

ABSTRACT

JUMP, ROMEO. Near Infrared Spectroscopy (NIRS). A Rapid Method for Nutrient Analysis of Eucalyptus and Pines in the Nursery. (Under the direction of Dr. Gary Ray Hodge).

Accurate and timely assessment of plant nutrient status is essential for optimizing fertilization practices, improving nursery efficiency, and supporting sustainable forestry production. Conventional laboratory-based foliar nutrient analyses, while precise, are time-consuming, destructive, and costly, limiting their practicality for frequent monitoring in operational settings. Near-Infrared Spectroscopy (NIRS) offers a rapid, non-destructive alternative, yet its effectiveness for predicting a broad range of macro- and micronutrients in nursery-grown forest species, particularly using portable devices, remains insufficiently understood.

This research evaluated the potential of NIRS to predict foliar nutrient content in nursery-grown eucalypt and pine seedlings using both portable and laboratory-based spectrometers. Seedlings of *Eucalyptus urophylla* × *Eucalyptus grandis* and *Pinus tecunumanii* were grown hydroponically under controlled greenhouse conditions and subjected to five nutrient regimes designed to generate variation in nitrogen, phosphorus, potassium, and selected micronutrients. Near-infrared spectra were collected at two growth stages, 15 and 30 days post-treatment, from intact foliage using two portable spectrometers, the Microphazir and the DLP NIRscan Nano EVM. Additional spectra were acquired from dried and ground foliage using the portable devices and a benchtop Foss NIRSystems 6500 spectrometer. All samples were analyzed using standard laboratory methods to provide reference nutrient concentrations.

Predictive models were developed using Partial Least Squares regression (PLSR) with appropriate spectral pre-processing, and model performance was evaluated using cross-validated coefficients of determination (R^2_{cv}) and root mean squared error of prediction (RMSEP_{cv}). Across species and growth stages, combining spectra from multiple foliage positions to represent whole-plant conditions consistently improved model performance compared to spectra collected from individual leaf or needle positions. Model accuracy was generally higher at 30 days post-treatment, reflecting greater physiological differentiation and spectral detectability as seedlings matured.

For eucalypt seedlings, portable spectrometers produced strong predictive models for nitrogen and moderate models for sulfur, calcium, and magnesium, particularly at early growth stages. Phosphorus predictability improved at later stages, while potassium models remained weak.

In pine seedlings, intact-needle models showed that nitrogen could be predicted with moderate to high accuracy using portable devices, with performance improving with plant maturity. Potassium and most micronutrients were difficult to predict reliably in intact foliage. Dried and ground foliage samples yielded substantially stronger models across nutrients and instruments. The Foss 6500 benchtop spectrometer consistently produced the most accurate predictions for nitrogen, phosphorus, potassium, calcium, magnesium, and sulfur. Among portable devices, the Microphazir demonstrated higher and more consistent accuracy for nitrogen across species and sample types, while the DLP Nano provided acceptable performance primarily for nitrogen and select nutrient ratios.

These findings demonstrate that NIRS is a viable tool for rapid nutrient assessment in nursery systems, particularly for nitrogen and selected macronutrients. Portable spectrometers offer practical advantages for *in situ* monitoring, while benchtop instruments remain preferable for comprehensive nutrient analysis. The results highlight both the operational potential and current limitations of NIRS, providing a foundation for improving calibration strategies and expanding its application in forestry nursery management.

© Copyright 2026 by Romeo Jump

All Rights Reserved

Near Infrared Spectroscopy (NIRS). A Rapid Method for Nutrient Analysis of
Eucalyptus and Pines in the Nursery.

by
Romeo Jump

A thesis submitted to the Graduate Faculty of
North Carolina State University
in partial fulfillment of the
requirements for the degree of
Master of Science

Forestry and Environmental Resources

Raleigh, North Carolina

2026

APPROVED BY:

Gary R. Hodge
Committee Chair

Juan J. Acosta

Miguel S. Castillo

DEDICATION

This thesis is dedicated to my wife, Anna Georgina, my children, Chris and Gracie, and my mother, Andrea Castañeda, who are the heart of everything I do.

To my wife, thank you for your love, understanding, and constant encouragement throughout this journey. Your patience and unwavering support during long nights, busy days, and moments of uncertainty gave me the strength to keep moving forward. I could not have completed this work without you by my side.

To my children, this work is for you. I hope it reminds you that learning is a lifelong journey and that education has the power to open doors, create opportunities, and shape the future. May you always be curious, resilient, and confident in your ability to overcome challenges. My greatest hope is that this work inspires you to pursue your dreams with dedication and to believe that your efforts can make a meaningful difference.

A mi madre, quien me enseñó con su ejemplo el valor del esfuerzo, la perseverancia y la dignidad. Tu amor, sacrificio y fe sembraron en mí el respeto por el conocimiento y el deseo de superarme. Este logro también es tuyo.

BIOGRAPHY

Romeo Jump is a researcher at Camcore, an international tree breeding and forest conservation cooperative housed within the Department of Forestry and Environmental Resources at North Carolina State University. With nearly fifteen years with the department, he has developed a strong record of applied research, international collaboration, and technical outreach in plantation forestry systems.

Romeo's interest in forestry began early in his life in Guatemala, where firsthand exposure to forestry shaped his understanding of sustainable forest management and regeneration. He later received a full scholarship to attend an agricultural boarding high school specializing in forestry and agricultural sciences, followed by completion of an Engineer degree in Agriculture with a concentration in tropical crops production. During his undergraduate training, he worked extensively with smallholder farmers across diverse regions, designing practical, resource-efficient production systems that integrated basic technologies and mechanization to improve productivity and sustainability.

After relocating to the United States, Romeo joined NC State University and Camcore, where he currently serves as Germplasm Bank Manager. In this role, he oversees the coordination, import, export, and global distribution of forest genetic material, ensuring strict compliance with international phytosanitary regulations. He works closely with government agencies, academic institutions, research partners, and private forestry organizations across more than 25 countries, supporting collaborative research initiatives and facilitating the transfer of technology and knowledge for breeding, testing, and conservation programs worldwide.

Romeo's research experience spans laboratory and field-based studies, including early work under the direction of Dr. William Dvorak on frost tolerance in temperate *Eucalyptus* species. He later led the development of *in vitro* propagation protocols to address phytosanitary and logistical challenges associated with international germplasm exchange. His work increasingly integrates novel technologies, including near-infrared spectroscopy, to assess wood properties and plant quality in different forest species.

Romeo is recognized for his commitment to applied, globally relevant research, his collaborative approach, and his ability to bridge science, technology, and operational forestry. His

professional work reflects a dedication to sustainable forest management, capacity building, and the responsible stewardship of forest genetic resources, values that continue to guide his academic and professional development.

Romeo currently lives in Raleigh, North Carolina, where he balances his professional and academic pursuits with a fulfilling family life. He shares his home with his wife, Anna Georgina, their two children, Chris and Gracie, and their dog, Calvin, who together provide constant inspiration, grounding, and joy beyond his professional work.

ACKNOWLEDGMENTS

First and foremost, I extend my sincere appreciation to the Camcore group worldwide for their ongoing support and sense of community throughout this research. I am especially grateful to my supervisors, Dr. Gary Hodge and Dr. Juan José Acosta, whose guidance and encouragement were essential to this work. From helping shape the initial research questions to offering technical insight and hands-on support along the way, Gary and JJ were generous mentors and a true pleasure to work with. Their leadership, expertise, and trust made this research both possible and deeply rewarding.

I would like to extend special thanks to the rest of the Camcore team—William Woodbridge, Elmer Guitierrez, Juan Luis López, Robert McGee, and Robert Jetton. Your mentorship, collaboration, and willingness to share your knowledge have meant a great deal to me, and I am truly honored to have worked alongside you. I am also grateful to Andy Whittier, former Camcore associate and now with the U.S. Forest Service, whose previous research inspired me to continue this line of work across different forestry species.

To the new generation of Camcore staff, friends, and colleagues—Dr. Ricardo Cavalheiro, Gabriela Brigatti Chaves, Dr. Aurelio Aguiar, Mindoro Razoki, and Gina Zabala—thank you for your support, collaboration, and camaraderie. A heartfelt thank you to Dr. Leonida Cherotich for your consistent help across multiple projects, and especially for your encouragement and steady support along the way.

Special thanks are extended to Dr. Miguel Castillo for serving on my committee. I greatly appreciate the opportunity to learn from your expertise and value your guidance and support throughout this process.

I am deeply grateful to my family. To my wife and children, thank you for patience and understanding during the many busy moments this work required. A mi madre, Andrea Castañeda, gracias por tu amor, tus oraciones y por enseñarme el valor de la fe, el esfuerzo y la educación. I am also thankful encouragement and constant support from my family in Guatemala.

Finally, I am profoundly grateful to my alma mater, Escuela Nacional Central de Agricultura, for providing the foundation of my education and for shaping the way I understand, question, and engage with science and the natural world.

AUTHORSHIP STATEMENT

Contributions of Romeo Jump and committee members are listed below for each chapter.

Chapter 1

- Romeo Jump: Sole author of Chapter 1
- Committee Members: Editorial feedback and revisions.

Chapter 2

- Romeo Jump: Experimental implementation; data collection; sample preparation; statistical analysis; interpretation of results; primary drafting and writing of the chapter.
- Dr. Hodge: Conceptual input on study design and biological interpretation; guidance throughout the research process; editorial feedback and revisions.
- Dr. Acosta: Conceptual input on experimental design; development of R code used for spectral analysis and model development; guidance and feedback on data analysis and interpretation; editorial feedback and revisions.
- Dr. Castillo: Edits to manuscript.

Chapter 3

- Romeo Jump: Experimental implementation; data collection; laboratory coordination; statistical analysis; interpretation of results; primary drafting and writing of the chapter.
- Dr. Gary Hodge: Guidance on study design and biological context; interpretation support; editorial feedback and revisions.
- Dr. Acosta: Guidance on experimental design and spectral modeling; feedback on data analysis and interpretation; editorial feedback and revisions.
- Dr. Castillo: editorial feedback and revisions.

Chapter 4

- Romeo Jump: Sole author of Chapter 4.
- Committee Members: Editorial feedback and revisions.

Use of Generative Artificial Intelligence

No generative artificial intelligence tools were used to create original content, data, analyses, or interpretations in this thesis. Writing assistance tools were used only for language editing and clarity.

TABLE OF CONTENTS

LIST OF TABLES	xi
LIST OF FIGURES	xii
CHAPTER 1: INTRODUCTION	1
1.1 Near-Infrared Spectroscopy	1
1.1.1 <i>Principles and Instrumentation</i>	2
1.1.2 <i>Portable Near-Infrared Spectroscopy: Definition and Significance</i>	2
1.1.3 <i>Technological Development of Portable NIR Spectrometers</i>	3
1.2 Application Domains of Portable Near-Infrared Spectroscopy	5
1.2.1 <i>Environmental Applications</i>	5
1.2.2 <i>Industrial Applications</i>	6
1.2.3 <i>Food and Beverages Applications</i>	6
1.2.4 <i>Agriculture and Crop Systems</i>	6
1.3 Forestry Applications of Portable NIRS	8
1.3.1 <i>Wood Chemistry and Wood Properties Assessment</i>	8
1.3.2 <i>Tree Seedling Applications</i>	9
1.4 NIRS for Foliar Nutrient Analysis in Pines and Eucalypts.....	10
1.4.1 <i>Comparison with Conventional Wet Chemistry Methods</i>	10
1.4.2 <i>Portable NIR Spectroscopy for Foliar Nutrient Assessment</i>	10
1.5 Research Gap and Study Rationale.....	12
1.6 References.....	13
CHAPTER 2: Prediction of Foliar Nutrient Concentration in Eucalypt Seedlings Using Portable Near-Infrared Spectroscopy	20
2.1 Introduction.....	22
2.2 Objectives	25
2.3 Materials and Methods	26
2.3.1 Plant material and nutrient regimes	26
2.3.2 Portable Spectrometers	28
2.3.3 Spectra Acquisition and Database Creation.....	28
2.3.4 Portable Spectrometers	31
2.3.5 NIR Model Dataset Creation	32
2.3.5.1 Spectral Transformations and Outlier Detection.....	33
2.3.5.2 Model Training, Cross-Validation, and Selection.....	33
2.4 Results.....	37
2.4.1 Nutrient concentration variation observed.....	37
2.4.1.1 Concentration Variation by Regime.....	37
2.4.1.2 Concentration Variation by Nutrient.....	37
2.4.2 Examination of Leaf-Pairs, Aggregates and Models for Macronutrients (Group 1)41	
2.4.2.1 Nitrogen.....	41
2.4.2.2 Phosphorus	42
2.4.2.3 Potassium.....	42
2.4.2.4 Effect of Leaf Aggregation and Model Selection	42
2.4.2.5 Rationale for Whole-Plant Dataset Selection.....	43

2.4.3 Models for the Rest of the Nutrients Using WP Dataset (Group 2)	46
2.4.3.1 Calcium, Magnesium, and Sulfur	46
2.4.3.2 Zinc, Copper, and Sodium	46
2.4.3.3 Iron, Manganese, Boron, Chloride, and Aluminum	46
2.4.3.4 Nutrient Ratios N:K, N:S, and Fe:Mn	47
2.5 Discussion	49
2.5.1 Overall Performance of Macronutrient Prediction Models	49
2.5.1.1 Nitrogen	49
2.5.1.2 Phosphorus	50
2.5.1.3 Potassium	51
2.5.2 Macronutrient Models Using Aggregated Leaf-Pair Datasets (Group 1)	51
2.5.3 Models for Additional Micronutrients Using the Whole-Plant Dataset (Group 2)	52
2.5.4 Comparative Performance of Portable NIR Spectrometers	53
2.6 Conclusion	55
2.7 References	56

CHAPTER 3: Protocol Use of Near-Infrared Spectroscopy to Predict Nutrient Concentration in Pines

3.1 Introduction	63
3.2 Objectives	66
3.3 Materials and methods	68
3.3.1 Plant material and nutrient regimes	68
3.3.2 NIR Spectrometers	70
3.3.3 Spectra Acquisition and Database Creation	70
3.3.4 NIR Model Dataset Creation	72
3.3.5 NIR Model Development	72
3.3.5.1 Spectral Transformations and Outlier Detection	73
3.3.5.2 Model Training, Cross-Validation, and Selection	73
3.4 Results	77
3.4.1 Nutrient concentration variation observed	77
3.4.1.1 Concentration Variation by Regime	77
3.4.1.2 Concentration Variation by Nutrient	77
3.4.2 Models for Nutrient Concentration Using Intact Foliage	81
3.4.2.1 Models at 15 Days Post-Treatment	83
3.4.2.2 Models at 30 Days Post-Treatment	83
3.4.2.3 Comparison of Primary Needles, Fascicles, and Whole-Plant Spectral Datasets	84
3.4.2.4 Comparison of Microphazir and DLP Nano Performance in Intact Foliage	84
3.4.3 Models for Nutrient Concentration in Dried and Ground Foliage	85
3.4.3.1 Models at 15 Days Post-Treatment	85
3.4.3.2 Models at 30 Days Post-Treatment	86
3.4.3.3 Comparison of Microphazir, DLP Nano, and Foss 6500 Performance	88
3.4.3.4 Comparison of Portable Spectrometers: DLP Nano vs. Microphazir	88
3.5 Discussion	90
3.6 Conclusion	96
3.7 References	97

CHAPTER 4: Thesis Conclusions	102
4.1 Scope.....	102
4.2 Key Findings.....	103
4.2.1 Freshly removed leaves of eucalypt seedlings.....	103
4.2.2 Intact needles of pine seedlings	104
4.2.3 Dried and ground needles of pine seedlings	105
4.3 Significance of the Results and Implications for Nursery Operations.....	105
4.4 Limitations of the Results and Implications	106
4.5 Recommendations.....	107
Appendixes	
Appendix A.....	109
Appendix B.....	115
Appendix C.....	125
Appendix D.....	134

LIST OF TABLES

Table 2.1	Composition of nutrient stock solutions, application volumes, and resulting concentrations of nitrate-nitrogen (NO ₃ -N), ammonium-nitrogen (NH ₄ -N), phosphorus (P), and potassium (K) in the complete Hoagland's nutrient solution	26
Table 2.2	Near infrared devices used to predict macronutrients and micronutrient levels in intact and processed samples of eucalypt leaves.....	27
Table 2.3	Partial least squares (PLS) regression fit statistics for predicting Nitrogen concentration in eucalypt foliage using the whole-plant dataset and Microphazir spectra collected 15 days after treatment application. Models were evaluated across multiple spectral preprocessing methods. For this dataset and this element, the SG7 transformation provided the most robust performance based on cross-validation statistics.....	33
Table 2.4	Summary statistics of observed foliar nutrient concentrations in eucalypt seedlings at 15 and 30 days post-treatment for samples used in NIR model development	39
Table 2.5	Observed Foliar Nitrogen Concentration Ranges at 15 and 30 Days Post-Treatment .	46
Table 2.6	Effect of different surface sterilization treatments on shoot proliferation on five different pine species (<i>P. tecunumanii</i> = TEC, <i>P. maximinoi</i> = MAX, <i>P. taeda</i> = TAE, <i>P. greggii</i> = GRE, and <i>P. patula</i> = PAT).	49
Table 2.7	Comparison of NIRS fit statistics for nutrient levels of macronutrients, micronutrients, and nutrient ratios in nursery material in pine†, eucalypts and teak (Whittier et al., 2021)	53
Table 3.1	Composition of nutrient stock solutions, application volumes, and resulting concentrations of nitrate-nitrogen (NO ₃ -N), ammonium-nitrogen (NH ₄ -N), phosphorus (P), and potassium (K) in the complete Hoagland nutrient solution.....	83
Table 3.2	Near-infrared devices used to predict macronutrient and micronutrient levels in intact and fried and ground samples of pine foliage	84
Table 3.3	Partial least squares (PLS) regression fit statistics for predicting Magnesium concentration in dried and ground pine needles using the Foss 6500 spectra collected 30 days after treatment application. Models were evaluated across multiple spectral preprocessing methods. For this sample dataset and nutrient, the MSC transformation provided the most robust performance based on cross-validation statistics.....	88
Table 3.4	Summary statistics of observed nutrient concentration of pine seedling foliage samples collected at 15 and 30 days post-treatments for samples used to build NIR models	94
Table 3.5	Comparison of NIRS fit statistics for nutrient levels of N, P, K, and Mg in teak (Whittier et al., 2021) and pine nursery material	106

LIST OF FIGURES

Figure 1.1 The electromagnetic spectrum is divided into several distinct regions, each characterized by a specific range of wavelengths and frequencies (Foss, 2024). This spectrum includes categories such as radio waves, microwaves, infrared, visible light, ultraviolet, X-rays, and gamma rays.....	1
Figure 1.2 Mini- and micro-spectrometer projected market will experience robust growth during the next decade (Data Insights Market, 2025)	5
Figure 1.3 The John Deere HarvestLab 3000, an advanced agricultural technology that uses NIR spectroscopy to evaluate the quality and composition of crops at harvesting. (Deere & Company, 2023).....	7
Figure 1.4 Times Cited and Publications Over Time on the use of TDZ in tissue culture.	12
Figure 2.1 Leaf selection and preparation workflow for NIR spectra data acquisition. A. The top four leaf-pairs were selected from each seedling. B. The eight leaves were removed for analysis. C. Leaves were arranged on a pre-labeled tray to maintain sample identity and position. D. Spectral measurements were collected with the spectrometer sensor positioned between the leaf margin and the midvein to ensure consistent sampling..	28
Figure 2.2 NIR spectral acquiring of eucalypt leaves using portable spectrometers. Top: Spectral measurements collected with the Microphazir scanning station. Bottom: Spectral measurements collected with the DLP NIRscan Nano EVM scanning station	29
Figure 2.3 Spectral data were collected from eight individual leaf positions (1a–8h) across each seedling and subsequently combined into four paired-leaf datasets (P1–P4) for NIR model development	31
Figure 2.4 RMSEP as a function of the number of latent variables for the SG7-transformed nitrogen model developed using the G234 dataset. The dotted gray vertical line indicates the model with the absolute minimum RMSEP (six latent variables), while the dashed blue vertical line indicates the selected model based on the one-sigma criterion. Although the minimum RMSEP occurred at six components, a five-component model was selected because its RMSEP was within one standard error of the minimum, favoring a more parsimonious model without loss of predictive performance.....	34
Figure 2.5 Box plots illustrate the variations in nitrogen, phosphorus, and potassium percentages in eucalypt seedling foliage collected at 15 and 30 days. Complete = Complete HNS. 50%NPK = Modified HNS with fifty percent nitrogen, phosphorus, and potassium. 10%N = Modified HNS with ten percent nitrogen. 10%P = Modified HNS with ten percent phosphorus. 10%K = Modified HNS ten percent potassium	38

- Figure 2.6 Line chart display showing R^2_{cv} (solid line) and $RMSEP_{cv}$ (dotted line) values of N, P, and K using all ten NIR spectra datasets at 15- (top) and 30-day (bottom) post-treatment for both portable spectrometers 43
- Figure 2.7 Observed versus predicted nitrogen concentrations (%) from whole-plant datasets. Top plots show models developed using Microphazir spectra, and bottom plots show models developed using DLP Nano spectra. Left plots correspond to 15 days post-treatment, and right plots to 30 days post-treatment. Models at 15 days post-treatment span a wider concentration range (1.16–5.08% N) and show stronger predictive performance, whereas models at 30 days post-treatment predict a narrower range (0.84–3.37% N), reflecting reduced variability at the later growth stage 44
- Figure 2.8 Bar charts comparing the R^2_{cv} values of nutrient models developed using whole plant spectral data from portable spectrometers: DLP Nano and Microphazir, at 15- and 30-days post-treatment. 47
- Figure 3.1 Acquisition of NIR spectra from intact pine seedlings using portable spectrometers. Left: DLP NIRscan Nano EVM (Texas Instruments) used to collect spectra from secondary needle fascicles located at the upper portion of the seedling. Right: Microphazir (Thermo Fisher Scientific) used to acquire spectra from primary needles located at the lower portion of the seedling 85
- Figure 3.2 Box plots illustrate the variations in nitrogen, phosphorus, and potassium percentages in pine seedling foliage collected at 15 and 30 days. Complete = Complete HNS. 50%NPK = Modified HNS with fifty percent nitrogen, phosphorus, and potassium. 0%N = Modified HNS with zero percent nitrogen. 0%P = Modified HNS with zero percent phosphorus. 0%K = Modified HNS with zero percent potassium 89
- Figure 3.3 Box plots illustrate the variations in nitrogen, phosphorus, and potassium percentages in pine seedling foliage collected at 15 and 30 days. Complete = Complete HNS. 50%NPK = Modified HNS with fifty percent nitrogen, phosphorus, and potassium. 0%N = Modified HNS with zero percent nitrogen. 0%P = Modified HNS with zero percent phosphorus. 0%K = Modified HNS with zero percent potassium 93
- Figure 3.4 Bar charts comparing model performance comparison for all nutrients at 15- and 30-days post-treatment for the three datasets: Primary needles, Fascicles, and Whole-Plant, with spectra acquired using Microphazir and DLP Nano spectrometers..... 96
- Figure 3.5 Bar charts displaying a model performance comparison for all nutrients at 15- and 30-days post-treatment of dried and ground samples with spectral data collected using Microphazir, DLP Nano spectrometers, and Foss 6500 spectrometers 101

CHAPTER 1

INTRODUCTION

In forestry and tree nursery operations, rapid assessment of foliar nutrient status is critical for optimizing fertilization regimes, ensuring seedling quality, and supporting early-stage plant development. Despite the demonstrated potential of portable Near-infrared spectroscopy (NIRS) across multiple disciplines, its application for quantitative foliar nutrient analysis in nursery-grown pine and eucalypt seedlings remains limited and unevenly validated. This literature review synthesizes existing research on portable NIRS, with an emphasis on its applicability, limitations, and performance in plant, agricultural, and forestry contexts, to establish the foundation for evaluating portable NIR instruments as tools for nutrient analysis in forest nursery operations.

1.1 Near-Infrared Spectroscopy

Near-infrared spectroscopy (NIRS) is a rapid, non-destructive analytical technique that utilizes the near-infrared region of the electromagnetic spectrum (Figure 1.1) to characterize the chemical composition of biological and industrial materials. The method is based on the absorption of near-infrared radiation by molecular overtones and combination vibrations, producing spectral patterns that can be related to chemical constituents through multivariate calibration models. The near-infrared region typically spans wavelengths from approximately 780 to 2500 nm, positioned adjacent to the visible spectrum and widely used for quantitative analysis across agricultural, industrial, and environmental systems (Gullifa et al., 2023).

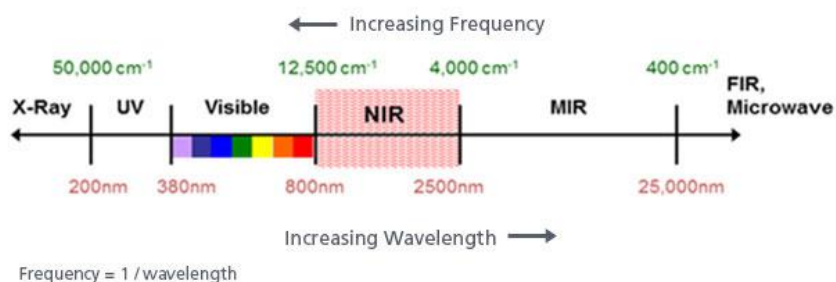


Figure 1.1 The electromagnetic spectrum is divided into several distinct regions, each characterized by a specific range of wavelengths and frequencies (Foss, 2024). This spectrum includes categories such as radio waves, microwaves, infrared, visible light, ultraviolet, X-rays, and gamma rays.

1.1.1 Principles and Instrumentation

This technology offers benefits like non-destructive analysis, providing immediate insights that can be linked to subsequent analyses on the same sample. Combining NIRS with chemometrics allows for focused and broad analyses through prediction models based on statistical evaluation. Results can be shared qualitatively or quantitatively, making them accessible to experts and non-experts (Gullifa et al., 2023).

NIRS has traditionally been implemented using laboratory-based, benchtop spectrometers that provide high spectral resolution and analytical stability and have demonstrated strong performance across a range of sectors, including agriculture, food & beverage, pharmaceuticals, textiles, and polymer & plastics industries. These systems typically require destructive sample preparation and access to centralized laboratory infrastructure, which introduces logistical constraints related to sample transport and processing. In operational settings where timely feedback is needed, these constraints can limit the practicality of benchtop approaches, motivating interest in alternative measurement strategies that enable on-site analysis.

Advances in optics, detector technology, and miniaturization over the past two decades have led to the development of portable and handheld NIR spectrometers capable of performing on-site measurements. These instruments offer substantial advantages, including reduced analysis time, non-destructive sampling, and the potential for high-throughput data collection. As a result, portable NIRS has gained increasing attention as a practical alternative to benchtop systems in applications requiring real-time or near-real-time assessment.

1.1.2 Portable Near-Infrared Spectroscopy: Definition and Significance

A NIR spectrometer is an analytical scientific instrument used to analyze and study the properties of light over a specific range of the electromagnetic spectrum (Beć et al., 2021). It works by splitting light into different wavelengths, allowing scientists to identify and measure its components. A NIR spectrometer is designed specifically for analyzing NIR light, providing insights into the molecular structure and composition of samples (Leary et al., 2021).

Over the past two decades, there has been increased interest in NIRS, resulting in the creation of portable devices for a range of applications. A portable spectrometer is a valuable analytical tool for quick and accurate sample analysis, whether in the laboratory or field (Leary et

al., 2021). Unlike traditional laboratory-based benchtop spectrometers, which require samples to be carried to the equipment, portable spectrometers are small and lightweight instruments that can be easily transported and can run on battery power for a reasonable time frame. The most apparent distinctiveness is the narrower spectral regions and/or lower spectral resolution with which the portable devices operate (Beć et al., 2021).

Portable spectrometers are compact, handheld devices that can be used to rapidly assess the chemical and physical properties of a sample. Such instruments offer the advantage of on-site scanning, potentially supporting quicker decision-making in laboratory, industrial, and field settings (Perez et al., 2019).

The ability to perform on-site and online analyses supports industrial applications, with the potential for easy automation and integration into the Internet of Things systems. Ongoing improvements in size, cost, durability, user-friendliness, portability, and design establish NIRS as a valuable tool for routine characterization (Gullifa et al., 2023).

1.1.3 Technological Development of Portable NIR Spectrometers

The history of portable spectroscopy has been shaped by safety, security, and military concerns, as well as by commercial and agricultural needs. Early uses of portable devices include military-related chemical detectors developed during the twentieth century and initial applications in forensic science. In parallel with these efforts, portable near-infrared spectroscopy began to emerge in agricultural contexts. In 1978, a research group developed a portable instrument mounted in a mobile van to deliver nutrient analysis of forages directly on-farm and at hay auctions, an approach that later evolved into university extension mobile NIR vans operating in Pennsylvania, Minnesota, Wisconsin, and Illinois. That same year, the USDA NIRS Forage Network was established to develop and test computer software and analytical methods for advancing NIRS-based grain and forage testing (Sapienza et al., 2008).

Additional milestones in the evolution of portable spectroscopy include the deployment of spectrometers for breath-alcohol measurements in the 1930s and the introduction of portable gas chromatography–mass spectrometry in 1996 (Leary et al., 2021). Following the events of September 11, 2001, the development of portable and handheld optical spectrometers accelerated

in response to security demands and subsequently expanded into emergency response, hazardous materials handling, and broader industrial and civilian applications (Crocombe, 2018).

In 2005, Thermo Fisher Scientific (formerly Polychromix) launched a groundbreaking NIR handheld device that transformed the industry, motivating the development of portable NIR instruments primarily for commercial purposes (Crocombe, 2018). Despite their potential, certain instruments failed to gain widespread acceptance due to limitations like restricted wavelength ranges or specific applications (e.g., Brix determination for apples only), which made these instruments less versatile and less appealing in the market (Saranwong & Kawano, 2005). The higher cost of some instruments compared to others also played a significant role in their lack of popularity (Crocombe, 2018).

The challenges related to calibration and the nonspecific nature of NIR spectra have influenced the pace of adoption, but ongoing technological improvements continue to shape the landscape of portable NIR instruments (Leary et al., 2021). NIR spectrometers are transforming to become even smaller and more affordable, and new devices capable of maintaining high performance will create new opportunities for utilization. They can be divided into two broad classes: 1) *Mini-spectrometers*, typically ranging in volume from about 250 cm³ (roughly the size of a large coffee mug) to 8,000 cm³ (comparable to a micro-wave oven), and 2) *Micro-spectrometers*, generally smaller than 250 cm³ (Bouyé & d'Humières, 2017).

Mini- and micro-spectrometers can make spectroscopy more accessible, potentially transforming numerous industries and enabling end-users to conduct on-field and in-line measurements across various applications, including chemistry, pharmaceuticals, agri-food, healthcare, and consumer areas. These spectrometers offer new possibilities, making spectroscopy more feasible and impactful across diverse fields (Bouyé & d'Humières, 2017).

Although high initial costs and the need for specialized technical expertise remain barriers to broader adoption, ongoing improvements in manufacturing efficiency and user-friendly software are reducing these constraints. Innovation and market expansion is driven by increasing demand from end-users for *in situ* measurement at low cost (Data Insights Market, 2025). The mini- and micro-spectrometer market, valued at approximately \$472 million in 2025, is projected

to experience sustained growth, with an estimated compound annual growth rate of 8.4% through 2033 (Figure 1.2).

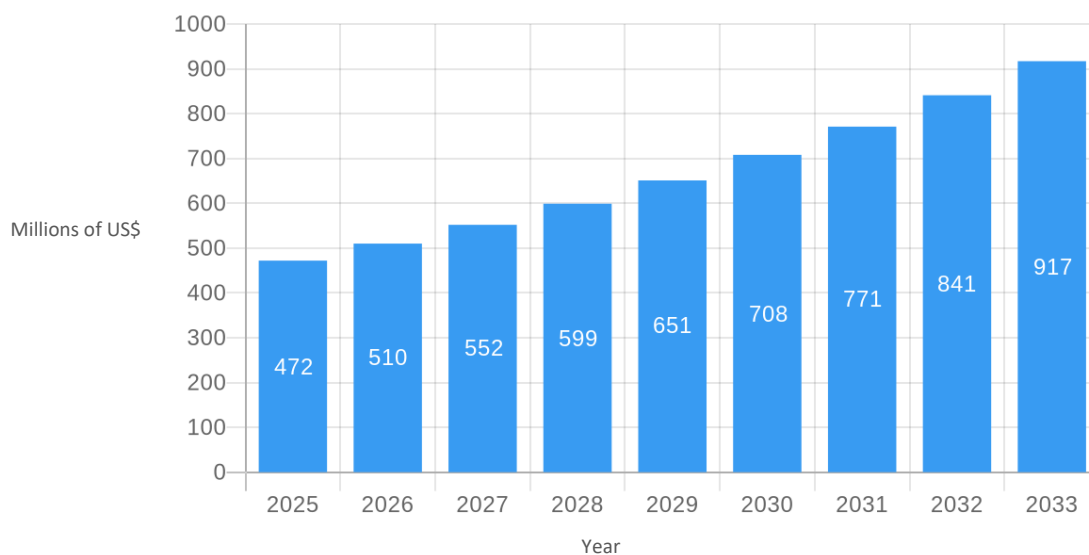


Figure 1.2 Mini- and micro-spectrometer projected market will experience robust growth during the next decade (Data Insights Market, 2025).

1.2 Application Domains of Portable Near-Infrared Spectroscopy

Portable near-infrared (NIR) spectrometers have been applied across a wide range of disciplines due to their ability to perform rapid, non-destructive, and on-site chemical analyses. While early adoption focused on laboratory-based systems, advances in miniaturization have enabled field-deployable instruments that support real-time decision-making across environmental, industrial, food, and agricultural contexts (Crocombe, 2018; Beć et al., 2021; Gullifa et al., 2023). The following sections briefly summarize key application areas to contextualize the versatility of portable NIR technology.

1.2.1 Environmental Applications

In environmental and exploration contexts, portable NIRS has been used for on-site characterization of soils and natural materials. Handheld instruments generally exhibit lower spectral resolution and analytical performance than benchtop systems. However, multiple studies indicate that they can provide sufficiently robust results for rapid screening applications, particularly in remote or logistically constrained settings (Yan et al., 2023). Applications include

soil property mapping, mineral exploration, and contamination assessment, such as the detection of total petroleum hydrocarbons, where portability and rapid data acquisition are prioritized over maximal analytical precision (Lopo et al., 2017; Miao et al., 2023).

1.2.2 Industrial Applications

Portable NIR spectrometers have also been adopted in industrial settings for material identification and quality monitoring. Reported applications include classification of textiles, characterization of polymer materials, and verification of fuel composition under field conditions (Maia Paiva et al., 2017; da Silva & Cavalcanti, 2015; Yan et al., 2023). These studies demonstrate the practical utility of portable NIR systems for industrial screening purposes. They also emphasize the importance of appropriate calibration strategies, wavelength coverage, and application-specific validation to ensure reliable use (Gullifa et al., 2023).

1.2.3 Food and Beverages Applications

In the food and beverage sector, portable NIRS has been widely investigated as a tool for quality assessment and fraud detection. Handheld instruments have been applied to a range of products, including meats, dairy, oils, flours, nuts, coffee, fruits, and juice primarily to detect compositional differences and potential adulteration (Dos Santos et al., 2013; Liu, et al., 2018; Beć et al., 2020; Perez et al., 2019; Silva et al., 2020; Pu et al., 2021; Ting et al., 2020; Ciaccheri et al., 2022; Netto et al., 2023; Boadu et al., 2023). In horticultural products, portable NIRS has been explored for estimating quality attributes such as soluble solids and sugar content, supporting applications in postharvest assessment and precision agriculture (Li et al., 2020; Donis-Gonzalez et al., 2020; Yan et al., 2023). Across food systems, reported results highlight the practicality of portable instruments for rapid screening. Performance variability is commonly attributed to differences in product type, calibration approach, and spectral range.

1.2.4 Agriculture and Crop Systems

Agriculture and plant systems represent a key application area for near-infrared spectroscopy (NIRS), particularly in contexts that require non-destructive, repeated measurements and rapid on-site analysis.

Forage analysis was among the earliest applications of NIR technology, with foundational studies demonstrating the ability of infrared reflectance spectroscopy to predict key chemical and nutritional attributes across a wide range of temperate and tropical forage species, including alfalfa,

tall fescue, bromegrass mixtures, bermudagrass, and pangola digit grass. This early work established NIRS as a rapid and practical alternative to conventional forage analysis (Norris et al., 1976).

Building on these initial advances, subsequent research demonstrated the feasibility of integrating diode array NIR spectrometers into self-propelled forage harvesters for real-time measurement of whole-plant silage moisture content under field conditions (Digman & Shinnars, 2006). This work informed the development of commercial platforms such as the John Deere HarvestLab™ 3000 (John Deere, Moline, IL, USA) (Figure 1.3), which applies NIRS to estimate crop moisture, dry matter, and dry yield during harvest operations (Long et al., 2016).



Figure 1.3 The John Deere HarvestLab 3000, an advanced agricultural technology that uses NIR spectroscopy to evaluate the quality and composition of crops at harvesting. (Deere & Company, 2023)

More recent studies have examined the use of portable and handheld NIR spectrometers for predicting nutritional attributes of forage crops. Comparative evaluations with benchtop instruments indicate that handheld devices can be used to develop prediction models for dry matter, neutral detergent fiber, true *in vitro* digestibility, sodium sulfite-treated neutral detergent fiber digestibility, acid detergent fiber, acid detergent lignin, and crude protein in dried and ground forages, including grass, alfalfa, switchgrass, and bermudagrass (Digman et al., 2022; Acosta et al., 2020).

Beyond forage, portable NIRS has been applied to specialty and commercial crops for chemical characterization and harvest-related decision support. In *Verbena officinalis*, miniaturized NIR devices enabled direct, non-invasive measurements on fresh and dried plant material for determining optimal harvest timing, although conventional instruments achieved slightly higher predictive performance for verbascoside content (Pezzei et al., 2017). Handheld NIR spectrometers have also been used to estimate reducing sugars, total alkaloids, and nicotine in flue-cured tobacco leaves, with more consistent performance reported for processed material than for unprocessed leaves (Castillo et al., 2023).

1.3 Forestry Applications of Portable NIRS

The applicability of portable NIRS becomes especially relevant within forestry, where rapid, non-destructive assessment of biological material is essential. Forestry operations demand analytical approaches capable of handling large sample volumes, heterogeneous plant tissues, and time-sensitive management decisions under field and nursery conditions that limit reliance on laboratory-based methods. NIRS has long been used to characterize wood and plant chemical properties using benchtop instruments, and recent advances in portable devices have extended this capability to on-site applications. These developments underscore the need to evaluate the performance of portable NIR spectrometers specifically within forestry and tree nursery contexts, which is the focus of the following section.

Forestry applications of NIRS have traditionally focused on wood chemistry and quality assessment, where the technique has been widely used to rapidly predict wood properties and support decision-making without destructive sampling. This approach has substantially advanced wood quality evaluation by enabling efficient characterization of key chemical and physical traits across large sample sets. More recently, the emergence of portable spectrometers has expanded the application of NIRS beyond laboratory settings, allowing for a range of on-site forestry applications (Beć et al., 2021). Emerging research suggests that extending these applications to foliar analysis using portable instruments may provide similarly valuable insights, particularly during early growth stages when management interventions are most impactful.

1.3.1 Wood Chemistry and Wood Properties Assessment

The NIRS method is highly effective in assessing wood quality and properties of various eucalypts (Bailleres et al., 2002; Raymond & Schimleck, 2002; Alves et al., 2011; Hodge et al.,

2018), and pine species (Hodge & Woodbridge, 2004; Hodge & Woodbridge, 2010; Fahey et al., 2018; Alves et al., 2020), particularly for wood chemistry traits such as soluble and insoluble lignin, SG ratio, glucose, xylose, and minor sugars. However, this powerful analytical technique has been developed mostly with the use of traditional laboratory-based or benchtop spectrometers.

A preliminary study compared the performance of benchtop and portable NIR spectrometers for measuring wood samples of *Eucalyptus pellita* and *E. benthamii*. The objective of this work was to compare the performance of spectra acquired with a benchtop and a portable spectrometer of sawdust samples. The bench spectrometer exhibited an overall better performance, but the portable instrument's parameters were satisfactory given its limitations in robustness and handling needs (Diniz et al., 2019). The collected NIR spectra and chemical analysis from the sawdust samples were used to develop prediction models for lignin and syringyl/guaiacol (S/G). The results showed that the benchtop instrument performed significantly better than the portable instrument (Diniz et al., 2019).

A recent study focused on developing on-site prediction models for kraft pulp yield and S/G ratio using portable NIRS, emphasizing the benefits of assessing pulpwood traits from standing eucalypts trees. This technique reduces the time required for measurements and eliminates the need for sample transport, grinding, and storage of samples typically used in benchtop NIR spectrometers (Ramadevi et al., 2022).

1.3.2 Tree Seedling Applications

NIRS has shown potential as a quick and non-destructive alternative to predict relative water content, leaf water potential, and stomatal conductance in *Eucalyptus grandis* seedlings. The technique could be very useful in studies involving plant water status, highlighting the advantages of using portable NIR instruments for on-site non-destructive, high-throughput monitoring of drought and recovery in the field (Warburton et al., 2014).

Traditional laboratory-based NIR spectrometers were found to be more accurate than handheld scanners in developing models to predict nitrogen, phosphorus, potassium, and boron in teak (*Tectona grandis*) seedlings. However, the handheld device has the advantage of offering non-destructive analysis and faster results, providing valuable insights for growers to manage their resources effectively (Whittier et al., 2021).

1.4 NIRS for Foliar Nutrient Analysis in Pines and Eucalypts

1.4.1 Comparison with Conventional Wet Chemistry Methods

Within forestry nurseries, foliar nutrient status serves as a critical indicator of seedling quality, reflecting both nutrient availability and physiological condition. Traditional wet chemistry methods for nutrient analysis, while accurate, are time-consuming, labor-intensive, and destructive, limiting their practicality for large-scale or repeated measurements. The integration of NIRS into foliar nutrient assessment offers the potential to overcome these limitations, enabling rapid evaluation of multiple nutrients from a single spectral measurement.

NIRS has several benefits over wet chemistry analysis for analyzing large sample sets once the predictive equation is established. The technique can quickly predict the chemical composition of a sample in a single measurement. This is done solely from the spectral properties, without the need for further analysis, eliminating the need for time-consuming and expensive chemical analyses for each separate nutrient (Fernández-Martínez et al., 2017).

Early stages of researching foliar content suggest that NIRS is a cost-effective and efficient alternative to wet chemistry methods for analyzing nitrogen, lignin, and cellulose concentrations in woody plants (McLellan et al., 1991). One study found suitable models to predict element concentrations in white pine and red oak using NIRS on ground foliage samples, highlighting the technique's potential for predicting aluminum, calcium, potassium, manganese, and magnesium in forest canopies (Hallett et al., 1997).

Researchers have assessed the potential of NIRS to predict mineral content in oven-dried, ground natural grassland samples collected in semiarid zones, suggesting that this technique may provide acceptable results. The study found suitable models to estimate nitrogen and acceptable for calcium and magnesium. However, models to estimate copper, manganese, and potassium content had limited utility, while the phosphorus, sodium, iron, and zinc models were unsuccessful (Vasquez et al., 1995).

1.4.2 Portable NIR Spectroscopy for Foliar Nutrient Assessment

The non-destructive nature of NIRS and the portability of modern miniaturized spectrometers could effectively enable individual leaves on a tree to be monitored on a regular

basis to provide longitudinal time data to be obtained. This could be used to study the uptake of fertilizer at several locations in a tree following the application of the fertilizer (Alwi et al., 2021).

Handheld NIR instruments that scan either a broader spectrum or specific sections across the NIR spectrum exhibit the ability to predict foliage nutrient content comparable to traditional laboratory-based NIR instruments (Whittier et al., 2021; Acosta et al., 2020). However, most of these devices lack comprehensive validation performed in well-equipped laboratories (Beć et al., 2021), highlighting the necessity for published and peer-reviewed research on the performance of portable NIR spectrometers.

For over 20 years, Camcore (based at North Carolina State University in the USA) has developed NIRS models to predict chemical and physical traits in wood and foliage, has used NIR canonical discriminant analysis to differentiate between pure and hybrid species, and confirm clonal identity in the nursery. Most recently, the program has developed global NIR models for wood characterization of pines and eucalypts and has worked in the assessment of foliar nutrient content in nurseries and plantations (Camcore, 2022). The program has been using portable spectrometers in a series of NIR projects from the last 10 years.

The studies cited above identify several commercially available portable NIRS devices with potential applicability for measuring foliar nutrient content. Among these, the mini-spectrometer MicroPHAZIR™ (Thermo Fisher Scientific) (Figure 1.4) and the micro-spectrometer DLP NIRscan Nano EVM (Texas Instruments) represent two widely used platforms with distinct technical characteristics. This study evaluates the effectiveness of these instruments for assessing foliar nutrient concentrations, with a specific focus on nursery-grown eucalypt and pine.



Figure 1.4 Pine seedlings, hydroponically grown, being scanned with MicroPHAZIR™ hand-held device.

1.5 Research Gap and Study Rationale

Despite extensive research demonstrating the utility of NIRS for chemical characterization of plant materials, most foliar nutrient studies in forestry have relied on laboratory-based benchtop instruments and processed samples. Portable and handheld NIR spectrometers have become increasingly available and have been explored across industrial, food, agricultural, and environmental applications; however, their performance for quantitative foliar nutrient analysis in nursery-grown pine and eucalypt seedlings remains insufficiently validated. Reported predictive accuracy varies across nutrients, species, and instrument platforms, and direct comparisons between portable devices and established laboratory systems under operational nursery conditions are limited. In addition, device-specific performance, variation in the nutrient concentrations, spectral preprocessing requirements, and robustness across nutrient concentration ranges are not consistently addressed in the literature. Collectively, these gaps underscore the need for a systematic evaluation of portable NIR spectrometers for foliar nutrient analysis in forest nursery operations.

1.6 References

- Acosta, J. J., Castillo, M. S., & Hodge, G. R. (2020). Comparison of benchtop and handheld near-infrared spectroscopy devices to determine forage nutritive value. *Crop Science*, *60*(6), 3410-3422. <https://doi-org.prox.lib.ncsu.edu/10.1002/csc2.20264>
- Alves, A., Simões, R., Lousada, J. L., Lima-Brito, J., & Rodrigues, J. (2020). Predicting the lignin H/G ratio of *Pinus sylvestris* L. wood samples by PLS-R models based on near-infrared spectroscopy. *Holzforschung*, *74*(7), 655 - 662. <https://doi-org.prox.lib.ncsu.edu/10.1515/hf-2019-0186>
- Alves, A., Simões, R., Stackpole, D. J., Vaillancourt, R. E., Potts, B. M., Schwanninger, M., & Rodriguez, J. (2011). Determination of the syringyl/guaiacyl ratio of Eucalyptus globulus wood lignin by near infrared-based partial least squares regression models using analytical pyrolysis as the reference method. *Journal Of Near Infrared Spectroscopy*, *19*(5), 343 - 348. <https://doi-org.prox.lib.ncsu.edu/10.1255/jnirs.946>
- Alwi, A., Meder, R., Japarudin, Y., Hamid, H. A., Sanusi, R., & Mohd Yusoff, K. H. (2021). Near infrared spectroscopy of *Eucalyptus pellita* for foliar nutrients and the potential for real-time monitoring of trees in fertiliser trial plots. *Journal Of Near Infrared Spectroscopy*, *29*(3) 158 - 167. <https://doi-org.prox.lib.ncsu.edu/10.1177/09670335211007971>
- Bailleres, H., Davrieux, F., & Ham-Pichavant, F. (2002). Near infrared analysis as a tool for rapid screening of some major wood characteristics in a *Eucalyptus* breeding program. *Wood, Breeding, Biotechnology and Industrial Expectations Conference*, *59*(5-6), 479 - 490. Villenave D'ornon: Annals of Forest Science. <https://doi.org/10.1051/forest:2002032>
- Beć, K. B., Grabska, J., & Huck, C. W. (2021). Principles and Applications of Miniaturized Near-Infrared (NIR) Spectrometers. *Chemistry-A European Journal*, *27* (5) 1514-1532. <https://doi-org.prox.lib.ncsu.edu/10.1002/chem.202002838>
- Beć, K. B., Grabska, J., Siesler, H. W., & Huck, C. W. (2020). Handheld near-infrared spectrometers: Where are we heading? *Nir News*, *31*(3-4), 28 - 35. <https://doi.org/10.1177/0960336020916815>
- Boadu, V. G., Teye, E., Amuah, C. L., Lamptey, F. P., & Sam-Amoah, L. K. (2023). Portable NIR Spectroscopic Application for Coffee Integrity and Detection of Adulteration with Coffee Husk. *Processes*, *11*(4), 1140. <https://doi.org/10.3390/pr11041140>

- Bouyé, C., & d'Humières, B. (2017). Miniature and micro spectrometers market: who is going to catch the value? *SPIE OPTO*, *10110*(1), 11. <https://doi-org.prox.lib.ncsu.edu/10.1117/12.2254033>
- Camcore. (2022). NIR fos assesment of Plantation Nutrient Status in Eucalyptus grandis. <https://www.camcore-ncsu.org/camcore-annual-meetings/#past-annual-meetings>
- Castillo, M. S., Acosta, J. J., Hodge, G. R., Vann, M. C., & Lewis, R. L. (2023). Analysis of alkaloids and reducing sugars in processed and unprocessed tobacco leaves using a handheld near infrared spectrometer. *Journal Of Near Infrared Spectroscopy*, *31*(2), 55 - 62. <https://doi-org.prox.lib.ncsu.edu/10.1177/09670335221148594>
- Ciaccheri, L., Adinolfi, B., Mencaglia, A. A., & Mignani, A. G. (2022). Bluetooth-Connected Pocket Spectrometer and Chemometrics for Olive Oil Applications. *Foods*, *11*(15), 2265. <https://doi.org/10.3390/foods11152265>
- Crocombe, R. A. (2018). Portable Spectroscopy. *Applied Spectroscopy*, *72*(12), 1701-1751. <https://doi-org.prox.lib.ncsu.edu/10.1177/0003702818809719>
- da Silva, N. C., & Cavalcanti, C. J. (2015). Standardization from a benchtop to a handheld NIR spectrometer using mathematically mixed NIR spectra to determine fuel quality parameters. *Analytica Chimica Acta*, *954*(1), 32 - 42. <https://doi-org.prox.lib.ncsu.edu/10.1016/j.aca.2016.12.018>
- Data Insights Market. (2025). Miniature and Micro Spectrometers Market Demand Dynamics: Insights 2025-2033. <https://www.datainsightsmarket.com/reports/miniature-and-micro-spectrometers-38165?tab=summary>
- Deere & Company. (2023). John Deere HarvestLab™ 3000 For S700 Series Combines. <https://www.deere.com/en/technology-products/precision-ag-technology/data-management/harvest-lab-3000/>
- Digman, M. F., & Shinnars, K. J. (2006). Real-Time Moisture Measurement On a Forage Harvester Using Near-Infrared Reflectance Spectroscopy. *Annual International Meeting of the American-Society-of-Agricultural-and-Biological-Engineers*, *51*(5), 1801-1810. <https://elibrary-asabe-org.prox.lib.ncsu.edu/abstract.asp?aid=25295&confalias=t2&t=1>

- Digman, M. F., Cherney, J. H., & Cherney, D. J. (2022). The Relative Performance of a Benchtop Scanning Monochromator and Handheld Fourier Transform Near-Infrared Reflectance Spectrometer in Predicting Forage Nutritive Value. *Sensors*, 22(2), 658. <https://doi.org/10.3390/s22020658>
- Diniz, C. P., Grattapaglia, D., & de Alencar Figueiredo, L. F. (2019). Comparative performance of bench and portable near infrared spectrometers for measuring wood samples of two Eucalyptus species (*E. pellita* and *E. benthamii*). *18th International Conference on Near Infrared Spectroscopy*. https://www.researchgate.net/publication/331203720_Comparative_performance_of_bench_and_portable_near_infrared_spectrometers_for_measuring_wood_samples_of_two_Eucalyptus_species_E_pellita_and_E_benthamii
- Diniz, C. P., Grattapaglia, D., & de Alencar Figueiredo, L. F. (2019). Near-infrared-based models for lignin syringyl/guaiacyl ratio of Eucalyptus benthamii and E. pellita using a streamlined thioacidolysis procedure as the reference method. *Wood Science And Technology*, 53(1), 521 - 533. <https://doi-org.prox.lib.ncsu.edu/10.1007/s00226-019-01090-3>
- Donis-Gonzalez, I. R., Valero, C., Momin, M. A., Kaur, A., & Slaughter, D. C. (2020). Performance evaluation of two commercially available portable spectrometers to non-invasively determine table grape and peach quality attributes. *Agronomy*, 10(1), 148. <http://dx.doi.org/10.3390/agronomy10010148>
- Dos Santos, C. A., Lopo, M., Páscoa, R. N., & Lopes, J. A. (2013). A Review on the Applications of Portable Near-Infrared Spectrometers in the Agro-Food Industry. *Applied Spectroscopy*, 67(11), 1215-1233. <https://doi-org.prox.lib.ncsu.edu/10.1366/13-07228>
- Fahey, L. M., Nieuwoudt, M. K., & Harris, P. J. (2018). Using near infrared spectroscopy to predict the lignin content and monosaccharide compositions of Pinus radiata wood cell walls. *International Journal Of Biological Macromolecules*, 113(1), 507 - 514. <https://doi-org.prox.lib.ncsu.edu/10.1016/j.ijbiomac.2018.02.105>
- Fernández-Martínez, J., Joffre, R., Zacchini, M., Fernández-Marín, B., García-Plazaola, J. I., & Fleck, I. (2017). NIRS allows rapid and simultaneous evaluation of chloroplast pigments and antioxidants, carbon isotope discrimination and nitrogen content. *Forest Ecology And Management*, 399(1), 227-234. <https://doi-org.prox.lib.ncsu.edu/10.1016/j.foreco.2017.05.041>

- Foss. (2024). NIR technology for routine analysis of food and agricultural products. <https://www.fossanalytics.com/de-de/news-articles/technologies/nir-technology>
- Gullifa, G., Barone, L., Papa, E., Giuffrida, A., Materazzi, S., & Risoluti, R. (2023). Portable NIR spectroscopy: the route to green analytical chemistry. *Frontiers in Chemistry*, *11*(1), 1214825. <https://doi.org/10.3389/fchem.2023.1214825>
- Hallett, R. A., Hornbeck, J. W., & Martin, M. E. (1997). Predicting elements in white pine and red oak foliage with visible-near infrared reflectance spectroscopy. *Journal Of Near Infrared Spectroscopy*, *5*(2), 77 - 82. <https://doi-org.prox.lib.ncsu.edu/10.1255/jnirs.101>
- Hastie, T., Tibshirani, R., & Friedman, J. (2009). The elements of statistical learning: data mining, inference, and prediction. *Springer Nature*, *27*(1), 83-85. <https://doi-org.prox.lib.ncsu.edu/10.1007/BF02985802>
- Hodge, G. R. & Woodbridge, W. C., (2004). Use of near infrared spectroscopy to predict lignin. *Journal of Near Infrared Spectroscopy*, *12*(6), 381-390. <https://doi-org.prox.lib.ncsu.edu/10.1255/jnirs.447>
- Hodge, G. R., & Woodbridge, W. C. (2010). Global near Infrared Models to Predict Lignin and Cellulose Content of Pine Wood. *Journal Of Near Infrared Spectroscopy*, *18*(6), 367 - 380. <https://doi-org.prox.lib.ncsu.edu/10.1255/jnirs.902>
- Hodge, G. R., Acosta, J. J., Unda, F., Woodbridge, W. C., & Mansfield, S. (2018). Global near infrared spectroscopy models to predict wood chemical properties of Eucalyptus. *Journal of Near Infrared Spectroscopy* *26*(2), 117-132. <https://doi-org.prox.lib.ncsu.edu/10.1177/0967033518770211>
- Leary, P. E., Crocombe, R. A., & Kammrath, B. W. (2021). Introduction to Portable Spectroscopy. In R. A. Crocombe, P. E. Leary, B. W. Kammrath, H. C. Lee, R. A. Crocombe, & P. E. Leary (Eds.), *Portable Spectroscopy and Spectrometry 1*, (1st ed., pp 1-13). Wiley. <https://doi.org/10.1002/9781119636489.ch1>
- Li, P., Li, S., Du, G., Jiang, L., Liu, X., Ding, S., & Shan, Y. (2020). A simple and nondestructive approach for the analysis of soluble solid content in citrus by using portable visible to near-infrared spectroscopy. *Food Science & Nutrition*, *8*(5), 2543 - 2552. <https://doi.org/10.1002/fsn3.1550>

- Liu, N., Parra, H. A., Pustjens, A., Hettinga, K., Mongondry, P., & van Ruth, S. M. (2018). Evaluation of portable near-infrared spectroscopy for organic milk authentication. *Talanta*, *184*(1), 128-135. <https://doi-org.prox.lib.ncsu.edu/10.1016/j.talanta.2018.02.097>
- Long, E. A., Ketterings, Q. M., Russell, D., Vermeulen, F., & Degloria, S. D. (2016). Assessment of yield monitoring equipment for dry matter and yield of corn silage and alfalfa/grass. *Presision Agriculture*, *17*(5), 546 - 563. <https://doi-org.prox.lib.ncsu.edu/10.1007/s11119-016-9436-y>
- Lopo, M., Páscoa, R. N., Graça, A. R., & Lopes, J. A. (2017). Classification of Vineyard Soils Using Portable and Benchtop Near-Infrared Spectrometers: A Comparative Study. *Soil Science Society Of America Journal*, *80*(3), 652 - 661. <https://doi-org.prox.lib.ncsu.edu/10.2136/sssaj2015.09.0324>
- Maia Paiva, E., Rodrigues Rohwedder, J. J., Pasquini, C., Pimentel, M. F., & Fernandes Pereira, C. (2017). Quantification of biodiesel and adulteration with vegetable oils in diesel/biodiesel blends using portable near-infrared spectrometer. *Fuel (Guildford)*, *160*(1), 57 - 63. <https://doi-org.prox.lib.ncsu.edu/10.1016/j.fuel.2015.07.067>
- McLellan, T. M., Martin, M. E., Aber, J. D., Melillo, J. M., Nadelhoffer, K. J., & Dewey, B. (1991). Comparison of wet chemistry and near infrared reflectance measurements of carbon-fraction chemistry and nitrogen concentration of forest foliage. *Canadian Journal Of Forest Research*, *21*(11), 1689 - 1693. <https://doi-org.prox.lib.ncsu.edu/10.1139/x91-233>
- Miao, T., Sihota, N., Pfeifer, F., McDaniel, C., & De Gea Neves, M. A. (2023). Rapid Determination of the Total Petroleum Hydrocarbon Content of Soils by Handheld Fourier Transform Near-Infrared Spectroscopy. *Analytical Chemistry*, *95*(17), 6888 - 6893. <https://doi.org/10.1021/acs.analchem.3c00021?urlappend=%3Fref%3DPDF&jav=VoR&rel=cite-as>
- Netto, J. M., Honorato, F. A., Celso, P. G., & Pimentel, M. F. (2023). Authenticity of almond flour using handheld near infrared instruments and one class classifiers. *Food Composition and Analysis*, *115*(1), 104981. <https://doi-org.prox.lib.ncsu.edu/10.1016/j.jfca.2022.104981>
- Norris, K. N., Barnes, R. F., Moore, J. E., & Shenk, J. S. (1976). Predicting Forage Quality by Infrared Reflectance Spectroscopy. *Journal of Animal Science*, *43*(4), 889-897. <https://doi.org/10.2527/jas1976.434889x>

- Perez, I. M., Cruz-Tirado, L. J., Badaro, A. T., de Oliveira, M. M., & Barbin, D. F. (2019). Present and future of portable/handheld near-infrared spectroscopy in chicken meat industry. *NIR News*, *30*(5-6), 26-29. <https://doi.org/10.1177/0960336019861476>
- Pu, Y., Pérez-Marín, D., O'Shea, N., & Garrido-Varo, A. (2021). Recent Advances in Portable and Handheld NIR Spectrometers and Applications in Milk, Cheese and Dairy Powders. *Foods*, *10*(10), 2377. <https://doi.org/10.3390/foods10102377>
- Ramadevi, P., Kamalakannan, R., Suraj, G. P., Hedge, D. V., & Varghese, M. (2022). Evaluation of Kraft pulp yield and syringyl/guaiacyl ratio from standing trees (*Eucalyptus camaldulensis*, *E. urophylla*, *Leucaena leucocephala* and *Casuarina junghuhniana*) using portable near infrared spectroscopy. *Journal Of Near Infrared Spectroscopy*, *30*(1), 40 - 47. <https://doi-org.prox.lib.ncsu.edu/10.1177/09670335211063634>
- Raymond, C. A., & Schimleck, L. R. (2002). Development of near infrared reflectance analysis calibrations for estimating genetic parameters for cellulose content in *Eucalyptus globulus*. *Canadian Journal Of Forest Research*, *32*(1), 170 - 176. <https://www.proquest.com/docview/230518523?parentSessionId=pKWajpA0SdiL6Sjj4R2Zs2KSk5ydk%2B19P%2BmjVG V2xMI%3D&accountid=12725&sourcetype=Scholarly%20Journals>
- Sapienza, D., Berzaghi, P., Martin, N., Taysom, D., Owens, F., Mahanna, B., Sevenich, D., & Allen, R. (2008). NIRS WHITE PAPER. Near Infrared Spectroscopy for forage and feed testing. https://www.foragelab.com/Media/nirs_white_paper.pdf
- Saranwong, S., & Kawano, S. (2005). Commercial Portable NIR Instruments in Japan. *Nir News*, *16*(7), 27-30. <https://doi.org/10.1255/nirn.859>
- Silva, L. C., Folli, G. S., Santos, L. P., Barras, I. H., Oliveira, B. G., Borghi, F. T., dos Santos, F. D., Filgueiras, P. R. & Romão, W. (2020). Quantification of beef, pork, and chicken in ground meat using a portable NIR spectrometer. *Vibrational Spectroscopy*, *111*(1), 103158. <https://doi-org.prox.lib.ncsu.edu/10.1016/j.vibspec.2020.103158>

- Ting, D. F., Pui, L. P., & Solihin, M. I. (2020). Feasibility of fraud detection in milk powder using a handheld near-infrared spectroscopy. Proceedings of the 7th international conference on electronic devices, systems and applications. <https://pubs-aip-org.prox.lib.ncsu.edu/aip/acp/article/2306/1/020017/749350/Feasibility-of-fraud-detection-in-milk-powder>
- Vasquez, B., Garcia, B., Garcia, A., & Perez, M. E. (1995). Estimation of mineral content in natural grasslands by near infrared reflectance spectroscopy. *Communications In Soil Science And Plant Analysis*, 26(9-10), 1383 - 1396. <https://doi-org.prox.lib.ncsu.edu/10.1080/00103629509369379>
- Warburton, P., Brawner, J., & Meder, R. (2014). Technical Note: Handheld near Infrared Spectroscopy for the Prediction of Leaf Physiological Status in Tree Seedlings. *Journal Of Near Infrared Spectroscopy*, 22(6), 433 - 438. <https://doi-org.prox.lib.ncsu.edu/10.1255/jnirs.1137>
- Whittier, W. A., Hodge, G. R., Lopez, J., Saravitz, C., & Acosta, J. J. (2021). Near Infrared Spectroscopy Studies of Teak Grown Under Varying Levels of Nitrogen, Phosphorus and Potassium. *Journal Of Near Infrared Spectroscopy*, 29(5), 301-310. <https://doi-org.prox.lib.ncsu.edu/10.1177/09670335211025649>
- Wilson, N. D., Watt, R. A., & Moffat, A. C. (2010). A near-infrared method for the assay of cineole in eucalyptus oil as an alternative to the official BP method. *Journal of Pharmancy and Pharmacology*, 53(1), 95-102. <https://doi-org.prox.lib.ncsu.edu/10.1211/0022357011775064>
- Yan, H., De Gea Neves, M., Noda, I., Guedes, G. M., Silva Ferreira, A. C., Pfeifer, F., Chen, X., & Siesler, H. W. (2023). Handheld Near-Infrared Spectroscopy: State-of-the-Art Instrumentation and Applications in Material Identification, Food Authentication, and Environmental Investigations. *Chemosensors*, 11(5), 272. <https://doi.org/10.3390/chemosensors11050272>

CHAPTER 2

Prediction of Foliar Nutrient Concentration in Eucalypt Seedlings Using Portable Near-Infrared Spectroscopy

ABSTRACT

This study aimed to develop NIR models to predict concentration of nutrients in freshly removed leaves of nursery-grown eucalypt seedlings. The nutrients (a total of 13) included macronutrients such as nitrogen, phosphorus, potassium, calcium, magnesium, and sulfur, as well as micronutrients like iron, boron, copper, chlorine, manganese, molybdenum, and zinc. The eucalypt seedlings were grown hydroponically in a greenhouse and were exposed to varying nitrogen, phosphorus, and potassium levels. Near-infrared spectroscopy was applied to foliar samples from 100 seedlings, with model calibration and validation supported by conventional laboratory nutrient analyses. Two portable NIR spectrometers were used and compared for accuracy: the DLP NIRscan Nano EVM by Texas Instruments and the Microphazir by Thermo Fisher Scientific. Initial NIR readings were taken distinct leaf positions within each intact seedling, first at 15 days post-treatments, and a second at 30 days. Following spectral acquisition, sampled leaves and remaining seedling foliage were collected, labeled, and submitted for standard laboratory foliar nutrient analysis.

The Microphazir demonstrated an advantage in comparison to the DLP Nano in producing moderately accurate to highly accurate nitrogen prediction models by analyzing spectra obtained from different segments of the plant foliage, especially 15 days after treatments. This advantage was amplified when spectral information from multiple leaf pairs was aggregated. Similarly, phosphorus models benefited from spectral aggregation across multiple leaf pairs when using the Microphazir, although predictive performance for potassium remained consistently poor. In contrast, the DLP Nano produced moderate to moderately high nitrogen models at 15 days post-treatment and moderate models at 30 days, with performance improving as spectra from additional leaf pairs were combined. However, models developed with this device for phosphorus and potassium were generally of lesser accuracy, ranging from weak to moderately low across datasets and growth stages. Both spectrometers showed potential for predicting selected micronutrients when whole-plant spectral data were used. Model performance for sulfur, calcium, magnesium, copper, and N:S ratio concentration ranged from moderately low to moderate, especially 15 days

after treatment applications using the Microphazir. In comparison, the DLP Nano demonstrated moderate performance only for sulfur at this early stage.

Collectively, these results indicate that the Microphazir is particularly well suited for assessing nitrogen status across developmental stages and, when whole-plant spectra are used, demonstrates moderate potential for predicting sulfur, calcium, magnesium, copper, and, to a limited extent, phosphorus during early growth. The DLP Nano showed acceptable predictive performance primarily for nitrogen at early developmental stages, but exhibited generally low predictive accuracy for phosphorus, potassium, and most micronutrients.

2.1 Introduction

Camcore (based at North Carolina State University in the USA) is an international gene conservation and tree breeding program at North Carolina State University (NCSU) that works with pine and eucalypt species. Camcore has been working with Near Infrared (NIR) models for prediction of wood chemical and physical traits for more than 20 years and has developed global (multi-species) NIR models for wood characterization of pines (Hodge & Woodbridge, 2004). Recently, Camcore has been working on global NIR models for eucalypt species, including *E. urophylla*, *E. dunnii*, *E. globulus*, and *E. nitens* (Hodge et al., 2018) allowing for the estimation of sugars, lignins, and S/G ratio, and has also used NIR to differentiate between pure and hybrid species and to confirm the identity of eucalyptus clones in the nursery. Camcore used NIR spectroscopy to create foliage nutrient concentration models for nursery-grown teak (*Tectona grandis*) seedlings with benchtop and portable NIR (Whittier et al., 2021).

A seedling is a young plant grown from a seed, but the term is also commonly used to refer to various types of nursery stock, including transplants, rooted cuttings, and emblings. Seedlings are grown in fields or controlled environments, in bareroot nurseries or in containers, with the objective of outplanting in the field (Landis, 2009). Seedling nutrition plays a fundamental role in ensuring the successful establishment, growth, and long-term survival of forest plant material (Grossnickle & MacDonald, 2018). By understanding nutrient requirements and deficiencies, growers can optimize fertilization strategies, leading to improved nursery health and productivity (Ge et al., 2014)

Plant tissue analysis helps identify nutrient-related issues like deficiencies, toxicities, or imbalances before visual symptoms appear. This analysis is crucial for research and crop production, providing insights into nutrient status and guiding fertilizer management decisions, and evaluates the effectiveness of fertility programs (Bhandari, 2018).

Conventional leaf tissue laboratory analysis is considered the most accurate method for determining nutrient concentration; these methods are well established and can quantify a wide range of nutrients and other analytes with high accuracy. This laboratory analysis involves destructive chemical or biochemical assays to directly measure the nutrient concentration of a sample. It tends to be costly, as it requires a multi-step, labor-intensive process with an extensive

amount of sample preparation, followed by complex procedures carried out by skilled personnel using specialized equipment. As a result, conventional lab analysis can be time-consuming, and this may be a problem in a nursery setting when answers are needed within a short window of time.

Spectroscopy has played a crucial role in plant tissue laboratory analysis, enabling precise measurement of nutrients. Techniques like Atomic Absorption Spectrometry (AAS), Inductively Coupled Plasma Atomic Emission Spectrometry (ICP-AES), and Inductively Coupled Plasma Mass Spectrometry (ICP-MS) are used to quantify nitrogen, phosphorus, and potassium. Variants like Flame Atomic Absorption Spectrometry (FAAS) and Graphite-Furnace Atomic Absorption Spectrometry (GF-AAS) offer increased sensitivity for trace elements. Inductively Coupled Plasma Optical Emission Spectrometry (ICP-OES) uses plasma to measure emitted light wavelengths. X-ray Fluorescence Spectrometry determines elemental composition, while Spectrophotometry quantifies specific compounds (Bhandari, 2018).

The ability to monitor nitrogen (N), phosphorus (P), potassium (K) status through remote sensing techniques is important for understanding plant nutrition and improving crop productivity (Pimstein et al., 2011). Macronutrients N, P, and K are essential for plant growth, but their optimal levels are crucial, as both deficiency and excess can adversely affect crop yield and quality. NIR spectroscopy is used in plant tissue analysis to estimate the concentrations of important biochemical components like N, P, and K (Zhai et al., 2013).

The use of NIR spectroscopy to evaluate foliar nutrient levels provides rapid, cost-effective, and potentially non-destructive results. The application of this technique to predict nutrient levels in the nursery would be an invaluable tool in allowing the nursery to address specific deficiencies, thereby minimizing expenses associated with excessive or inadequate fertilization (Whittier et al., 2021).

Near-infrared reflectance spectroscopy utilizes NIR light interacting with organic molecular bonds in a substance, causing absorption due to changes in molecular states (Zhang et al., 2022). This technique relies on the principle that different molecular structures absorb and reflect light at specific wavelengths in the near-infrared region of the electromagnetic spectrum, allowing for the identification and quantification of various compounds present in a sample. By

analyzing the patterns of light absorption and reflection, NIR spectroscopy can be used for qualitative and quantitative analysis of a wide range of materials, including agricultural products, food industry, health sector and chemicals (Gullifa et al., 2023).

A NIR spectrometer is an analytical scientific instrument used to analyze and study the properties of light over a specific range of the electromagnetic spectrum (Beć et al., 2021). It works by splitting light into different wavelengths, allowing scientists to identify and measure its components. A NIR spectrometer is designed specifically for analyzing NIR light, providing insights into the molecular structure and composition of samples (Leary et al., 2021). The main parts of a NIR spectrometer system are generally a light source, beam splitter system, reflector, sample chamber/detector inlet valve, diffuse reflection detector, transmission detector, control and data processing system (Cen & He, 2007).

Traditional NIR devices have a benchtop-type configuration and require samples to be carried to the equipment (Beć et al., 2021). Benchtop devices have been mainly used by trained personnel working in commercial and research laboratories and are typically relatively expensive (Acosta et al., 2020). Over the past two decades, an increased interest in NIR spectroscopy has resulted in the creation of portable spectrometers for a range of applications. A portable spectrometer is a valuable analytical tool for quick and accurate sample analysis, whether in the laboratory or field (Leary et al., 2021).

Unlike conventional laboratory-based devices, portable spectrometers are small and lightweight instruments that can be easily transported and run on battery power for a reasonable time frame. The most apparent distinctives are narrower spectral regions and/or lower spectral resolution with which the portable devices operate (Beć et al., 2021). However, these portable devices can provide accurate measurements and generate NIR reflectance data at a given wavelength with precision comparable to those produced by laboratory-grade spectrometers (Sorak et al., 2012).

Portable spectrometers provide the benefit of conducting on-site analysis, enabling immediate decision-making in laboratory, industrial and field environments (Perez et al., 2019). This technology offers benefits such as non-destructive analysis, providing instant insights that can be linked to subsequent analyses on the same sample. Combining NIR spectroscopy with

chemometrics allows for focused and broad analyses through prediction models based on statistical evaluation. Results can be shared qualitatively or quantitatively, making them accessible to experts and non-experts (Gullifa et al., 2023).

NIR spectroscopy applications are assumed to provide reliable results when their prediction models are developed using accurate biochemical data, hence, they are considered spectrochemical models. Consequently, the accuracy of predictions for response values obtained from NIR spectra depends on the ability to generate appropriate NIR models (Acosta et al., 2020). In addition, the accuracy of the technique depends on factors such as device specifications, algorithms used in the analysis, and range of nutrient levels in the samples (Pimstein et al., 2011).

2.2 Objectives

This research addresses the following objectives:

- To evaluate the applicability of near-infrared spectroscopy (NIRS) for measuring nutrient concentration in freshly removed foliage of nursery-grown eucalypt seedlings.
- To establish useful protocols for acquiring high-quality NIR spectra from freshly harvested eucalypt foliage grown under varying nutrient regimes, and to develop predictive models for predicting macronutrient and micronutrient concentrations.
- To assess the performance of portable NIR spectrometers, specifically the DLP NIRscan Nano EVM (Texas Instruments) and the Microhazir (Thermo Fisher Scientific), as practical tools for acquiring NIR spectra and evaluating foliar nutrient status under operational nursery conditions.

2.3 Materials and Methods

2.3.1 Plant material and nutrient regimes

Three hundred 11.5-cm square vacuum pots, each containing 1 L of washed and steam-sterilized silica river sand, were arranged in a greenhouse on the NC State University campus. Approximately three seeds of the hybrid *Eucalyptus urophylla* × *E. grandis* were sown in each pot at a depth of 0.5 cm. The pots were monitored daily and watered using an automated mist system, and no fertilizer was applied during germination. The first germinants emerged on day six, and by day ten, all pots contained at least one seedling.

All 300 pots were initially treated with a Complete Hoagland's nutrient solution to promote seedling health and ensure uniform nutritional status prior to treatment initiation. Hoagland's nutrient solution (HNS), originally developed for water culture systems, is widely used in controlled plant nutrition studies due to its well-defined and reproducible composition. It supplies essential macro- and micronutrients (Table 2.1) at concentrations that support healthy physiological development while allowing precise manipulation of individual nutrient levels, making it a standard framework for evaluating nutrient sufficiency and deficiency responses across plant species (Hoagland & Arnon, 1950). In this study, its use provided a consistent and controlled nutritional baseline for subsequent experimental regimes. The nutrient solution was applied twice daily for 50 days, with 25 mL administered per pot in the early morning and an additional 25 mL in the afternoon. During this period, regular irrigation was provided by an automated system programmed to operate for 10–20 seconds every hour between 7:00 a.m. and 5:00 p.m. Five days after the initial fertilization, seedlings were thinned to retain one plant per pot.

Following seedling grading, 200 pots were selected and randomized to begin nutrient regimes. The experiment consisted of five treatment groups using modified HNS prepared in the laboratory. Nutrient solutions were formulated from reagent-grade stock solutions containing potassium nitrate (KNO_3), calcium nitrate tetrahydrate [$\text{Ca}(\text{NO}_3)_2 \cdot 4\text{H}_2\text{O}$], potassium dihydrogen phosphate (KH_2PO_4), magnesium sulfate heptahydrate ($\text{MgSO}_4 \cdot 7\text{H}_2\text{O}$), iron diethylenetriamine-pentaacetic acid (FeDTPA), manganese chloride tetrahydrate ($\text{MnCl}_2 \cdot 4\text{H}_2\text{O}$), zinc chloride (ZnCl_2), cupric chloride dihydrate ($\text{CuCl}_2 \cdot 2\text{H}_2\text{O}$), boric acid (H_3BO_3), and sodium molybdate dihydrate ($\text{Na}_2\text{MoO}_4 \cdot 2\text{H}_2\text{O}$). Stock solutions were diluted with tap water with an electrical conductivity of

0.24 mS cm⁻¹, and pH was adjusted to 6.0 using sodium hydroxide (NaOH). (Barnes et al., 2012).

Table 2.1 Composition of nutrient stock solutions, application volumes, and resulting concentrations of nitrate-nitrogen (NO₃-N), ammonium-nitrogen (NH₄-N), phosphorus (P), and potassium (K) in the complete Hoagland's nutrient solution.

Composition (Formula)	Stock Solution	mL used per 100 L	PPM			
			NO ₃ -N	NH ₄ -N	P	K
Ca(NO ₃) ₂ ·4H ₂ O	35.42 g/100 mL	185	77.74	—	—	—
KNO ₃	12.85 g/100 mL	276.4	49.22	—	—	137.38
MgSO ₄ ·7H ₂ O	29.58 g/100 mL	171.4	—	—	—	—
K ₂ HPO ₄ ·3H ₂ O	20.00 g/100 mL	0	—	—	—	—
KH ₂ PO ₄	8.17 g/100 mL	53.8	—	—	10.00	12.62
K ₂ SO ₄	10.00 g/100 mL	0	—	—	—	—
(NH ₄) ₂ HPO ₄	11.50 g/100 mL	0	—	—	—	—
NH ₄ NO ₃	17.15 g/100 mL	33.3	10.00	10.00	—	—
(NH ₄) ₂ SO ₄	13.21 g/100 mL	0	—	—	—	—
Mg(NO ₃) ₂	25.64 g/100 mL	10.87	3.05	—	—	—
CaSO ₄ ·2H ₂ O	17.22 g/100 mL	0	—	—	—	—
KCl	7.46 g/100 mL	0	—	—	—	—
Fe-DTPA	40 g/L	100	—	—	—	—
MnCl ₂ ·4H ₂ O	3.96 g/L	90	—	—	—	—
ZnCl ₂ ·7H ₂ O	2.73 g/L	15	—	—	—	—
CuCl ₂ ·2H ₂ O	3.41 g/L	15	—	—	—	—
H ₃ BO ₃	6.18 g/L	45	—	—	—	—
Na ₂ MoO ₄ ·2H ₂ O	0.24 g/L	10	—	—	—	—
		Total	140.00	10.00	10.00	150.00
		Total N	150.00			

Treatment 1 received the complete HNS used during the establishment phase. Treatment 2 received a modified solution with nitrogen (N), phosphorus (P), and potassium (K) reduced to 50% of full strength. Treatments 3, 4, and 5 received solutions in which N, P, and K were reduced to 10% of full strength, respectively, while all other nutrients were maintained at full concentration. Each seedling received 25 mL of nutrient solution per pot in the morning and an additional 25 mL in the afternoon, with supplemental watering provided by the automated sprinkler system as described above.

2.3.2 Portable Spectrometers

Two portable spectrometers with differing spectral coverage and resolution were evaluated in this study to assess their suitability for foliar nutrient analysis (Table 2.2). The instruments differ in optical design, wavelength interval, and spectral range, factors that influence their ability to capture absorption features relevant to macronutrient and micronutrient prediction in plant tissues.

Table 2.2 Near infrared devices used to predict macronutrients and micronutrient levels in intact and processed samples of eucalypt leaves

Device	Type	Spectral Range	Wavelength Interval	No. of Wavelengths
Microphazir (Thermo Fisher Scientific)	Handheld	1600–2400 nm	8 nm	100
DLP Nano EVM (Texas Instruments)	Handheld	900–1700 nm	5 nm	160

Evaluating instruments operating in distinct regions of the near-infrared spectrum allowed assessment of how spectral range and resolution influence predictive performance for foliar nutrient concentrations in nursery-grown eucalypt leaves.

2.3.3 Spectra Acquisition and Database Creation

In this phase of the experiment, each treatment group was subdivided into two sets, each comprising 20 randomly selected seedlings. NIR spectra were acquired two times:

- The first set of seedlings **15 days** post treatment and second set **30 days** post treatment.

At each measurement time, NIR spectra were acquired using the **two** portable spectrometers:

- The **Microphazir** by Thermo Fisher Scientific and the **DLP NIRscan Nano EVM** by Texas Instruments.

The spectra were collected from distinct positions within each intact seedling in preparation for acquiring spectral data, the first four pairs of leaves attached to the stem were removed from each seedling, beginning with the topmost pair with a width greater than 15 mm.

- The eight removed leaves were then placed on a pre-labeled tray (**1a, 2b, 3c, 4d, 5e, 6f, 7g, and 8h**) (Figure 2.1A, 2.1B, and 2.1C).

Spectra were collected on each of the eight individual leaves using handheld spectrometers positioned between the leaf margin and midvein directly on the upper leaf blade over healthy tissue (Figure 2.1D), with a flat piece of black plastic as a background. (Figure 2.2).

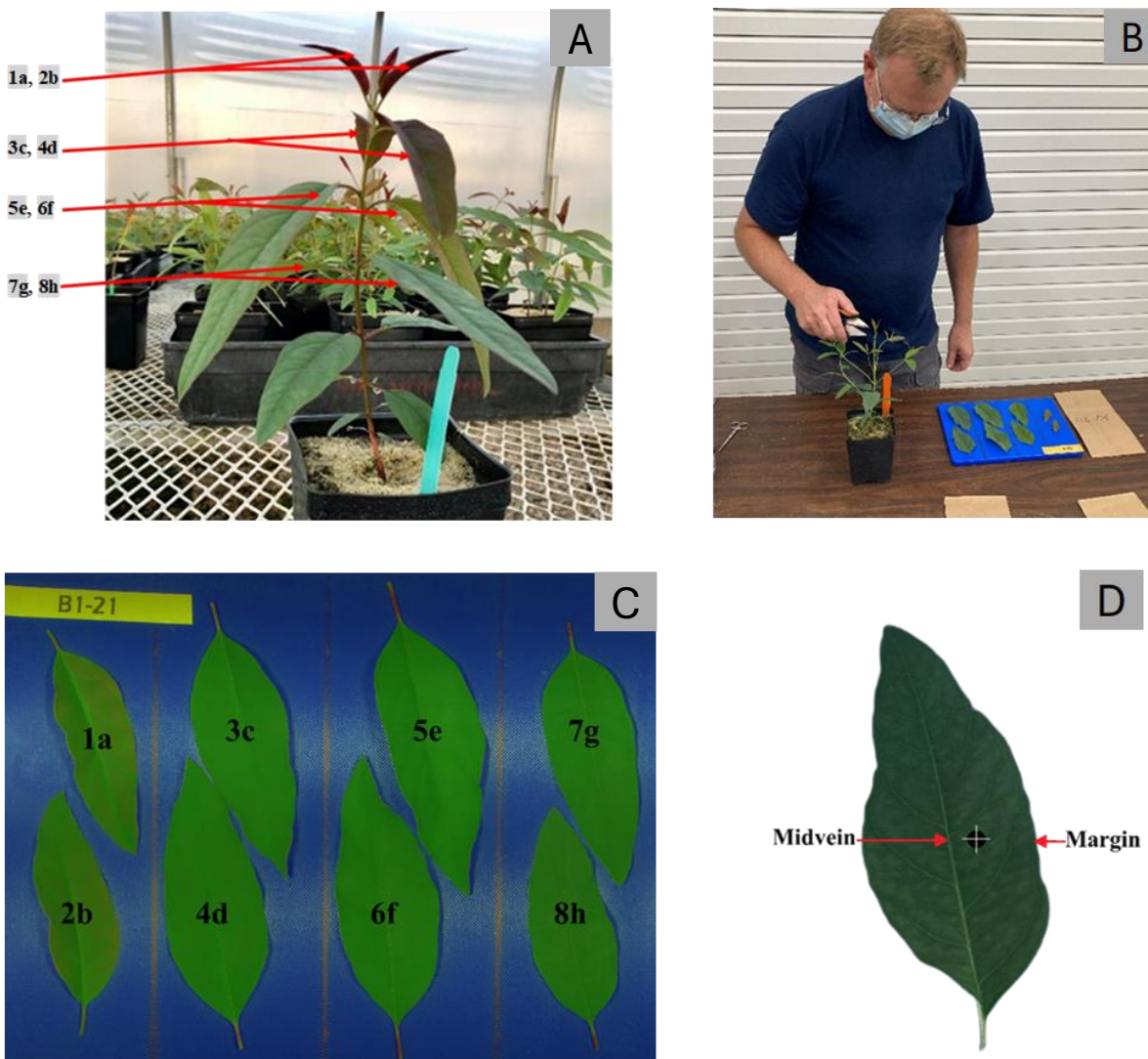


Figure 2.1 Leaf selection and preparation workflow for NIR spectra data acquisition. **A.** The top four leaf-pairs were selected from each seedling. **B.** The eight leaves were removed for analysis. **C.** Leaves were arranged on a pre-labeled tray to maintain sample identity and position. **D.** Spectral measurements were collected with the spectrometer sensor positioned between the leaf margin and the midvein to ensure consistent sampling.

After acquiring the spectra of each growth stage, the eight leaves were placed into separate craft paper bags along with the remaining seedling foliage. Each paper bag was labeled and submitted to the North Carolina Department of Agriculture & Consumer Services (NCDA&CS) for standard nutrient laboratory analysis.



Figure 2.2 NIR spectral acquiring of eucalypt leaves using portable spectrometers. **Top:** Spectral measurements collected with the Microphazir scanning station. **Bottom:** Spectral measurements collected with the DLP NIRscan Nano EVM scanning station.

Total N was determined by oxygen combustion gas chromatography with subsequent quantification by thermal conductivity detector. Total concentrations of P, K, Ca, Mg, S, Fe, Mn, Zn, Cu, B, Na, Cl, and Al were determined with Inductively Coupled Plasma-Optical Emission Spectrometry. N, P, K, Ca, Mg, S, and Na are reported in percentage (%), and all other elements (Fe, Mn, Zn, Cu, B, Al, and ratios of N:S, N:K, Fe:Mn) are reported in parts per million (ppm - mg kg⁻¹). All results are reported on a dry weight basis. Detailed results of the standard laboratory foliar nutrient analyses for all samples, organized by nutrient regime and growth stage, are provided in Appendix B (*a-j*) of this thesis.

2.3.4 NIR Model Dataset Creation

NIR model development was conducted in two sequential phases. Phase 1 focused on the macronutrients N, P, and K and was designed to evaluate the influence of leaf position and sample aggregation strategy on model performance. Phase 2 extended the analysis to additional nutrients and nutrient ratios using the most robust leaf sample dataset identified in Phase 1.

Phase 1: N, P, and K

Models were developed using spectra collected from individual leaves sampled from different positions across the seedling (Figure 2.1A–C). These individual leaf spectra were subsequently combined to generate multiple datasets representing different levels of leaf-pair aggregation. In total, ten datasets were constructed:

- Four datasets consisting of average spectra for each individual leaf pair (1a, 2b = **P1**; 3c, 4d = **P2**; 5e, 6f = **P3**; 7g, 8h = **P4**) (Figure 2.3),
- Three datasets consisting of averaged spectra combining two consecutive leaf pairs (P1, P2 = **G12**; P2, P3 = **G23**; P3, P4 = **G34**),
- Two datasets consisting of averaged spectra combining three consecutive leaf pairs (P1, P2, P3 = **G123**; P2, P3, P4 = **G234**),
- One dataset consisting of averaged spectra combining all four leaf pairs (P1, P2, P3, P4 = **G1234**, hereafter referred to as the whole-plant (**WP**) dataset).

Phase 2: Ca, Mg, S, Na, Fe, Mn, Zn, Cu, B, Al, and N:S, N:K, and Fe:Mn ratios

Based on the results of Phase 1, the whole-plant (WP) dataset, which provided the most

robust and consistent performance across N, P, and K models, was selected for subsequent analyses. This dataset was used to develop prediction models for calcium, magnesium, sulfur, sodium, iron, manganese, zinc, copper, boron, and aluminum, as well as for nutrient ratios including N:S, N:K, and Fe:Mn.

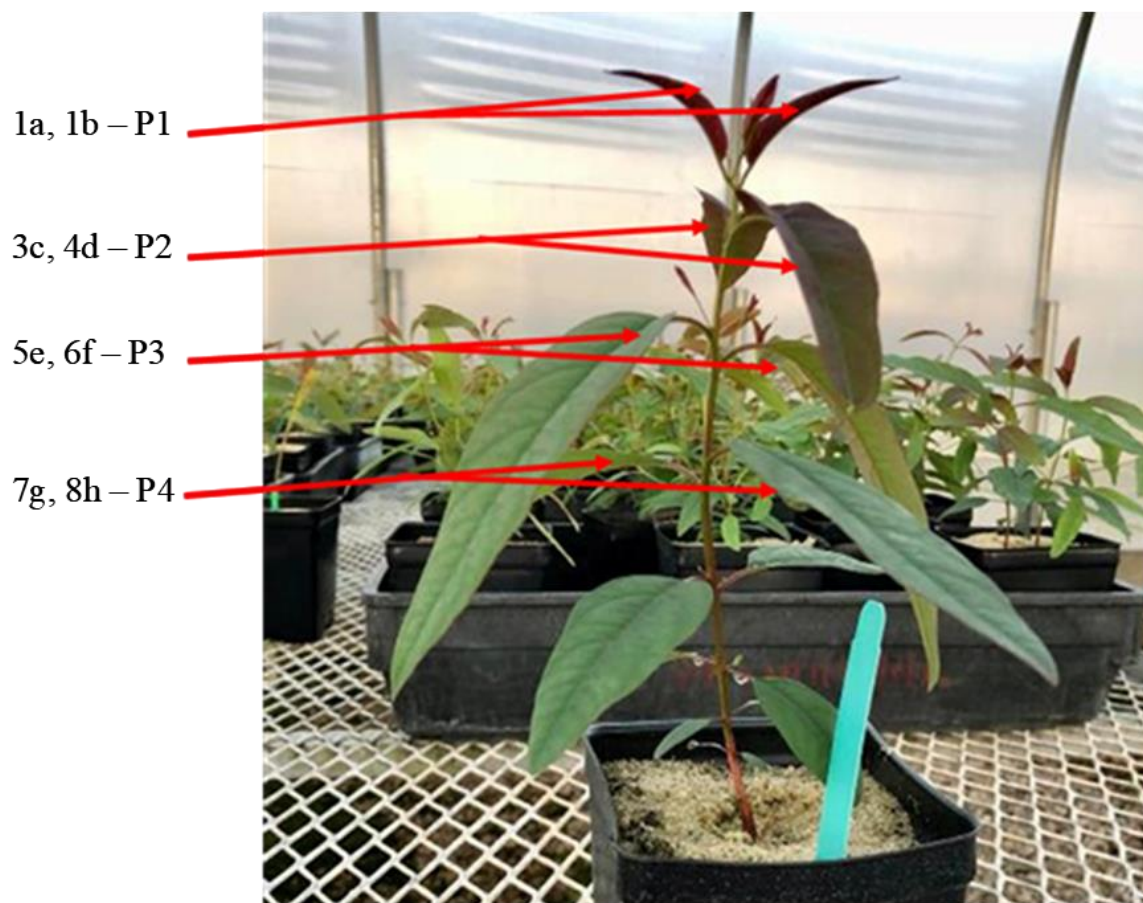


Figure 2.3 Spectral data were collected from eight individual leaf positions (1a–8h) across each seedling and subsequently combined into four paired-leaf datasets (P1–P4) for NIR model development.

2.3.5 NIR Model Development

NIR model development was conducted using a data analysis pipeline implemented in the R statistical environment, following the procedure described by Hodge et al. (2018) and Acosta et

al. (2020). This workflow has been successfully applied in previous studies for developing NIR calibration models to predict foliar nutrients in teak (Whittier et al., 2021), and chemical properties of wood (Hodge et al., 2018), as well as the nutritive value of tobacco and nutritional content of forage species (Castillo et al., 2023; Castillo et al., 2020; Bekewe et al., 2020; Acosta et al., 2020). The modeling procedure consisted of two main stages: spectral transformation and outlier detection, and model training, cross-validation, and selection.

2.3.5.1 Spectral Transformations and Outlier Detection

Raw NIR reflectance spectra ($\log 1/R$) were subjected to a series of mathematical transformations to reduce the effects of light scattering, baseline shifts, instrumental noise, wavelength-dependent scattering, and sample-related variability. Scatter-correction techniques included multiplicative scatter correction (MSC), standard normal variate (SNV), and detrend (DT). In addition, spectral derivative preprocessing was performed using Savitzky–Golay smoothing with second-order polynomial fitting and window sizes of five and seven points (SG5 and SG7). Combinations of scatter-correction and derivative preprocessing methods, including SNV + SG5, SNV + SG7, MSC + SG5, MSC + SG7, DT + SG5, and DT + SG7, were also evaluated to optimize spectral information. In total, fourteen spectral datasets were generated for each modeling scenario, consisting of the raw spectra and thirteen transformed datasets.

Outlier detection was performed using the Local Outlier Factor (LOF) algorithm (Breunig et al., 2000), which identifies observations that exhibit anomalous local density relative to their nearest neighbors. LOF scores were calculated using ten nearest neighbors, and samples with LOF values greater than 2 were removed from subsequent analyses, following the approach described by Castillo et al. (2023).

2.3.5.2 Model Training, Cross-Validation, and Selection

Outlier-filtered datasets were used to develop NIR calibration models relating spectral data to reference nutrient concentrations obtained through laboratory analyses. Partial least squares regression (PLSR) was applied using the *pls* package in R (Mevik & Wehrens, 2016). Model performance was evaluated using leave-one-out (LOO) cross-validation, in which each observation is sequentially excluded from the calibration set and used for validation (Diana & Tommasi, 2002).

For each transformation, model performance metrics included the coefficient of determination for calibration (R^2_{cal}) and cross-validation (R^2_{cv}), the root mean squared error of prediction for calibration ($RMSEP_{cal}$) and cross-validation ($RMSEP_{cv}$), and the explained variance of both predictor variables ($ExpVar X$) and response variables ($ExpVar Y$). These metrics were used to compare preprocessing strategies and select the most robust models for each nutrient (Table 2.3).

TABLE 2.3 Partial least squares (PLS) regression fit statistics for predicting Nitrogen concentration in eucalypt foliage using the whole-plant dataset and Microphazir spectra collected 15 days after treatment application. Models were evaluated across multiple spectral preprocessing methods. For this dataset and this element, the SG7 transformation provided the most robust performance based on cross-validation statistics.

Transformation	Components	Calibration		Cross Validation		ExpVar Y	ExpVar X
		R^2_{cal}	$RMSEP_{cal}$	R^2_{cv}	$RMSEP_{cv}$		
<i>SNV+SG7</i>	4	0.91	0.30	0.89	0.35	91.44	96.92
<i>SNV+SG5</i>	4	0.89	0.34	0.84	0.42	88.94	92.20
<i>SNV+DT</i>	4	0.89	0.35	0.86	0.39	88.53	96.81
<i>SNV</i>	5	0.90	0.32	0.88	0.36	90.29	98.18
<i>SG7*</i>	5	0.93	0.28	0.89	0.34	92.53	97.62
<i>SG5</i>	5	0.90	0.33	0.83	0.42	89.72	94.05
<i>NIR</i>	7	0.89	0.34	0.86	0.39	89.35	99.86
<i>MSC+SG7</i>	4	0.88	0.36	0.84	0.41	87.98	99.05
<i>MSC+SG5</i>	4	0.88	0.35	0.79	0.46	88.48	96.94
<i>MSC+DT</i>	4	0.89	0.35	0.86	0.39	88.53	96.81
<i>MSC</i>	5	0.87	0.37	0.82	0.43	87.12	99.88
<i>DT+SG7</i>	4	0.91	0.30	0.89	0.35	91.44	96.92
<i>DT+SG5</i>	4	0.89	0.34	0.84	0.42	88.94	92.20
<i>DT</i>	4	0.89	0.35	0.86	0.39	88.53	96.81

Nitrogen, Dataset G234

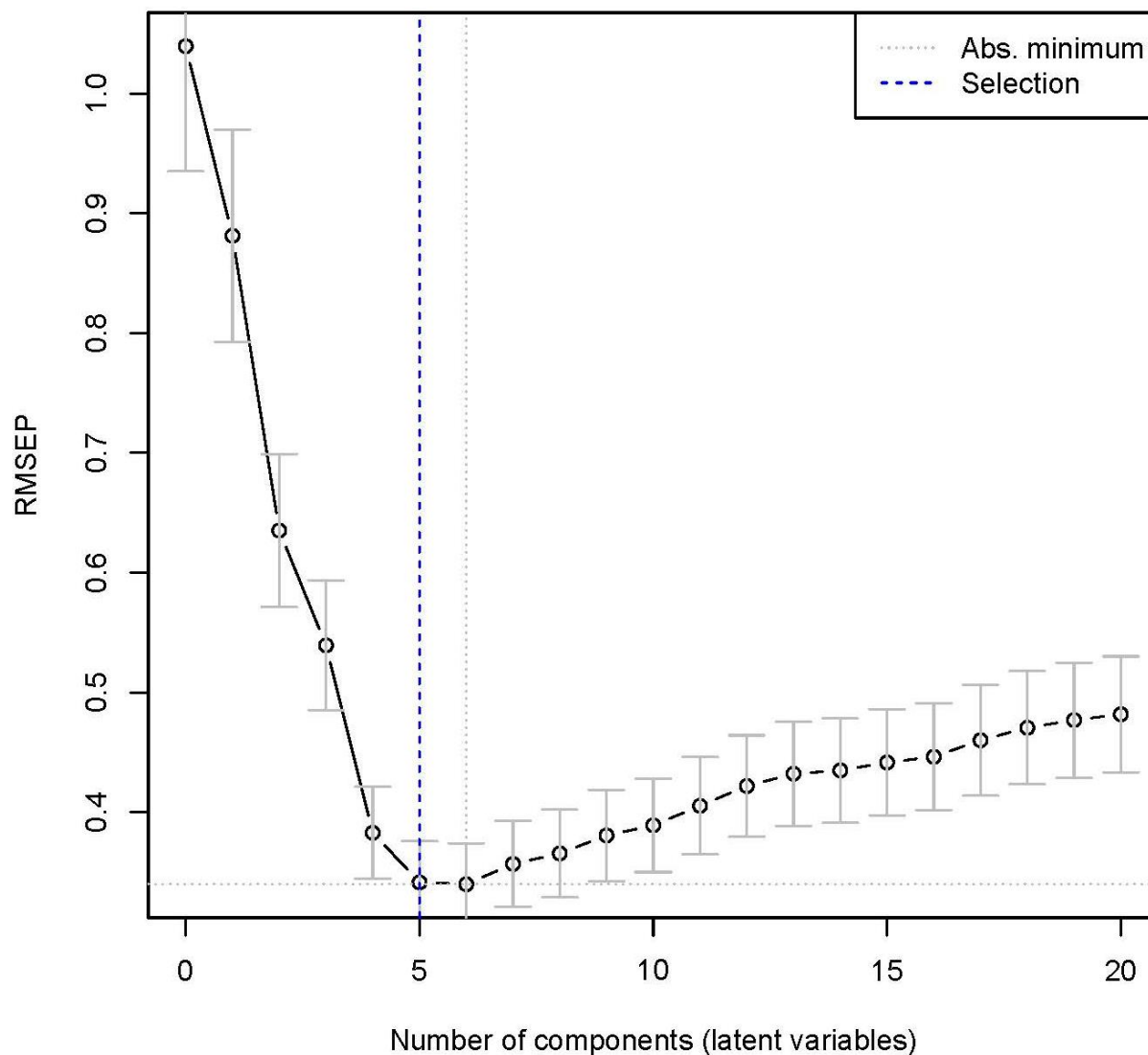


Figure 2.4 RMSEP as a function of the number of latent variables for the SG7-transformed nitrogen model developed using the G234 dataset. The dotted gray vertical line indicates the model with the absolute minimum RMSEP (six latent variables), while the dashed blue vertical line indicates the selected model based on the one-sigma criterion. Although the minimum RMSEP occurred at six components, a five-component model was selected because its RMSEP was within one standard error of the minimum, favoring a more parsimonious model without loss of predictive performance.

The R-based analysis pipeline identifies an “optimal” model using the one-sigma criterion, which balances predictive performance and model complexity by minimizing overfitting. This approach evaluates models with 1 to 20 latent variables and selects the model with the fewest factors whose root mean squared error of prediction from RMSEP_{cv} falls within one standard error of the minimum RMSEP (Castillo et al., 2023; Figure 2.4). Models selected using this criterion exhibited strong fit statistics.

As an example, for nitrogen models developed using NIR spectra acquired with the Microphazir device at 15 days post-treatment and the G234 dataset, all spectral transformations and raw NIR spectra were evaluated. The model selection algorithm identified the SG7 transformation with five latent factors as the optimal model, as it produced the highest cross-validated coefficient of determination ($R^2_{CV} = 0.89$) and the lowest RMSEP_{cv} (0.35) among the candidate models (Table 2.3).

In other modeling scenarios, alternative models may be selected for the same nutrient depending on tradeoffs among performance metrics and model complexity. For example, the selected five-factor SG7 model and the four-factor SNV+SG7 and DT+SG7 models exhibited identical R^2_{CV} values (0.89), with only a marginal increase in RMSEP_{cv} from 0.34 to 0.35 for the latter two models (Table 2.3). In applied settings, a model with fewer latent variables may be preferred as more robust for routine or operational use. However, the minor differences observed among the top-ranked models do not affect conclusions regarding spectrometer performance or the overall feasibility of developing reliable NIR models for nutrient prediction (Acosta et al., 2020).

2.4 Results

The performance of NIR predictive models varied as a function of the range in nutrient concentration observed, growth stage (15 vs. 30 days post-treatment), spectral acquisition position, and spectrometer type (Microphazir and DLP Nano). Complete calibration and cross-validation statistics for all evaluated PLS regression models are reported in Appendix A of this thesis..

2.4.1 Nutrient concentration variation observed

2.4.1.1 Concentration Variation by Regime

The results from the standard nutrient laboratory analysis indicate that the five nutrient regimes produced varying levels of nutrient concentration based on the quantity of nutrients added to each modified HNS. The box plots in Figure 2.5 illustrate the differences in foliar nitrogen, phosphorus, and potassium concentration across the different treatments and time points (15 and 30 days) for eucalypt foliage.

These results emphasize how nutrient availability in the solution directly affects foliar nutrient concentration. This is particularly evident in the treatments with reduced nutrient concentration (10% N, 10% P, and 10% K), where foliar nutrient concentration remained consistently low.

2.4.1.2 Concentration Variation by Nutrient

Table 2.4 provides a detailed comparison of the observed foliar nutrient concentration dynamics, highlighting a notable decline trend of nutrient concentration over time and reduced variability as the treatments progress.

Nitrogen, phosphorus, and potassium all exhibit a progressive reduction in value ranges from 15 to 30 days post-treatment, reflecting a trend toward more uniform nutrient concentrations over time, suggesting a natural stabilization of nutrient levels, which impacts their model accuracy at later growth stages.

For nitrogen, the range narrows significantly from 1.16–5.08% at 15 days to 0.84–3.37% at 30 days, with the two-standard deviation interval (2σ) shrinking from 1.23–5.36% to 0.79–2.91%, indicating increased uniformity and concentration within a narrower range.

Phosphorus follows a similar pattern, with its range decreasing from 0.08–0.37% at 15 days to 0.05–0.29% at 30 days. The 2σ interval tightens from 0.10–0.35% to 0.02–0.26%, confirming a shift toward lower phosphorus levels over time.

For potassium, the range contracts from 0.97–2.43% at 15 days to 0.49–2.19% at 30 days, while 2σ narrows from 0.95–2.26% to 0.52–2.14%. Despite minor variability in outliers, potassium concentrations also stabilize within a more consistent range as the plants develop.

The analysis of other nutrients, such as Calcium, Magnesium, and Sulfur, shows consistent trends of reduced variability and narrower ranges over time. For example, Calcium's interval within 2σ narrows from 0.72–1.68% to 0.66–1.40%. Magnesium and Sulfur follow similar patterns, demonstrating lower variability and more predictable nutrient concentrations. Trace nutrients, such as Iron, Manganese, Zinc, Copper, and Boron, show significant reductions in maximum values and corresponding 2σ values, signaling reduced variability and tighter ranges in the 30-day analysis. For instance, Iron's interval within 2σ shifts from 54.63–128.51 mg kg⁻¹ to 29.53–118.55 mg kg⁻¹, indicating stabilization as the growing period progresses.

The standard nutrient analysis at 30-day after-treatments consistently reveals narrower ranges, lower maximum values, and reduced variability for most nutrients compared to the analysis at 15-day.

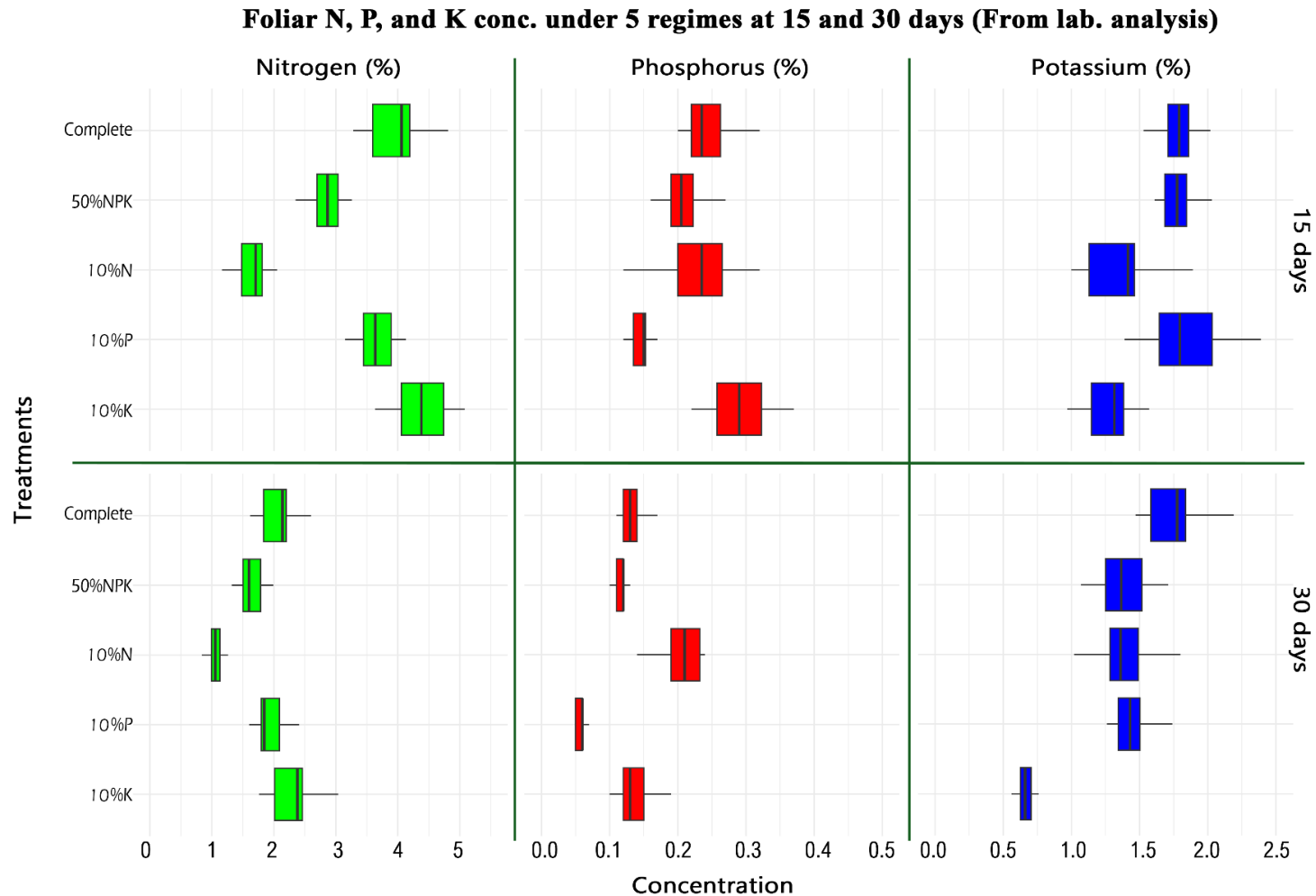


Figure 2.5 Box plots illustrate the variations in nitrogen, phosphorus, and potassium percentages in eucalypt seedling foliage collected at 15 and 30 days. **Complete** = Complete HNS. **50%NPK** = Modified HNS with fifty percent nitrogen, phosphorus, and potassium. **10%N** = Modified HNS with ten percent nitrogen. **10%P** = Modified HNS with ten percent phosphorus. **10%K** = Modified HNS ten percent potassium.

Table 2.4 Summary statistics of observed foliar nutrient concentrations in eucalypt seedlings at 15 and 30 days post-treatment for samples used in NIR model development.

Nutrient	Unit	15-day Standard Nutrient Analysis					30-day Standard Nutrient Analysis				
		Min	Max	Mean	2 σ	Range within 2 σ	Min	Max	Mean	2 σ	Range within 2 σ
Nitrogen	%	1.16	5.08	3.30	2.07	(1.23, 5.36)	0.84	3.37	1.85	1.06	(0.79, 2.91)
Phosphorus	%	0.08	0.37	0.22	0.12	(0.10, 0.35)	0.05	0.29	0.14	0.12	(0.02, 0.26)
Potassium	%	0.97	2.43	1.61	0.66	(0.95, 2.26)	0.49	2.19	1.33	0.81	(0.52, 2.14)
Calcium	%	0.43	1.69	1.20	0.48	(0.72, 1.68)	0.63	1.64	1.03	0.37	(0.66, 1.4)
Magnesium	%	0.2	0.5	0.39	0.12	(0.27, 0.51)	0.23	0.53	0.33	0.11	(0.21, 0.44)
Sulfur	%	0.11	0.3	0.22	0.09	(0.13, 0.31)	0.09	0.27	0.16	0.08	(0.09, 0.24)
Iron	mg kg ⁻¹	54.2	149	91.57	36.94	(54.63, 128.51)	36	162	74.04	44.51	(29.53, 118.55)
Manganese	mg kg ⁻¹	92.7	275	178.55	76.27	(102.28, 254.81)	67.4	267	139.27	94.49	(44.78, 233.77)
Zinc	mg kg ⁻¹	19.8	53.4	33.17	11.84	(21.33, 45.01)	17.6	48.2	27.25	10.59	(16.67, 37.84)
Copper	mg kg ⁻¹	6.21	26.5	14.93	9.40	(5.53, 24.32)	3.7	18.1	9.98	5.97	(4.01, 15.96)
Boron	mg kg ⁻¹	17.9	48.3	28.00	11.50	(16.49, 39.50)	18.9	44.2	28.92	10.63	(18.29, 39.55)
Sodium	mg kg ⁻¹	0.15	0.62	0.35	0.19	(0.16, 0.55)	0.13	0.8	0.36	0.35	(0.01, 0.71)
Aluminum	mg kg ⁻¹	1.79	30.9	8.42	10.44	(-2.02, 18.86)	1.43	27.1	8.71	10.78	(-2.07, 19.49)
N:S	mg kg ⁻¹	7.16	20.6	14.59	5.20	(9.39, 19.80)	5.52	16.9	11.35	4.64	(6.71, 15.98)
N:K	mg kg ⁻¹	0.94	4.35	2.11	1.59	(0.52, 3.70)	0.63	4.29	1.64	1.99	(-0.35, 3.63)
Fe:Mg	mg kg ⁻¹	0.31	1.22	0.53	0.31	(0.22, 0.84)	0.19	1.06	0.58	0.41	(0.17, 0.99)

Overall, the nutrient concentrations and elemental ratios exhibit broad and well-distributed variability within the $\pm 2\sigma$ ranges at both 15 and 30 days post-treatment, providing an appropriate dynamic range for evaluating NIR spectrometer performance. The macronutrients nitrogen, phosphorus, and potassium show approximately two- to three-fold variation across sampling times, reflecting the imposed nutrient regimes and temporal effects on foliar nutrient accumulation. These controlled yet substantial gradients are particularly well suited for assessing model sensitivity and predictive stability.

2.4.2 Examination of Leaf-Pairs, Aggregates and Models for Macronutrients (Group 1)

Predictive NIR models for the macronutrients nitrogen (N), phosphorus (P), and potassium (K) were initially developed using all ten spectral datasets derived from individual leaf pairs and their successive aggregations (P1–P4, G12, G23, G34, G123, G234, and the whole-plant dataset, WP). This dataset structure enabled systematic evaluation of how leaf position and spectral aggregation influence model performance.

Figure 2.6 presents a comparative analysis of cross-validated coefficients of determination (R^2_{cv}) and cross-validated root mean squared error of prediction (RMSEP_{cv}) for N, P, and K across datasets, spectrometers, and growth stages (15 and 30 days post-treatment). Across nutrients and datasets, models developed using spectra acquired with the Microphazir generally achieved higher R^2_{cv} values and lower RMSEP_{cv} than those developed with the DLP Nano, particularly for nitrogen.

2.4.2.1 Nitrogen

Nitrogen models exhibited a clear stage-dependent response for both spectrometers. At 15 days post-treatment, Microphazir-based models showed strong to moderate predictive performance across datasets, with R^2_{cv} values ranging from 0.91 to 0.79 and RMSEP_{cv} values between 0.29 and 0.47. At 30 days post-treatment, even though RMSEP_{cv} values were generally lower than at 15 days (0.22–0.36), model performance declined in terms of explained variance ($R^2_{cv} = 0.82$ –0.53). This reflects reduced absolute variability (i.e., a smaller range) in foliar nitrogen concentration at later growth stages (see Figure 2.5).

The DLP Nano spectrometer followed a similar pattern but with consistently lower predictive performance. At 15 days, R^2_{cv} values ranged from moderately high to moderate (0.73–0.60), with RMSEP_{cv} values between 0.53 and 0.65. At 30 days, nitrogen models showed a marked reduction in predictive strength ($R^2_{cv} = 0.59–0.05$), even though RMSEP_{cv} values were lower overall (0.34–0.52), again reflecting diminished concentration variability.

2.4.2.2 Phosphorus

For phosphorus, neither spectrometer produced useful predictive models at 15 days post-treatment. Microphazir-based models at this stage yielded very low R^2_{cv} values (<0.10), with only the G123 and WP datasets producing marginally usable models (RMSEP_{cv} ≈ 0.06). At 30 days post-treatment, Microphazir models improved, with R^2_{cv} values ranging from weak to moderate (0.26–0.64) across datasets and RMSEP_{cv} values below 0.05.

Similarly, the DLP Nano spectrometer did not produce usable phosphorus models at 15 days. At 30 days, R^2_{cv} values remained weak (≤ 0.40) or negligible, although RMSEP values were comparable to those obtained with Microphazir for the limited number of viable models.

2.4.2.3 Potassium

Potassium prediction proved challenging for both spectrometers. At 15 days post-treatment, models exhibited weak predictive performance ($R^2_{cv} < 0.25$) with RMSEP_{cv} values between 0.28 and 0.30. At 30 days post-treatment, neither spectrometer produced useful potassium models for any dataset, indicating limited sensitivity of portable NIR spectra to foliar potassium under the conditions evaluated.

2.4.2.4 Effect of Leaf Aggregation and Model Selection

Across nutrients and spectrometers, datasets derived from individual leaf pairs (P1–P4) consistently produced lower R^2_{cv} values and higher RMSEP_{cv}, indicating weaker and less stable predictive performance. As spectral information was progressively aggregated across multiple leaf pairs—first two (G12, G23, G34), then three (G123, G234), and ultimately all four pairs (WP)—model performance improved, with higher R^2_{cv} and lower RMSEP_{cv}. This pattern confirms that spectral averaging across a larger portion of the plant reduces within-sample variability and noise, leading to more stable and generalizable models.

Model selection within each dataset followed the one-sigma criterion, favoring models that balanced predictive accuracy and parsimony by minimizing RMSEP_{cv} while limiting the number of latent variables. In cases where multiple preprocessing strategies produced similar R²_{cv} and RMSEP_{cv} values, preference was given to models with fewer latent variables, consistent with best practices for avoiding overfitting and enhancing robustness for future application.

2.4.2.5 Rationale for Whole-Plant Dataset Selection

The whole-plant (WP) dataset consistently produced the highest R²_{cv} and the lowest RMSEP_{cv} for nitrogen, phosphorus, and potassium, independent of spectrometer or growth stage. The improved performance of the WP dataset reflects its ability to integrate spectral information across multiple leaf positions, thereby capturing a broader representation of spatial and physiological variability within each seedling. Based on these results, the WP dataset was selected for subsequent model development for the rest of the nutrients, including Ca, Mg, S, Na, Fe, Mn, Zn, Cu, B, and Al, as well as nutrient ratios (N:K, N:S, and Fe:Mn). This approach ensures that additional nutrient models are developed using the most stable and representative spectral dataset identified during macronutrient model evaluation.

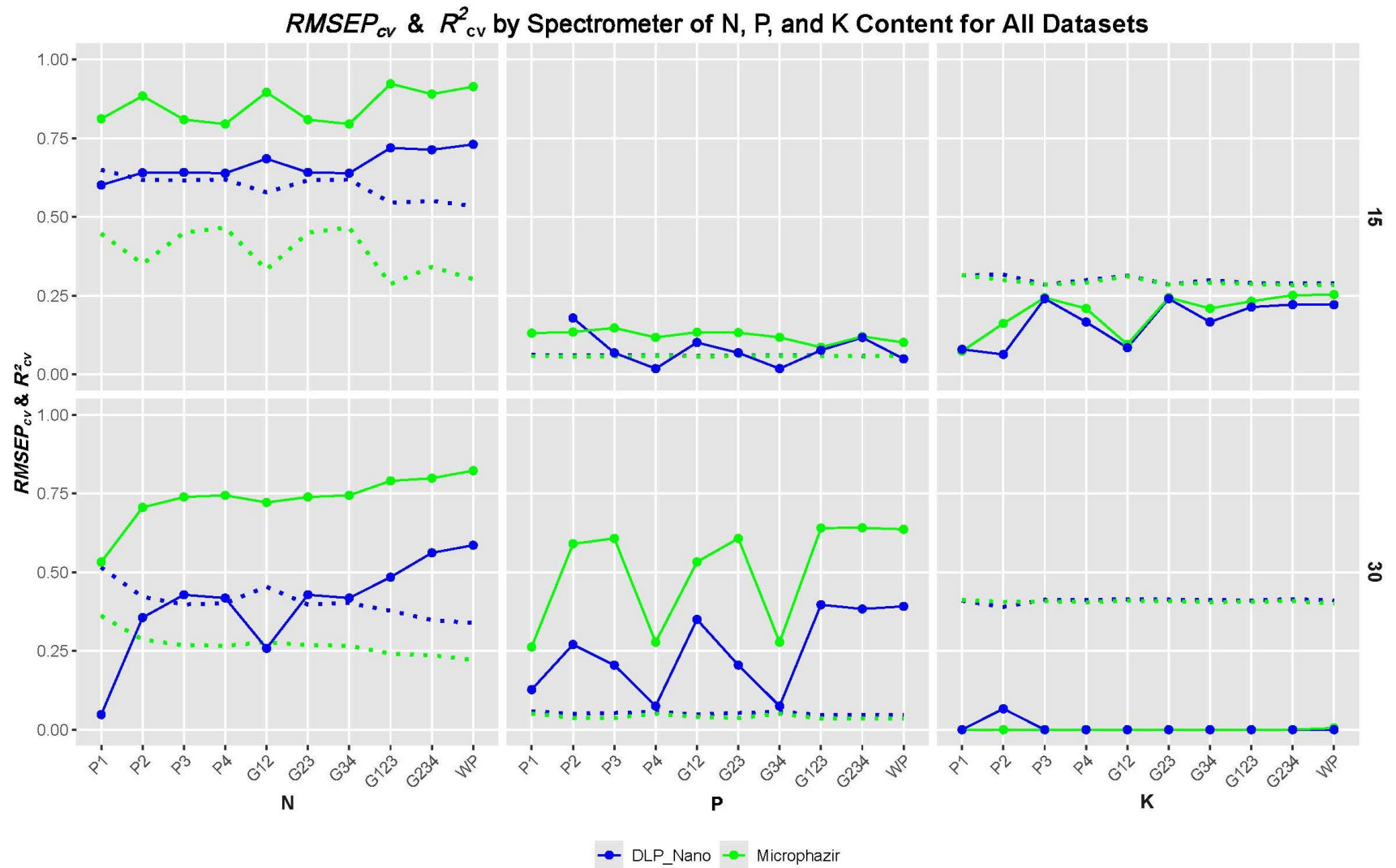


Figure 2.6 Line chart display showing R^2_{cv} (solid line) and $RMSEP_{cv}$ (dotted line) values of N, P, and K using all ten NIR spectra datasets at 15- (top) and 30-day (bottom) post-treatment for both portable spectrometers.

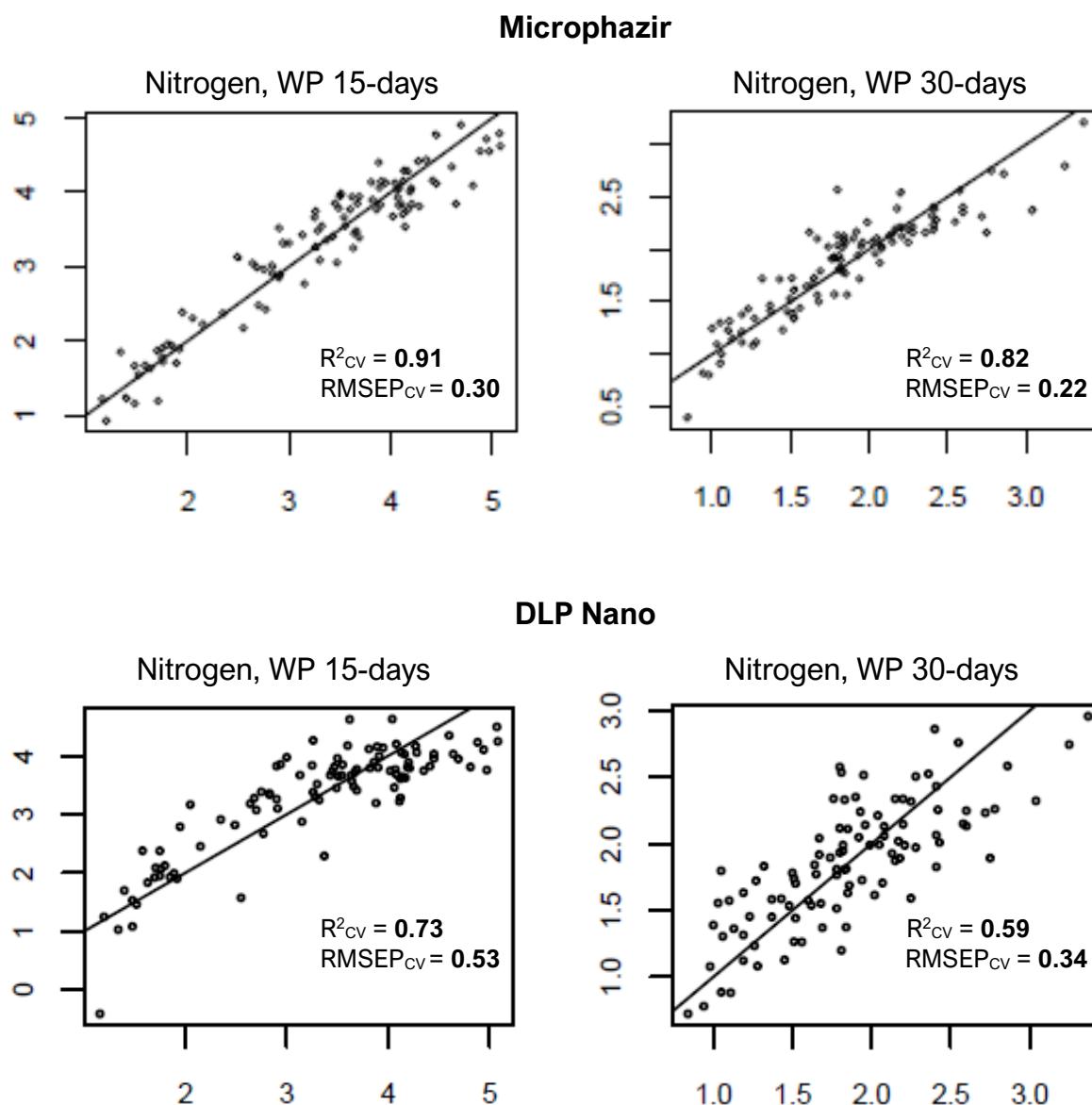


Figure 2.7 Observed versus predicted nitrogen concentrations (%) from whole-plant datasets. Top plots show models developed using Microphazir spectra, and bottom plots show models developed using DLP Nano spectra. Left plots correspond to 15 days post-treatment, and right plots to 30 days post-treatment. Models at 15 days post-treatment span a wider concentration range (1.16–5.08% N) and show stronger predictive performance, whereas models at 30 days post-treatment predict a narrower range (0.84–3.37% N), reflecting reduced variability at the later growth stage.

2.4.3 Models for the Rest of the Nutrients Using WP Dataset (Group 2)

Model performance differed between spectrometers, with Microphazir generally producing higher R^2_{cv} values and lower RMSEP_{cv} than the DLP Nano across most nutrients (Table 2.5). Despite this overall trend, both instruments showed some predictive capability for several micronutrients, particularly at the later growth stage.

2.4.3.1 Calcium, Magnesium, and Sulfur

At 15 days post-treatment, Microphazir produced moderate to highly moderate models for sulfur ($R^2_{cv} = 0.74$, RMSEP_{cv} = 0.02), calcium ($R^2_{cv} = 0.63$, RMSEP_{cv} = 0.15), and magnesium ($R^2_{cv} = 0.62$, RMSEP_{cv} = 0.04). In comparison, DLP Nano exhibited slightly lower predictive performance for these nutrients, with R^2_{cv} values of 0.61 (S), 0.54 (Ca), and 0.57 (Mg), and comparable RMSEP_{cv} values.

By 30 days post-treatment, model performance declined for both spectrometers. Microphazir R^2_{cv} values decreased to 0.57 (S), 0.43 (Ca), and 0.38 (Mg), with slightly increased values of RMSEP_{cv}. A similar decline was observed for DLP Nano, with R^2_{cv} values of 0.35 (S), 0.40 (Ca), and 0.30 (Mg).

2.4.3.2 Zinc, Copper, and Sodium

At 15 days, Microphazir exhibited weak to moderate models for zinc ($R^2 = 0.26$), copper ($R^2_{cv} = 0.55$), and sodium ($R^2 = 0.23$), with RMSEP_{cv} values of 5.08, 3.12, and 0.08, respectively. DLP Nano produced lower R^2_{cv} values for these nutrients, with similar RMSEP_{cv} values.

At 30 days post-treatment, predictive performance decreased for both instruments, with Microphazir R^2_{cv} values dropping to 0.18 (Zn), 0.05 (Cu), and 0.20 (Na), and DLP Nano showing similarly weak performance.

2.4.3.3 Iron, Manganese, Boron, Chloride, and Aluminum

Both spectrometers exhibited poor predictive performance for iron, manganese, boron, chloride, and aluminum at both sampling times. At 15 days, Microphazir R^2_{cv} values were ≤ 0.19 across these nutrients, with high RMSEP_{cv} particularly for iron and manganese. DLP Nano performed similarly poorly, with R^2_{cv} values near zero.

By 30 days post-treatment, predictive accuracy further declined for both instruments, with consistently low R^2_{cv} values and high RMSE P_{cv} , indicating limited model predictability for these elements.

2.4.3.4 Nutrient Ratios N:K, N:S, and Fe:Mn

For nutrient ratios, Microphazir showed moderate predictive performance at 15 days post-treatment for N:S ($R^2_{cv} = 0.58$, RMSE $P_{cv} = 1.67$) and N:K ($R^2_{cv} = 0.52$, RMSE $P_{cv} = 0.55$). DLP Nano produced lower R^2_{cv} values for both ratios. At 30 days post-treatment, predictive accuracy declined substantially for both instruments. The Fe:Mn ratio showed consistently poor predictability at both time points, with R^2_{cv} values below 0.10 and high RMSEP.

Table 2.5 Cross-validated model performance (R^2_{cv}) for nutrient and nutrient-ratio models developed at 15 and 30 days post-treatment using Microphazir and DLP Nano spectrometers.

Nutrient	DLP Nano		Microphazir	
	15 days R^2_{cv}	30 days R^2_{cv}	15 days R^2_{cv}	30 days R^2_{cv}
Sulfur	0.61	0.35	0.74	0.57
Calcium	0.54	0.40	0.63	0.43
Magnesium	0.57	0.30	0.62	0.38
N:S	0.51	0.00	0.58	0.31
Copper	0.38	0.00	0.55	0.05
N:K	0.18	0.00	0.52	0.07
Zinc	0.21	0.00	0.26	0.18
Sodium	0.16	0.12	0.23	0.20
Manganese	0.00	0.00	0.00	0.30

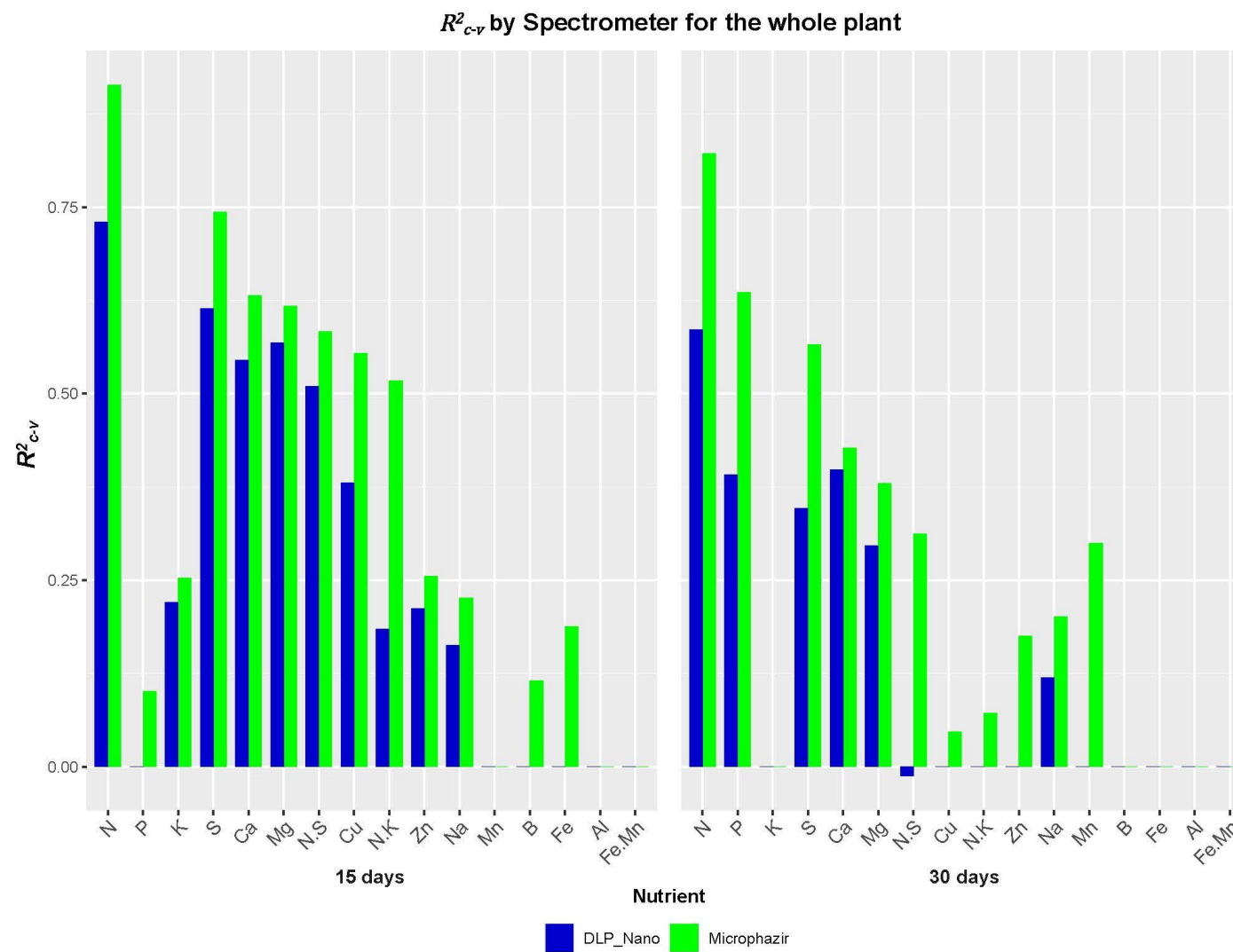


Figure 2.8 Bar charts comparing the R^2_{c-v} values of nutrient models developed using whole plant spectral data from portable spectrometers: DLP Nano and Microphazir, at 15- and 30-days post-treatment.

2.5 Discussion

Near-infrared spectroscopy can be a helpful tool that can rapidly and accurately analyze plant nutrients in real time (Prananto et al., 2021). Portable NIRS technology is an emerging technique that can offer a rapid, cost-effective, and efficient alternative to the time-consuming and expensive laboratory analysis required to measure foliar levels of nutrients accurately (García-Martínez et al., 2012; Azadnia et al., 2023).

Better-fitting models in freshly removed foliage were developed using aggregated leaf pairs, particularly Whole-Plant aggregates, which was derived from the average spectral data from all four-leaf pairs. These models exhibited the highest predictive accuracy compared to those based on individual leaf pairs.

The observed reduction in variability and narrower concentration ranges for N, P, K, and most micronutrients at 30 days post-treatment suggest a natural stabilization of nutrient concentration as seedlings mature. In this context, stabilization refers to foliar nutrient concentrations converging toward narrower physiological ranges as nutrient uptake and plant growth become more balanced over time, reducing differences among treatments. This process significantly affected spectral detectability and model accuracy, as shown by the marked decline in R^2_{cv} values across all nutrient models between 15- and 30-days post-treatment (Figure 2.8).

This pattern aligns with findings from other NIR spectroscopy research, such as studies on potato nitrogen models in Visible-Near Infrared (Vis-NIR) Spectroscopy for leaf nutrient analysis, which demonstrated that nutrient variability at different growth stages influences spectral model predictability. These studies found that the variation in nitrogen content at different growth stages did influence the predictability of the models, with better performance at certain stages and moderate-to-poor performance at others (Rawal et al., 2024).

2.5.1 Overall Performance of Macronutrient Prediction Models

2.5.1.1 Nitrogen

The nitrogen models exhibited superior accuracy and prediction consistency at 15 days, with higher R^2_{cv} values and lower $RMSEP_{CV}$ values, compared to models developed at 30 days post-treatment. This trend is evident in Figure 2.7, where at 15 days, the nitrogen model for

Microphazir reached an R^2_{cv} of 0.91 and $RMSEP_{CV}$ of 0.30, whereas at 30 days, these values declined to $R^2_{cv} = 0.82$ and $RMSEP_{CV} = 0.22$. Similarly, DLP Nano's nitrogen model at 15 days ($R^2_{cv} = 0.73$, $RMSEP_{CV} = 0.53$) deteriorated at 30 days to $R^2_{cv} = 0.59$, $RMSEP_{CV} = 0.34$.

This predictability trend observed in nitrogen models can be explained by the variation in observed nitrogen values obtained from standard laboratory foliar nutrient analysis, as detailed in Table 2.4. There was a significant 55% decrease in the range of observed nitrogen values between 15 and 30 days, meaning that the range of values used to develop nitrogen prediction models at 15 days was much broader than at 30 days. Specifically, foliar nitrogen concentration at 15 days ranged from 1.16% to 5.08%, whereas at 30 days, it narrowed to 0.84% to 3.37%.

The broader range of observed nitrogen concentration values at 15 days post-treatment (Table 2.6) allowed for higher variance in model performance, meaning both greater predictability (higher R^2_{cv} values) and greater error potential (higher $RMSEP_{CV}$ values). In contrast, at 30 days, the narrowing range of observed nitrogen values constrained both R^2_{cv} and $RMSEP_{CV}$, making the models appear more conservative but also potentially less applicable for broader predictive uses. This trend is clearly visible in Figure 2.8, where R^2_{cv} values are significantly lower for most nutrients at 30 days post-treatment compared to 15 days.

Table 2.6 Observed Foliar Nitrogen Concentration Ranges at 15 and 30 Days Post-Treatment

Lab Analysis	15 days		30 days	
	Min %	Max %	Min %	Max %
Nitrogen	1.16	5.08	0.84	3.37

2.5.1.2 Phosphorus

The observed values of phosphorus concentration obtained from each standard laboratory foliar nutrient analysis (Table 2.4) fell within normal range for plants, which is 0.05 to 0.5% (Johri et al., 2015).

Unlike nitrogen, the models for phosphorus performed poorly with spectral data collected 15 days post-treatments for both portable spectrometers. The performance improved at 30 days,

especially for Microphazir using spectra from G123, G234, and WP, which are the datasets that aggregate the most leaf pairs. The $RMSEP_{CV}$ remained consistently low (0.04-0.05) within datasets. A study in corn discusses the challenges in predicting phosphorus concentration during the early growth stages of the plant, where nutrient uptake variability and uneven distribution leads to less accurate predictions based on near-infrared (NIR) technology (Osborne et al., 2002).

2.5.1.3 Potassium

For potassium, the predictive models showed inadequate performance when analyzing the spectral data obtained 15- and 30-days following treatments, for both portable spectrometers. Even though this nutrient is one of the most abundant inorganic elements in plant cellular media and is highly concentrated in the most active plant organs, such as leaves (Sardans & Penuelas, 2021), NIR techniques face challenges in predicting potassium concentration due to its inorganic form, lack of direct spectral features, and reliance on indirect correlations with organic compounds, factors that result in poorer model performance compared to other macronutrients, such as nitrogen and phosphorus (Prananto et al., 2021).

2.5.2 Macronutrient Models Using Aggregated Leaf-Pair Datasets (Group 1)

For the macronutrients, the raw NIR spectra acquired with both portable spectrometers from each treatment at the two stages were combined to create multiple datasets consisting of paired leaves that were aggregated to form ten outlier-free datasets (P1, P2, P3, P4, G12, G23, G34, G123, G234, and G1234 or Whole Plant - WP).

Prediction of Nitrogen concentration was best using spectra from aggregated datasets G123 and WP obtained with the Microphazir at 15 days, with an R^2_{cv} of 0.92 and 0.91 and $RMSEP_{CV}$ of 0.29 and 0.30 respectively. For phosphorus concentration, prediction models were adequate using spectra from datasets G123, G234, and WP, all of them with R^2_{cv} of 0.64 and $RMSEP_{CV}$ of 0.04. This aligns with a recent study on *Eucalyptus pellita* leaf samples based on portable near-infrared technology at different growth stages from nursery to the field, where models yielded an R^2_{cv} of 0.88 and $RMSEP_{CV}$ of 0.21 for nitrogen and 0.61 and 0.02 for phosphorus (Alwi et al., 2021). Comparable results for nitrogen concentration were obtained in leaf samples taken from rice, corn, sesame, soybean, tea, grass, shrub, and vines with *pls* and support vector machine regression (SVMR) models performing moderately to moderately high (Zhai et al., 2013). An

assessment in individual fresh leaves of cucumber using a handheld spectrometer found a prediction model with a moderate validation accuracy ($R^2_{cv} = 0.75$) (Zhang & Li, 2008).

Nitrogen and phosphorus are mineral nutrients required for plants in concentration exceeding one part per million (ppm) as they play essential structural and metabolic roles in the plant (Pandey, 2018). NIR can detect macronutrients such as nitrogen and phosphorus directly because they are major constituents of NIR-sensitive organic compounds, whereas potassium, another macronutrient that exist mostly in inorganic forms, is detected through association with organic compounds and indirect correlations with organic compounds (Prananto et al., 2020).

The significance of specific absorbances of proteins at 1490 nm and 1539 nm for estimating nitrogen has been highlighted for *E. pellita*, where calibration of foliar N on fresh leaves has been successful for nitrogen. However, it was found to be challenging to predict phosphorus (Alwi et al., 2021), which is consistent with NIR foliar analysis in other crops (Zhai et al., 2013).

2.5.3 Models for Additional Micronutrients Using the Whole-Plant Dataset (Group 2)

After the initial analyses of nitrogen, phosphorus, and potassium, it was observed that better-fitted models resulted from aggregating more NIR spectra from each leaf pair (Figure 2.6). As a result of this trend, all the remaining nutrients, including Ca, Mg, S, Fe, Mn, Zn, Cu, B, Na, Cl, Al, as well as nutrient ratios N:K, N:S, and Fe:Mg were subsequently analyzed exclusively using the whole-plant (WP) dataset, which combines averaged NIR spectra from all the leaf pairs

This study has determined that NIR models can effectively estimate the sulfur, calcium, and magnesium concentration in freshly removed leaves using the Microphazir 15 days after applying the treatments. The models yielded a moderately high prediction accuracy for sulfur, with an R^2_{cv} value of 0.74 and $RMSEP_{CV}$ of 0.02. For calcium, R^2_{cv} was 0.63 with an $RMSEP_{CV}$ of 0.15. Lastly, for magnesium, R^2_{cv} was 0.62 and $RMSEP_{CV}$ 0.04. Moderately accurate models were also determined for copper, with R^2_{cv} of 0.55 and $RMSEP_{CV}$ 3.12; N:K ratio, with R^2_{cv} of 0.52 and $RMSEP_{CV}$ 0.55; and for N:S ratio, with R^2_{cv} of 0.58 and $RMSEP_{CV}$ 1.67.

Mineral nutrients such as aluminum, boron, iron, manganese, sodium, and zinc, categorized as micronutrients, are essential for plants and are required in small quantities, ranging from 0.1 to 100 mg per kg of plant dry matter (Pandey, 2018). The performance of models generated by analyzing these micronutrients nutrients, including ratio of Fe:Mn, varied when using NIR spectra

acquired by the portable spectrometers used in this study.

NIR spectrometry has low sensitivity due to low absorption coefficients, resulting in higher detection limits that can compromise accurate detection of low concentrations of analytes like micronutrients. (Menezes et al., 2009). Unfortunately, the current study failed to develop suitable predictive models for the remaining nutrients. All developed models for these nutrients showed weak performance, with most of the cross-validated coefficient of determination (R^2_{cv}) values falling below 0.30. Therefore, these models were excluded from the analysis because they lacked the predictive capability, acknowledging the limitations of portable NIR technique to predict micronutrients in plant leaf tissue (Prananto et al., 2020; Prananto et al., 2021). This limitation can be attributed to the low concentration of nutrient concentration in plant foliage and their inability to affect NIR reflectance at such low levels. (Whittier et al., 2021).

Some inorganic and organic molecules present at low concentrations in samples of compounds and medicines may not be effectively detected and measured when applying chemometric techniques. This is due to several limitations associated with Near-Infrared Spectroscopy, including low sensitivity, increased noise, calibration range constraints, interference from other sample components, non-linearity, and variations in the sample matrix. These factors complicate the isolation and accurate measurement of these nutrients. The low concentration and the small magnitude of spectral changes caused by variations in their concentration make it particularly challenging to capture them accurately in calibration models. (Menezes et al., 2009).

2.5.4 Comparative Performance of Portable NIR Spectrometers

In general, for spectra acquired at 15- and 30-days post treatment, in all 10 datasets across the plant, the Microphazir spectrometer produced better fit statistics for nitrogen and phosphorus models than the DLP Nano spectrometer.

Results in predicting foliar nutrient levels in hydroponically grown teak seedlings (Table 2.7) revealed that the Microphazir device produced robust models for nitrogen, phosphorus, and potassium, with R^2_{cv} values exceeding 0.80 for these nutrients. Nevertheless, these authors acknowledged that reduced precision of a portable device in predicting nutrient levels is anticipated due to the more significant environmental variability during spectral data collection from fresh foliage and the higher water concentration within the leaves (Whittier et al., 2021).

Table 2.7 Comparison of NIRS fit statistics for nutrient levels of macronutrients, micronutrients, and nutrient ratios in nursery material in pine[†], eucalypts and teak (Whittier et al., 2021).

Nutrient	Teak	Pine [†]	Eucalypt
	Microphazir ¹	Best Portable NIR ¹	Best Portable NIR ²
	----- R^2_{cv} -----		
Nitrogen (%)	0.82	0.86	0.92
Phosphorus (%)	0.68	0.19	0.64
Potassium (%)	0.75	0.45	0.25
Calcium (%)	0.10	0.47	0.63
Magnesium (%)	0.09	0.25	0.62
Sulfur (%)	0.11	0.15	0.74
Iron (ppm)	0.05	0.12	0.19
Manganese (ppm)	0.01	0.00	0.62
Zinc (ppm)	-0.37	0.32	
Copper (ppm)	0.14	0.33	0.55
Boron (ppm)	0.43	0.00	0.26
Molybdenum (ppm)	0.06		
Sodium (%)	0.16	0.00	0.23
N:K		0.64	0.52
N:S		0.27	0.58
Fe:Mn		0.17	

[†]See chapter 3 of this thesis for results on NIR spectroscopy of pine.

Spectra taken from ¹needles still attached to the stem, and ²freshly removed green leaves.

2.6 Conclusion

Near-infrared spectroscopy (NIRS) represents a promising and efficient approach for the rapid, non-destructive assessment of macro- and micronutrient concentrations in freshly removed foliage of nursery-grown eucalypt seedlings using portable spectrometers. While the technique demonstrates clear potential, the results also indicate inherent limitations in spectral modeling, particularly for nutrients present at low concentrations in foliar tissues. These constraints underscore the need for continued refinement of NIRS calibration strategies to improve predictive performance across a broader range of nutrients.

The development of accurate NIR models for predicting foliar macronutrient and micronutrient concentrations benefits from leveraging spectral information collected from multiple positions and developmental stages. By utilizing spectra from different points and growth stages, these models can better capture the variability in nutrient distribution across the plant. This integrative approach improves model stability and predictive performance and supports the development of more robust NIR-based tools for evaluating plant nutrient status.

Across all evaluated scenarios, the Microphazir consistently outperformed the DLP Nano in developing models for nitrogen and demonstrated moderate predictive capability for phosphorus, sulfur, calcium, magnesium, and copper when whole-plant spectra were used. This superior performance highlights the Microphazir as a highly promising tool for nutrient analysis, particularly when assessing freshly harvested leaves. Its ability to produce models with moderate to moderately high predictive performance across a range of these essential nutrients supports its potential utility in the research applications and in operational nutrient management contexts where rapid, non-destructive assessment is desirable.

2.7 References

- Acosta, J. J., Castillo, M. S., & Hodge, G. R. (2020). Comparison of benchtop and handheld near-infrared spectroscopy devices to determine forage nutritive value. *Crop Science*, *60*(6), 3410-3422. <https://doi-org.prox.lib.ncsu.edu/10.1002/csc2.20264>
- Alwi, A., Meder, R., Japarudin, Y., Hamid, H. A., Sanusi, R., & Mohd Yusoff, K. H. (2021). Near infrared spectroscopy of *Eucalyptus pellita* for foliar nutrients and the potential for real-time monitoring of trees in fertiliser trial plots. *Journal Of Near Infrared Spectroscopy*, *29*(3) 158 - 167. <https://doi-org.prox.lib.ncsu.edu/10.1177/09670335211007971>
- Azadnia, R., Rajabipour, A., Jamshidi, B., & Omid, M., (2023). New approach for rapid estimation of leaf nitrogen, phosphorus, and potassium contents in apple-trees using Vis/NIR spectroscopy based on wavelength selection coupled with machine learning. *Computers and Electronics in Agriculture*, *207*(1), 107746. <https://doi-org.prox.lib.ncsu.edu/10.1016/j.compag.2023.107746>
- Barnes, J., Whipker, B., McCall, I., & Frantz, J. (2012). Nutrient disorders of 'evolution' mealy-cup sage. *Hort Technology*, *22*(4), 502 - 508. <https://doi.org/10.21273/HORTTECH.22.4.502>
- Beć, K. B., Grabska, J., & Huck, C. W. (2021). Principles and Applications of Miniaturized Near-Infrared (NIR) Spectrometers. *Chemistry-A European Journal*, *27*(5) 1514-1532. <https://doi-org.prox.lib.ncsu.edu/10.1002/chem.202002838>
- Bhandari, N. (2018). Review: Techniques Used in Plant Tissue Analysis for Essential Elements on Horticultural Plants and Correlate with Nutrient. *North American Academic Research*, *1*(2), 94-113. <https://twasp.info/journal/Zq3423H/review-techniques-used-in-plant-tissue-analysis-for-essential-elements-on-horticultural-plants-and-correlate-with-nutrient-requirement>
- Breunig, M., Kriegel, H., Ng, R., & Sander, J. (2000). LOF: identifying density-based local outliers. *Sigmod Record*, *29*(2), 93-104. <https://doi-org.prox.lib.ncsu.edu/10.1145/335191.335388>
- Castillo, M. S., Acosta, J. J., Hodge, G. R., Vann, M. C., & Lewis, R. L. (2023). Analysis of alkaloids and reducing sugars in processed and unprocessed tobacco leaves using a handheld near infrared spectrometer. *Journal Of Near Infrared Spectroscopy*, *31*(2), 55 - 62. <https://doi-org.prox.lib.ncsu.edu/10.1177/09670335221148594>

- Castillo, M. S., Tiezzi, F., & Franzluebbers, A. J. (2020). Tree species effects on understory forage productivity and microclimate in a silvopasture of the Southeastern USA. *Agriculture, Ecosystems & Environment*, 295(1), 106917. <https://doi-org.prox.lib.ncsu.edu/10.1016/j.agee.2020.106917>
- Cen, H., & He, Y. (2007). Theory and application of near infrared reflectance spectroscopy in determination of food quality. *Trends in Food Science & Technology*, 18(2), 72 - 83. <https://doi-org.prox.lib.ncsu.edu/10.1016/j.tifs.2006.09.003>
- Diana, G., & Tommasi, C. (2002). Cross-validation methods in principal component analysis: A comparison. *Statistical Methods & Applications*, 11(1), 71-82. <https://doi.org/10.1007/BF02511446>
- García-Martínez, S., Gálvez-Sola, L.N., Alonso, A., Agulló, E., Rubio, F., Ruiz, J. J., & Moral, R. (2012). Quality assessment of tomato landraces and virus-resistant breeding lines: quick estimation by near infrared reflectance spectroscopy. *Journal of the Science of Food and Agriculture*, 92(6), 1178-85. <https://doi.org/10.1002/jsfa.4661>
- Ge, S., Zhu, Z., Peng, L., Chen, Q., & Jiang, Y. (2018). Soil Nutrient Status and Leaf Nutrient Diagnosis in the Main Apple Producing Regions in China. *Horticultural Plant Journal*, 4(4), 89-93. <https://doi.org/10.1016/j.hpj.2018.03.009>
- Grossnickle, S. C., & MacDonald, J. E. (2018). Why seedlings grow: influence of plant attributes. *New Forests*, 49(1), 1-34. <https://doi.org/10.1007/s11056-017-9606-4>
- Gullifa, G., Barone, L., Papa, E., Giuffrida, A., Materazzi, S., & Risoluti, R. (2023). Portable NIR spectroscopy: the route to green analytical chemistry. *Frontiers in Chemistry*, 11(1), 1214825. <https://doi.org/10.3389/fchem.2023.1214825>
- Hoagland, D. R., & Arnon, D. I. (1950). The water-culture method for growing plants without soil. *Circular: California Agricultural Experiment Station*, 347(1), 1-32. <https://archive.org/details/watercultureme3450hoag/page/n3/mode/2up>
- Hodge, G. R., Acosta, J. J., Unda, F., Woodbridge, W. C., & Mansfield, S. (2018). Global near infrared spectroscopy models to predict wood chemical properties of Eucalyptus. *Journal of Near Infrared Spectroscopy* 26(2), 117-132. <https://doi-org.prox.lib.ncsu.edu/10.1177/0967033518770211>

- Hodge, G. R., & Woodbridge, W. C. (2004). Use of near infrared spectroscopy to predict lignin. *Journal of Near Infrared Spectroscopy*, 12(6), 381-390. <https://doi-org.prox.lib.ncsu.edu/10.1255/jnirs.447>
- Johri, A. K., Oelmüller, R., Dua, M., Yadav, V., Kumar, M., Tuteja, N., Varma, A., Bonfante, P., Persson, B. L., & Stroud, R. M. (2015). Fungal association and utilization of phosphate by plants: success, limitations, and future prospects. *Frontiers In Microbiology*, 6(1), 984. <https://doi.org/10.3389/fmicb.2015.00984>
- Landis, T. D. (2009). Nursery Practices . In F. T. Bonner& R. P. Karrfalt (Eds.), *The Woody Plant Seed Manual* (1st. ed., pp. 125-145). U.S. Department of Agriculture, Forest Service.
- Leary, P. E., Crocombe, R. A., & Kammrath, B. W. (2021). Introduction to Portable Spectroscopy. In R. A. Crocombe, P. E. Leary, B. W. Kammrath, H. C. Lee, R. A. Crocombe, & P. E. Leary (Eds.), *Portable Spectroscopy and Spectrometry 1*, (1st ed., pp 1-13). Wiley. <https://doi.org/10.1002/9781119636489.ch1>
- Menezes, J. C., Ferreira, A. P., Rodrigues L. O., Brás, L. P., & Alves, T. P. (2009). Chemometrics Role within the PAT Context: Examples from Primary Pharmaceutical Manufacturing. In S. D. Brown, R. Tauler & W. Beata (Eds.), *Comprehensive Chemometrics* (1st ed. pp. 313-355). Elsevier. <https://doi-org.prox.lib.ncsu.edu/10.1016/B978-044452701-1.00012-0>
- Mevik, B. & Wehrens, R. (2016). *Introduction to the pls Package*. The Comprehensive R Archive Network. <https://cran.r-project.org/web/packages/pls/vignettes/pls-manual.pdf>
- Osborne, S. L., Schepers, J. S., Francis, D. D. & Schlemmer, M. R. (2002). Detection of phosphorus and nitrogen deficiencies in corn using spectral radiance measurements. *Agronomy Journal*, 94(6), 1215-1221. <https://doi-org.prox.lib.ncsu.edu/10.2134/agronj2002.1215>
- Pandey, N. (2018). Role of Plant Nutrients in Plant Growth and Physiology. In: *Plant Nutrients and Abiotic Stress Tolerance*. Singapur: Springer Singapore (1st. ed. pp. 51-93. https://doi.org/10.1007/978-981-10-9044-8_2

- Perez, I. M., Cruz-Tirado, L. J., Badaro, A. T., de Oliveira, M. M., & Barbin, D. F. (2019). Present and future of portable/handheld near-infrared spectroscopy in chicken meat industry. *NIR News*, 30(5-6), 26-29. <https://doi.org/10.1177/0960336019861476>
- Pimstein, A., Karnieli, A., Bansal, S. K., & Bonfil, D. J. (2011). Exploring Remotely Sensed Technologies for Monitoring Wheat Potassium and Phosphorus Using Field Spectroscopy. *Field Crops Research*, 121(1), 125-135. <https://doi-org.prox.lib.ncsu.edu/10.1016/j.fcr.2010.12.001>
- Prananto, J., Minasny, B., & Weaver, T. (2020). Chapter One - Near infrared (NIR) spectroscopy as a rapid and cost-effective method for nutrient analysis of plant leaf tissues. In D. L. Sparks, *Advances in Agronomy* (1st ed. pp. 1-49). Elsevier.
- Prananto, J. A., Minasny, B., & Weaver, T. (2021). Rapid and cost-effective nutrient content analysis of cotton leaves using near-infrared spectroscopy (NIRS). *PeerJ*, 9(1), <https://doi.org/10.7717/peerj.11042>
- Rawal, A., Hartemink, A., Zhang, Y., Wang, Y., Lankau, R. A., & Ruark, M. D. (2024). Visible and near-infrared spectroscopy predicted leaf nitrogen contents of potato varieties under different growth and management conditions. *Precision Agriculture*, 25(2), 751-770. <https://doi.org/10.1007/s11119-023-10091-z>
- Sardans, J., & Peñuelas, J. (2021). Potassium control of plant functions: Ecological and agricultural implications. *Plants*, 10(2), 419. doi:<https://doi.org/10.3390/plants10020419>
- Sorak, D., Herberholz, L., Iwascek, S., Altinpinar, S., Pfeifer, F., & Siesler, H. W. (2012). New Developments and Applications of Handheld Raman, Mid-Infrared, and Near-Infrared Spectrometers. *Applied Spectroscopy Reviews*, 47(2), 83. <https://doi.org/10.1080/05704928.2011.625748>
- Whittier, W. A., Hodge, G. R., Lopez, J., Saravitz, C., & Acosta, J. J. (2021). Near Infrared Spectroscopy Studies of Teak Grown Under Varying Levels of Nitrogen, Phosphorus and Potassium. *Journal Of Near Infrared Spectroscopy*, 29(5) 301-310. <https://doi-org.prox.lib.ncsu.edu/10.1177/09670335211025649>

- Zhai, Y., Cui, L., Zhou, X., Gao, Y., Fei, T., & Gao, W. (2013). Estimation of nitrogen, phosphorus, and potassium contents in the leaves of different plants using laboratory-based visible and nearinfrared reflectance spectroscopy: comparison of partial least-square regression and support vector machine regression meth. *International Journal of Remote Sensing*, *34*(7), 2502–2518. <https://doi-org.prox.lib.ncsu.edu/10.1080/01431161.2012.746484>
- Zhang, W., Kasun, L. C., Wang, Q. J., Zheng, Y., & Lin, Z. (2022). A Review of Machine Learning for Near-Infrared Spectroscopy. *Sensors*, *22*(24), 9764. <https://doi.org/10.3390/s22249764>
- Zhang, X. & Li, M. (2008). Analysis and Estimation of the Phosphorus Content in Cucumber Leaf in Greenhouse by Spectroscopy. *Spectroscopy and Spectral Analysis*, *10*(1), 2404-2408. <https://pubmed.ncbi.nlm.nih.gov/19123417/>

CHAPTER 3

Use of Near-Infrared Spectroscopy to Predict Nutrient Concentration in Pines

ABSTRACT

This study aimed to develop predictive models for nutrient concentration in the foliage of pine seedlings using near-infrared (NIR) reflectance spectra. The targeted nutrients included macronutrients—nitrogen (N), phosphorus (P), potassium (K), calcium (Ca), magnesium (Mg), sulfur (S)—and micronutrients—iron (Fe), boron (B), copper (Cu), chlorine (Cl), manganese (Mn), molybdenum (Mo), and zinc (Zn). Pine seedlings were grown hydroponically in a greenhouse in Raleigh, North Carolina, USA, under varying levels of N, P, and K. Foliage samples from 100 seedlings across five nutrient regimes were analyzed using NIR spectroscopy. Traditional standard nutrient analyses were also conducted on all foliage samples to calibrate the NIR models. Two portable NIR spectrometers—the DLP NIRscan Nano EVM by Texas Instruments and the Microphazir by Thermo Fisher Scientific—were compared with a Foss NIRSystems 6500 benchtop spectrometer. NIR readings were taken nondestructively from intact (i.e., live, green, fresh) primary needles at the bottom and secondary needles (fascicles) at the top of the seedlings at 15- and 30-days post-treatments. Subsequently, the foliage was harvested, dried, ground, and analyzed again with both portables and the benchtop spectrometer.

For intact foliage, reliable models were developed only for N concentration. The Microphazir produced a good model for N concentration 15 days after treatment ($R^2_{CV} = 0.66$), with improved accuracy at 30 days ($R^2_{CV} = 0.86$). In contrast, the DLP Nano showed poorer performance at 15 days ($R^2_{CV} = 0.46$) and moderate accuracy at 30 days ($R^2_{CV} = 0.67$), indicating that the Microphazir is the preferred tool for measuring N in intact pine foliage. Neither portable spectrometer developed suitable models for other macronutrients or micronutrients on intact samples. For dried and ground samples, both portable devices showed moderate accuracy for N concentration at 15 days ($R^2_{CV} = 0.67$ for the DLP Nano and $R^2_{CV} = 0.73$ for the Microphazir), with much higher accuracy at 30 days ($R^2_{CV} = 0.89$ and $R^2_{CV} = 0.94$, respectively). The Foss 6500 benchtop spectrometer produced very high accuracy models for N ($R^2_{CV} = 0.78$ at 15 days and $R^2_{CV} = 0.94$ at 30 days), and for K ($R^2_{CV} = 0.84$ at 15 days and $R^2_{CV} = 0.85$ at 30 days). Moderate models were developed for P using the benchtop unit ($R^2_{CV} = 0.58$ at 15 days and $R^2_{CV} = 0.60$ at 30 days).

These results suggest that while the benchtop spectrometer remains the best option for analyzing N, P, and K in pine foliage, portable devices, particularly the Microphazir, are effective for N measurement in both intact and processed foliage. The development of accurate NIR models for N, P, and K will provide nursery and plantation managers with a rapid, non-destructive tool for monitoring the nutrient status of seedlings and improving nutrient management practices.

3.1 Introduction

Pinus tecunumanii has emerged as an important species in tropical and subtropical forestry, with extensive studies conducted since 1981 by Camcore (based at North Carolina State University in the USA), an international tree improvement and forest gene conservation program. The program's work includes seed collections made across the Mesoamerican region, and provenance trials and conservation banks established worldwide, resulting in invaluable insights into the evolution of this species, its productivity, and genetic diversity.

P. tecunumanii exhibits substantial genetic and provenance variation, particularly between low- and high-elevation sources, resulting in strong differences associated with growth rate, stress tolerance, and disease resistance (Hodge & Dvorak, 2007; Hodge & Dvorak, 2014).

In addition, *Pinus tecunumanii* combines rapid early growth, high nursery productivity, and favorable wood properties for both pulp and sawtimber applications, which has led to its widespread use in commercial plantations and breeding programs across tropical and subtropical regions (Dvorak, 2000; Mbinga et al., 2019). The species has gained increasing importance as a pure species in countries such as Colombia, Brazil, and South Africa, and is widely deployed as a hybrid parent in combination with *P. patula* and *P. greggii*. These hybrids have demonstrated improved growth rates, enhanced disease tolerance, acceptable wood properties, and better adaptation to warmer sites (Kanzler et al., 2014). The increasing deployment of *P. tecunumanii* as a pure species and as a hybrid parent in operational forestry underscores the need for rapid, non-destructive tools to assess nutrient status, supporting its suitability as a model species for NIRS-based nutrient prediction in pine systems.

A seedling is a young plant grown from a seed, but the term is also commonly used to refer to various types of nursery stock, including transplants, rooted cuttings, and emblings. Seedlings are grown outdoors in the field, and in controlled environments, bareroot nurseries and in containers, with the objective of outplanting in the field (Landis, 2009). Seedling nutrition plays a fundamental role in ensuring the successful establishment, growth, and long-term survival of forest trees (Grossnickle & MacDonald, 2018). By understanding nutrient requirements and deficiencies, growers can optimize fertilization strategies, leading to improved nursery health and productivity (Ge et al., 2014)

Plant tissue analysis helps identify nutrient-related issues like deficiencies, toxicities, or imbalances before visual symptoms appear. This analysis is crucial for research and crop production, providing insights into plant nutrient status and guiding fertilizer management decisions and evaluates the effectiveness of fertilization programs (Bhandari, 2018).

Conventional leaf tissue laboratory analysis is considered the most accurate method for determining nutrient concentration; these methods are well established and can quantify a wide range of nutrients and other analytes with high accuracy. This laboratory method involves destructive chemical or biochemical assays to directly measure the nutrient concentration of a sample. It tends to be costly as it requires a multi-step, labor-intensive process with an extensive amount of sample preparation, followed by complex procedures carried out by skilled personnel using specialized equipment. As a result, conventional lab analysis can be time consuming, and this may be a limitation in a nursery setting when answers are needed within a short time window.

Spectroscopy has played a crucial role in plant tissue laboratory analysis, enabling precise measurement of nutrients. Techniques like Atomic Absorption Spectrometry (AAS), Inductively Coupled Plasma Atomic Emission Spectrometry (ICP-AES), and Inductively Coupled Plasma Mass Spectrometry (ICP-MS) are used to quantify nitrogen, phosphorus, and potassium. Variants like Flame Atomic Absorption Spectrometry (FAAS) and Graphite-Furnace Atomic Absorption Spectrometry (GF-AAS) offer increased sensitivity for trace elements. Inductively Coupled Plasma Optical Emission Spectrometry (ICP-OES) uses plasma to measure emitted light wavelengths. X-ray Fluorescence Spectrometry determines elemental composition, while Spectrophotometry quantifies specific compounds (Bhandari, 2018).

The ability to monitor nitrogen (N), phosphorus (P), and potassium (K) status through remote sensing techniques is important for understanding plant nutrition and improving crop productivity (Pimstein et al., 2011). Macronutrients N, P, and K are essential for plant growth, but their optimal levels are crucial, as both deficiency and excess can adversely affect crop yield and quality. NIR spectroscopy is used in plant tissue analysis to estimate the concentrations of these important biochemical components (Zhai et al., 2013).

The use of NIR spectroscopy to evaluate foliar nutrient levels provides a rapid, cost-effective, and potentially non-destructive method to evaluate foliar nutrient levels. Applications of this technique to predict nutrient levels in the nursery would be an invaluable tool in the nursery

to address specific deficiencies, thereby minimizing expenses associated with excessive or inadequate fertilization (Whittier et al., 2021).

NIR reflectance spectroscopy utilizes the interactions of NIR light with organic molecular bonds in a substance to evaluate variation in molecular states (Zhang et al., 2022). This technique relies on the principle that different molecular structures absorb and reflect light at specific wavelengths in the near-infrared region of the electromagnetic spectrum, allowing for the identification and quantification of various compounds present in a sample. By analyzing the patterns of light absorption and reflection, NIR spectroscopy can be used for qualitative and quantitative analysis of a wide range of materials, including agricultural products, food industry, health sector and chemicals (Gullifa et al., 2023).

An NIR spectrometer is an analytical scientific instrument used to analyze and study the properties of light over a specific range of the electromagnetic spectrum (Beć et al., 2021). It works by splitting light into different wavelengths, allowing scientists to identify and measure its components. An NIR spectrometer is designed specifically for analyzing NIR light, providing insights into the molecular structure and composition of samples (Leary et al., 2021) The main parts of an NIR spectrometer system are generally a light source, beam splitter system, reflector, sample chamber/detector inlet valve, diffuse reflection detector, transmission detector, control and data processing system (Cen & He, 2007).

Traditional NIR devices have a benchtop configuration and require samples to be carried to the equipment (Beć et al., 2021). Benchtop devices have mainly been used by trained personnel working in commercial and research laboratories and are typically relatively expensive (Acosta et al., 2020). Over the past two decades, an increased interest in NIR spectroscopy has resulted in the creation of portable spectrometers for a range of applications. A portable spectrometer is a valuable analytical tool for quick and accurate sample analysis, whether in the laboratory or field (Leary et al., 2021).

Unlike conventional laboratory-based equipment, portable spectrometers are small and lightweight instruments that can be easily transported and run on battery power for a reasonable length of time frame. The most apparent distinctions are narrower spectral regions and/or lower spectral resolution within which the portable devices operate (Beć et al., 2021). However, these devices can provide accurate measurements and generate NIR reflectance data at a given

wavelength with precision comparable to those produced by laboratory-grade spectrometers (Sorak et al., 2012).

Portable spectrometers provide the benefit of conducting on-site analysis, enabling immediate decision making in laboratory, industrial and field environments (Perez et al., 2019). This technology offers benefits such as non-destructive sampling, providing immediate insights that can be linked to subsequent analyses on the same sample. Combining NIR spectroscopy with chemometrics allows for focused and broad analyses through prediction models based on statistical evaluation. Results can be shared qualitatively or quantitatively, making them accessible to experts and non-experts (Gullifa et al., 2023).

NIR spectroscopy applications can provide reliable results when their prediction models are developed using accurate biochemical data, hence, they are considered spectrochemical models. Consequently, the accuracy of predictions for response values obtained from NIR spectra depends on the ability to generate appropriate NIR models (Acosta et al., 2020). In addition, the accuracy of the technique depends on factors such as device specifications, algorithms used in the analysis, and the range of nutrient levels in the samples (Pimstein et al., 2011).

3.2 Objectives

The aim of this study is to acquire near-infrared (NIR) spectra using two portable spectrometers, the DLP NIRscan Nano EVM (Texas Instruments) and the Microphazir (Thermo Fisher Scientific), as well as a laboratory-based benchtop spectrometer, the Foss 6500 (Foss NIRSystems), in order to address the following objectives:

- To evaluate the use of near-infrared spectroscopy (NIRS) as a rapid, non-destructive approach for estimating foliar nutrient concentration in pine seedlings, with emphasis on both macronutrients and micronutrients.
- To establish useful protocols for acquiring high-quality NIR spectra from intact, still-attached needle foliage and from dried, ground foliage samples of pine seedlings grown under varying nutrient regimes, and to develop predictive models for predicting macronutrient and micronutrient concentrations.
- To evaluate and compare the performance of portable NIR spectrometers for in situ nutrient assessment in pine seedlings, and to benchmark their predictive capability against the

laboratory-based spectrometer to determine their suitability for operational nursery conditions and laboratory-based nutrient monitoring applications.

3.3 Materials and Methods

3.3.1 Plant material and nutrient regimes

Three hundred 11.5-centimeter square vacuum pots, each containing 1 L of washed and steam-sterilized silica river sand, were arranged on the NCSU Campus. Two seeds of *Pinus tecunumanii* seeds were sown in each pot, one centimeter deep and two centimeters apart. The pots were monitored daily and watered with an automated mist system. No fertilizer was added during germination. The first germinants were observed on the fifth day after sowing. On the sixteenth day, a few extra germinants were transplanted into empty pots so that all pots contained at least one germinant.

All 300 pots were initially treated with a Complete Hoagland's nutrient solution to promote seedling health and ensure uniform nutritional status prior to treatment initiation. Hoagland's nutrient solution (HNS), originally developed for water culture systems, is widely used in controlled plant nutrition studies due to its well-defined and reproducible composition. It supplies essential macro- and micronutrients (Table 3.1) at concentrations that support healthy physiological development while allowing precise manipulation of individual nutrient levels, making it a standard framework for evaluating nutrient sufficiency and deficiency responses across plant species (Hoagland & Arnon, 1950). In this study, its use provided a consistent and controlled nutritional baseline for subsequent experimental regimes. The nutrient solution was applied twice daily for 65 days, with a dose of 25 mL per in the early morning and an additional 25 milliliters in the afternoon. During this period, regular irrigation was provided by an automated sprinkler system programmed to operate for 10–20 seconds every hour between 7:00 a.m. and 5:00 p.m. Five days after the initial fertilization, seedlings were thinned to retain one plant per pot.

Following seedling grading, 200 pots were selected and randomized to begin nutrient regimes. The experiment consisted of five treatment groups using modified HNS prepared in the laboratory. Nutrient solutions were formulated from reagent-grade stock solutions containing potassium nitrate (KNO_3), calcium nitrate tetrahydrate [$\text{Ca}(\text{NO}_3)_2 \cdot 4\text{H}_2\text{O}$], potassium dihydrogen phosphate (KH_2PO_4), magnesium sulfate heptahydrate ($\text{MgSO}_4 \cdot 7\text{H}_2\text{O}$), iron diethylenetriaminepentaacetic acid (FeDTPA), manganese chloride tetrahydrate ($\text{MnCl}_2 \cdot 4\text{H}_2\text{O}$), zinc chloride (ZnCl_2), cupric chloride dihydrate ($\text{CuCl}_2 \cdot 2\text{H}_2\text{O}$), boric acid (H_3BO_3), and sodium

molybdate dihydrate ($\text{Na}_2\text{MoO}_4 \cdot 2\text{H}_2\text{O}$). Stock solutions were diluted with tap water with an electrical conductivity of 0.24 mS cm^{-1} , and pH was adjusted to 6.0 using sodium hydroxide (NaOH). (Barnes et al., 2012).

Table 3.1 Composition of nutrient stock solutions, application volumes, and resulting concentrations of nitrate-nitrogen ($\text{NO}_3\text{-N}$), ammonium-nitrogen ($\text{NH}_4\text{-N}$), phosphorus (P), and potassium (K) in the complete Hoagland nutrient solution.

Composition (Formula)	Stock Solution	mL used per 100 L	PPM			
			$\text{NO}_3\text{-N}$	$\text{NH}_4\text{-N}$	P	K
$\text{Ca}(\text{NO}_3)_2 \cdot 4\text{H}_2\text{O}$	35.42 g/100 mL	185	77.74	—	—	—
KNO_3	12.85 g/100 mL	276.4	49.22	—	—	137.38
$\text{MgSO}_4 \cdot 7\text{H}_2\text{O}$	29.58 g/100 mL	171.4	—	—	—	—
$\text{K}_2\text{HPO}_4 \cdot 3\text{H}_2\text{O}$	20.00 g/100 mL	0	—	—	—	—
KH_2PO_4	8.17 g/100 mL	53.8	—	—	10.00	12.62
K_2SO_4	10.00 g/100 mL	0	—	—	—	—
$(\text{NH}_4)_2\text{HPO}_4$	11.50 g/100 mL	0	—	—	—	—
NH_4NO_3	17.15 g/100 mL	33.3	10.00	10.00	—	—
$(\text{NH}_4)_2\text{SO}_4$	13.21 g/100 mL	0	—	—	—	—
$\text{Mg}(\text{NO}_3)_2$	25.64 g/100 mL	10.87	3.05	—	—	—
$\text{CaSO}_4 \cdot 2\text{H}_2\text{O}$	17.22 g/100 mL	0	—	—	—	—
KCl	7.46 g/100 mL	0	—	—	—	—
Fe-DTPA	40 g/L	100	—	—	—	—
$\text{MnCl}_2 \cdot 4\text{H}_2\text{O}$	3.96 g/L	90	—	—	—	—
$\text{ZnCl}_2 \cdot 7\text{H}_2\text{O}$	2.73 g/L	15	—	—	—	—
$\text{CuCl}_2 \cdot 2\text{H}_2\text{O}$	3.41 g/L	15	—	—	—	—
H_3BO_3	6.18 g/L	45	—	—	—	—
$\text{Na}_2\text{MoO}_4 \cdot 2\text{H}_2\text{O}$	0.24 g/L	10	—	—	—	—
Total			140.00	10.00	10.00	150.00
Total N			150.00			

Treatment 1 received the complete HNS used during the establishment phase. Treatment 2 received a modified solution with nitrogen (N), phosphorus (P), and potassium (K) reduced to 50% of full strength. Treatments 3, 4, and 5 were excluded to all N, P, and K respectively, while all other nutrients were maintained at full concentration. Each seedling received 25 mL of nutrient solution per pot in the morning and an additional 25 mL in the afternoon, with supplemental watering provided by the automated sprinkler system as described above.

3.3.2 NIR Spectrometers

The three spectrometers used in this study differ in their wavelength coverage, spectral intervals, and resolution (Table 3.2). The DLP NIRscan Nano EVM and the Microphazir operate over spectral ranges of 900–1700 nm and 1600–2400 nm, respectively, whereas the Foss 6500 benchtop spectrometer provides the broadest coverage, spanning the visible to near-infrared region (400–2498 nm). For consistency across instruments and analyses, only spectral information within the near-infrared region (1100–2498 nm) was used for model development.

Table 3.2 Near-infrared devices used to predict macronutrient and micronutrient levels in intact and fried and ground samples of pine foliage

Device	Type	Spectral Range	Wavelength Interval	No. of wavelengths
Microphazir	Handheld	<i>1600–2400</i>	<i>8 nm</i>	<i>100</i>
DLP Nano	Handheld	<i>900–1700</i>	<i>5 nm</i>	<i>160</i>
Foss 6500	Benchtop	<i>1100–2498</i>	<i>2 nm</i>	<i>700</i>

3.3.3 Spectra Acquisition and Database Creation

During this phase of the experiment, each treatment group was subdivided into two sets, each consisting of 20 randomly selected seedlings. Near-infrared (NIR) spectra were acquired at two growth stages: **15 days** and **30 days** after the nutrient treatments started. Spectra collected at 15 days were obtained from the first set of seedlings, while spectra collected at 30 days were obtained from the second set.

At each growing stage, NIR spectra were first acquired using two portable spectrometers: the **Microphazir** (Thermo Fisher Scientific) and the **DLP NIRscan Nano EVM** (Texas Instruments). Spectral measurements were collected from two distinct positions on each intact seedling: primary needles located at the lower portion of the stem and secondary needles (fascicles) located near the upper portion of the seedling.

To ensure consistent and accurate measurements, needles at each position were gently clamped together, and the handheld spectrometers were placed directly against the intact needle

bundle. A flat piece of black plastic was positioned behind the needles to minimize background interference during spectral acquisition (Figure 3.1).

After acquiring the spectra from intact needles of each growth stage, the entire foliage of each seedling was removed, placed into individually labeled craft paper bags, and transported to a laboratory at North Carolina State University. The foliage samples were then dried in a forced-air oven at 60 °C until a constant weight was achieved prior to further processing.

The dried foliage was subsequently ground into fine particles (≤ 1 mm) using a Marconi MA048 knife mill fitted with an 18-mesh screen. The resulting ground material was stored in labeled glass test tubes. Approximately 1 g of ground tissue from each sample was transferred into spinning-sample module cups fitted with quartz covers, and a new set of NIR spectra was acquired using a laboratory-grade Foss NIRSystems 6500 spectrometer (Foss 6500). In addition, NIR spectra of the dried and ground samples were collected through the quartz covers of the Foss sample cups using the two portable spectrometers.



Figure 3.1 Acquisition of NIR spectra from intact pine seedlings using portable spectrometers. **Left:** DLP NIRscan Nano EVM (Texas Instruments) used to collect spectra from secondary needle fascicles located at the upper portion of the seedling. **Right:** Microphazir (Thermo Fisher Scientific) used to acquire spectra from primary needles located at the lower portion of the seedling

After acquiring the spectra of each growth stage, the entire seedling's dried and ground foliage samples were bagged, labeled, and submitted to the North Carolina Department of Agriculture & Consumer Services (NCDA&CS) for standard nutrient laboratory analysis.

Total N was determined by oxygen combustion gas chromatography with subsequent quantification by thermal conductivity detector. Total concentrations of P, K, Ca, Mg, S, Fe, Mn, Zn, Cu, B, Na, Cl, and Al were determined with Inductively Coupled Plasma-Optical Emission Spectrometry. N, P, K, Ca, Mg, S, Na, and Cl are reported in percentage (%), and all other elements are reported in parts per million (ppm, equivalent to mg kg^{-1}). All results are reported on a dry weight basis. Detailed results of the standard laboratory foliar nutrient analyses for all samples, organized by nutrient regime and growth stage, are provided in Appendix D (*a-j*) of this thesis.

3.3.4 NIR Model Dataset Creation

A total of four NIR spectral datasets were generated for model development:

- **Two datasets** derived from spectra collected at distinct positions within each intact seedling, including primary needles from the lower portion of the plant and secondary needles (fascicles) from the upper portion.
- **One dataset** created by combining spectra from both needle positions within each intact seedling to form a **whole-plant (WP)** spectral dataset.
- **One dataset** derived from spectra collected from dried and ground foliage samples, acquired through the glass covers of the Foss module sampling cups.

3.3.5 NIR Model Development

NIR model development was conducted using a data analysis pipeline implemented in the R statistical environment, following the procedure described by Hodge et al. (2018) and Acosta et al. (2020). This workflow has been successfully applied in previous studies for developing NIR calibration models to predict foliar nutrients in teak (Whittier et al., 2021), and chemical properties of wood (Hodge et al., 2018), as well as the nutritive value of tobacco and nutritional content of forage species (Castillo et al., 2023; Castillo et al., 2020; Bekewe et al., 2020; Acosta et al., 2020). The modeling procedure consisted of two main stages: spectral transformation and outlier detection, and model training, cross-validation, and selection.

3.3.5.1 Spectral Transformations and Outlier Detection

Raw NIR reflectance spectra ($\log 1/R$) were subjected to a series of mathematical transformations to reduce the effects of light scattering, baseline shifts, instrumental noise, wavelength-dependent scattering, and sample-related variability. Scatter-correction techniques included multiplicative scatter correction (MSC), standard normal variate (SNV), and detrend (DT). In addition, spectral derivative preprocessing was performed using Savitzky–Golay smoothing with second-order polynomial fitting and window sizes of five and seven points (SG5 and SG7). Combinations of scatter-correction and derivative preprocessing methods, including SNV + SG5, SNV + SG7, MSC + SG5, MSC + SG7, DT + SG5, and DT + SG7, were also evaluated to optimize spectral information. In total, fourteen spectral datasets were generated for each modeling scenario, consisting of the raw spectra and thirteen transformed datasets.

Outlier detection was performed using the Local Outlier Factor (LOF) algorithm (Breunig et al., 2000), which identifies observations that exhibit anomalous local density relative to their nearest neighbors. LOF scores were calculated using ten nearest neighbors, and samples with LOF values greater than 2 were removed from subsequent analyses, following the approach described by Castillo et al. (2023).

3.3.5.2 Model Training, Cross-Validation, and Selection

Outlier-filtered datasets were used to develop NIR calibration models relating spectral data to reference nutrient concentrations obtained through laboratory analyses. Partial least squares regression (PLSR) was applied using the *pls* package in R (Mevik & Wehrens, 2016). Model performance was evaluated using leave-one-out (LOO) cross-validation, in which each observation is sequentially excluded from the calibration set and used for validation (Diana & Tommasi, 2002).

For each transformation, model performance metrics included the coefficient of determination for calibration (R^2_{cal}) and cross-validation (R^2_{cv}), the root mean squared error of prediction for calibration (RMSEP_{cal}) and cross-validation (RMSEP_{cv}), and the explained variance of both predictor variables (ExpVar X) and response variables (ExpVar Y). These metrics were used to compare preprocessing strategies and select the most robust models for each nutrient (Table 3.3).

Table 3.3 Partial least squares (PLS) regression fit statistics for predicting Magnesium concentration in dried and ground pine needles using the Foss 6500 spectra collected 30 days after treatment application. Models were evaluated across multiple spectral preprocessing methods. For this sample dataset and nutrient, the MSC transformation provided the most robust performance based on cross-validation statistics.

Transformation	Factors	Calibration		Cross Validation		ExpVar Y	ExpVar X
		R^2_{cal}	RMSEP_{cal}	R^2_{cal}	RMSEP_{cv}		
<i>DT</i>	7	0.73	0.02	0.61	0.03	73.16	99.41
<i>DT+SG5</i>	4	0.71	0.02	0.42	0.03	70.93	75.73
<i>DT+SG7</i>	5	0.71	0.02	0.52	0.03	71.21	88.75
<i>MSC*</i>	8	0.74	0.02	0.63	0.03	74.04	99.66
<i>MSC+DT</i>	7	0.73	0.02	0.61	0.03	73.16	99.41
<i>MSC+SG5</i>	4	0.71	0.02	0.42	0.03	70.97	75.79
<i>MSC+SG7</i>	5	0.71	0.02	0.52	0.03	71.25	88.78
<i>NIR</i>	8	0.73	0.02	0.60	0.03	72.74	99.82
<i>SG5</i>	5	0.77	0.02	0.46	0.03	77.27	79.96
<i>SG7</i>	6	0.79	0.02	0.59	0.03	79.24	90.06
<i>SNV</i>	6	0.70	0.02	0.59	0.03	69.54	99.00
<i>SNV+DT</i>	7	0.73	0.02	0.61	0.03	73.16	99.41
<i>SNV+SG5</i>	4	0.71	0.02	0.42	0.03	70.93	75.73
<i>SNV+SG7</i>	5	0.71	0.02	0.52	0.03	71.21	88.75

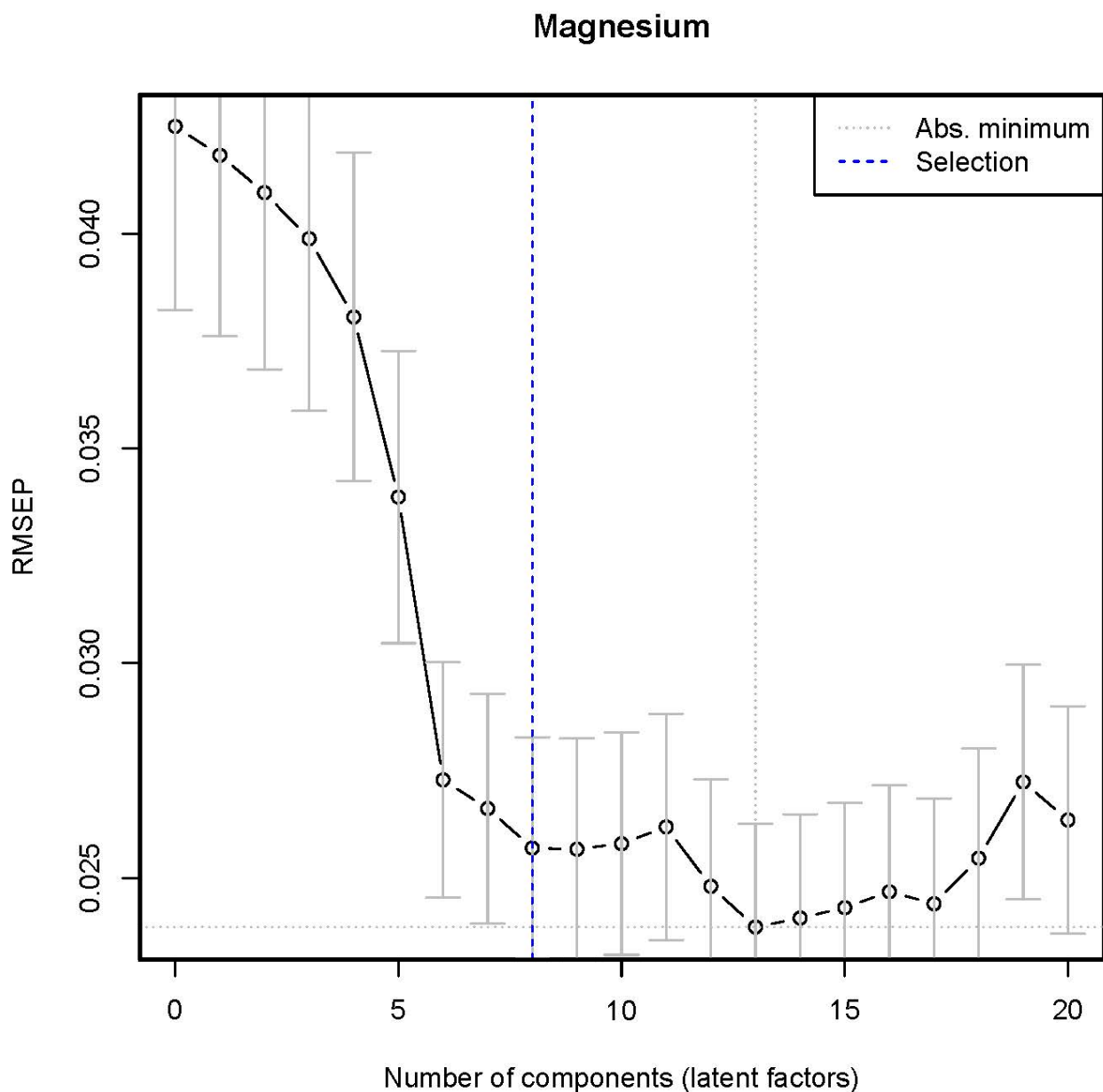


Figure 3.2 RMSEP as a function of the number of latent variables for the MSC-transformed Magnesium model developed from spectra collected from dried and ground pine needles. The dotted gray vertical line indicates the model with the absolute minimum RMSEP (thirteen latent variables), while the dashed blue vertical line indicates the selected model based on the one-sigma criterion. Although the minimum RMSEP occurred at thirteen components, an eight-component model was selected because its RMSEP was within one standard error of the minimum, favoring a more parsimonious model without loss of predictive performance.

The R-based analysis pipeline identifies an “optimal” model using the one-sigma criterion, which balances predictive performance and model complexity by minimizing overfitting. This approach evaluates models with 1 to 20 latent variables and selects the model with the fewest factors whose root mean squared error of prediction from RMSEP_{cv} falls within one standard error of the minimum RMSEP (Castillo et al., 2023; Figure 3.2). Models selected using this criterion exhibited strong fit statistics.

As an example, for magnesium models developed using NIR spectra acquired with the Foss 6500 at 30 days post-treatments, all spectral transformations and raw NIR spectra were evaluated. The model selection algorithm identified the MSC transformation with eight latent factors as the optimal model, as it produced the highest cross-validated coefficient of determination ($R^2_{cv} = 0.63$) and the lowest RMSEP_{cv} (0.033) among the candidate models (Table 3.3).

In other modeling scenarios, alternative models may be selected for the same nutrient depending on tradeoffs among performance metrics and model complexity. For example, when comparing the selected eight-factor MSC model to models DT, MSC+DT, and SNV-DT, these three models with seven factors (Table 3.3) may be preferred as more robust for routine or operational use. However, the minor differences observed among the top-ranked models do not affect conclusions regarding spectrometer performance or the overall feasibility of developing reliable NIR models for nutrient prediction (Acosta et al., 2020).

3.4 Results

The performance of NIR predictive models varied depending on the range of nutrient concentration observed, sampling method (intact vs. dried and ground foliage), developmental stage (15 vs. 30 days post-treatment), spectral acquisition position (primary needles, fascicles, or whole plant), and the spectrometer used (Microphazir, DLP Nano, Foss 6500).

Complete calibration and cross-validation statistics for all evaluated PLS regression models are reported in Appendix C.

3.4.1 Nutrient concentration variation observed

3.4.1.1 Concentration Variation by Regime

The results from the standard nutrient laboratory analysis indicate that the five treatments produced varying levels of nutrient concentration depending on the amount of nutrients added to each modified HNS. The box plots in Figure 3.3 illustrate the differences in foliar nitrogen, phosphorus, and potassium concentration across the different treatments and time points (15 and 30 days) for pine seedling foliage.

These results highlight how the availability of nutrients in the solution directly impacts the nutrient concentration of the leaves. This effect is especially noticeable in the treatments with deficient nutrients (0% N, 0% P, and 0% K), where nutrient levels consistently remained low. Furthermore, the changes observed over time indicate that the nutrient uptake by the seedlings continues as long as sufficient nutrients are available. This leads to slightly higher foliar concentrations at 30 days compared to those at 15 days.

3.4.1.2 Concentration Variation by Nutrient

Table 3.4 provides a detailed comparison of the observed nutrient concentration dynamics, highlighting each nutrient's stability, accumulation, or reduction as the treatments progress.

For nitrogen, the minimum concentration decreased from 1.07% at 15 days to 0.81% at 30 days, while the maximum concentration also showed a slight decrease from 2.80% to 2.72%. This shift results in a narrower range at 30 days, though the mean remains fairly consistent, 1.96% at 15 days and 1.95% at 30 days. The interval within two standard deviations narrows slightly, changing from (1.16 to 2.76) at 15 days to (0.97 to 2.72) at 30 days. This minor shift suggests a

stabilization in nitrogen concentration as the samples mature, with a very small reduction in variability by the 30-day stage.

Phosphorus concentration shows a marked increase in maximum concentration over time, rising from 0.37% at 15 days to 0.49% at 30 days, while the minimum value remains relatively constant at around 0.18–0.19%. This results in an expanded range for phosphorus by 30 days. The interval within two standard deviations for phosphorus broadens as well, from (0.19 to 0.35) at 15 days to (0.18 to 0.41) at 30 days. This indicates increased variability in phosphorus concentration in later stages of development.

Potassium concentration exhibits a noticeable decrease over time. The minimum value drops from 1.17% at 15 days to 0.89% at 30 days, while the maximum decreases from 2.93% to 2.35%. This decrease in both minimum and maximum potassium levels results in a reduced range at 30 days. The interval within two standard deviations narrows as well, from (1.18 to 2.35) to (0.91 to 2.34), indicating a shift toward lower potassium concentrations and reduced variability in the nutrient's distribution over time.

For the rest of the nutrients, the standard nutrient over 15-day and 30-day stages reveals minor changes in calcium, magnesium, and sulfur, with slight increases in their maximum values by 30 days, resulting in minimal variation in their range. Iron, manganese, zinc, copper, and boron, however, display more pronounced shifts. Iron's maximum concentration decreases significantly over time, indicating stabilization, while manganese and zinc show increases in maximum values, suggesting accumulation. Copper's range narrows due to a decrease in its maximum, while boron's range expands, likely reflecting gradual concentration increases.

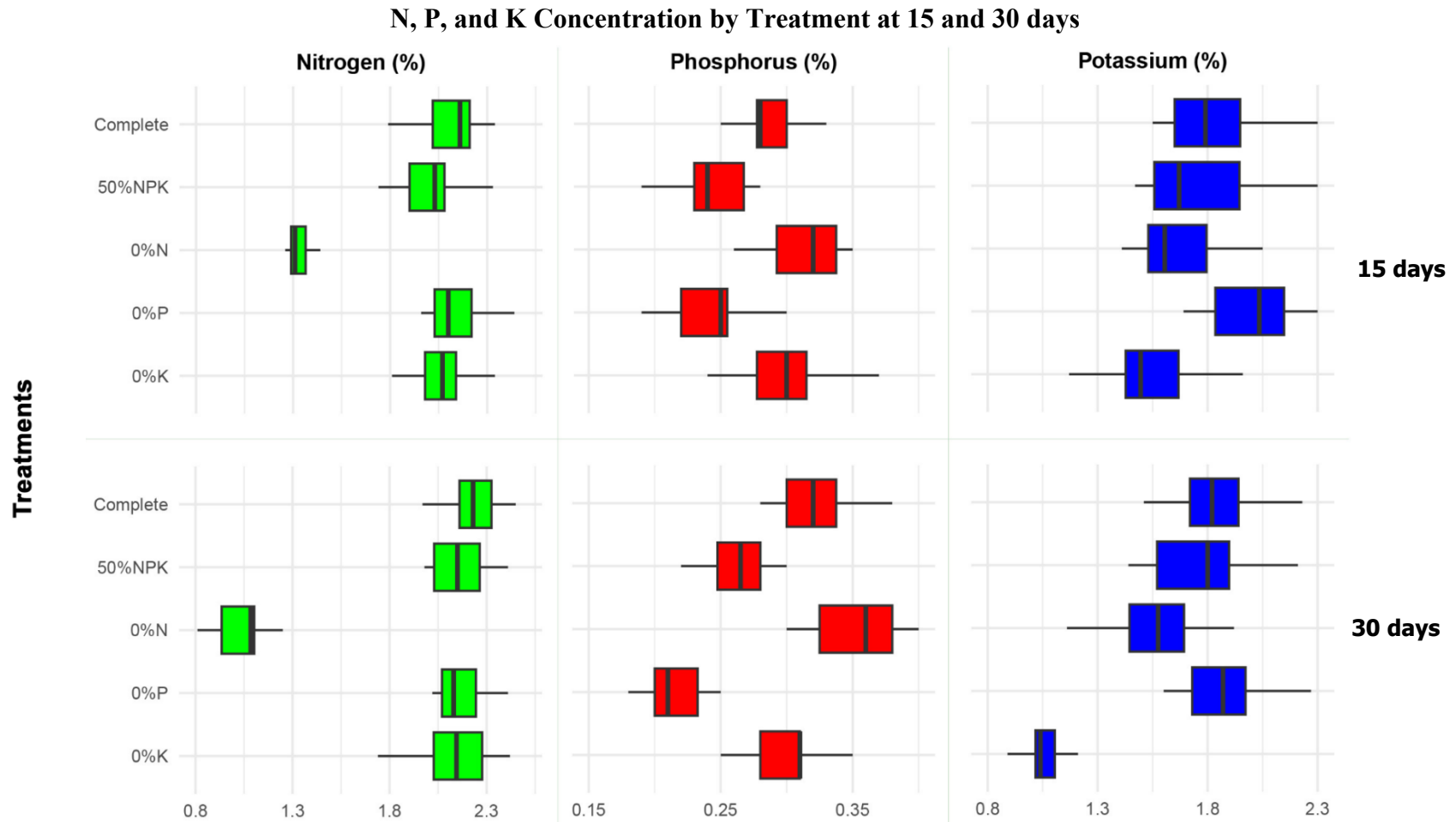


Figure 3.3 Box plots illustrate the variations in nitrogen, phosphorus, and potassium percentages in pine seedling foliage collected at 15 and 30 days. **Complete** = Complete HNS. **50%NPK** = Modified HNS with fifty percent nitrogen, phosphorus, and potassium. **0%N** = Modified HNS with zero percent nitrogen. **0%P** = Modified HNS with zero percent phosphorus. **0%K** = Modified HNS with zero percent potassium.

Table 3.4 Summary statistics of observed nutrient concentration of pine seedling foliage samples collected at 15 and 30 days post-treatments for samples used to build NIR models.

Nutrient	Unit	15-day Standard Nutrient Analysis					30-day Standard Nutrient Analysis				
		Min	Max	Mean	2 σ	Range within 2 σ	Min	Max	Mean	2 σ	Range within 2 σ
Nitrogen	%	1.07	2.80	1.96	0.80	(1.16, 2.76)	0.80	2.72	1.95	0.98	(0.97, 2.72)
Phosphorus	%	0.19	0.37	0.27	0.08	(0.19, 0.35)	0.20	0.49	0.29	0.12	(0.18, 0.41)
Potassium	%	1.17	2.93	1.77	0.59	(1.18, 2.35)	0.90	2.35	1.62	0.72	(0.91, 2.34)
Calcium	%	0.30	0.68	0.43	0.15	(0.30, 0.58)	0.30	0.70	0.46	0.18	(0.28, 0.64)
Magnesium	%	0.17	0.36	0.24	0.07	(0.17, 0.31)	0.20	0.36	0.25	0.08	(0.17, 0.34)
Sulfur	%	0.21	0.52	0.37	0.15	(0.21, 0.52)	0.20	0.62	0.39	0.17	(0.22, 0.57)
Iron	mg kg ⁻¹	30.20	632.00	62.06	153.61	(30.20, 215.67)	39.0	126.00	60.03	32.53	(39.30, 92.57)
Manganese	mg kg ⁻¹	167.00	387.00	262.89	84.21	(178.68, 347.10)	147.00	485.00	311.22	114.58	(196.64, 425.80)
Zinc	mg kg ⁻¹	14.30	41.00	26.46	12.64	(14.30, 39.10)	17.00	50.50	28.04	12.58	(17.00, 40.62)
Copper	mg kg ⁻¹	4.72	15.80	7.27	2.87	(4.72, 10.14)	4.70	10.30	7.40	2.41	(4.99, 9.81)
Boron	mg kg ⁻¹	29.40	66.20	48.78	12.97	(35.81, 61.74)	37.00	74.70	49.70	15.04	(37.00, 64.74)
Sodium	mg kg ⁻¹	0.04	0.21	0.09	0.06	(0.04, 0.16)	0.00	0.16	0.10	0.06	(0.04, 0.16)
Aluminum	mg kg ⁻¹	1.56	178.00	8.17	36.42	(1.56, 44.60)	2.70	14.30	6.22	4.97	(2.67, 11.20)
N:S	mg kg ⁻¹	2.90	12.60	5.52	2.90	(2.90, 8.42)	2.00	10.10	5.07	2.79	(2.28, 7.87)
N:K	mg kg ⁻¹	0.61	1.74	1.12	0.51	(0.61, 1.64)	0.50	2.39	1.26	0.91	(0.51, 2.18)
Fe:Mg	mg kg ⁻¹	0.10	1.96	0.24	0.52	(0.10, 0.75)	0.10	0.53	0.20	0.14	(0.11, 0.34)

Nutrient ratios provide additional insights into the evolving balance between nutrient pairs. The nitrogen-to-sulfur (N:S) ratio shows a slight decrease in maximum, suggesting a stable relationship over time, while the nitrogen-to-potassium (N:K) ratio expands, reflecting changes due to potassium's overall decrease. The iron-to-magnesium (Fe:Mn) ratio slightly narrows by 30 days.

Based on the values in Table 3.4, the observed ranges ($\pm 2\sigma$) for all nutrients and ratios indicate significant variability in both macronutrient and micronutrient concentration. Macronutrient concentrations exhibit two to three-fold variation at both growing stages, confirming that the nutrient treatments effectively created diverse nutrient conditions. Similarly, micronutrient ranges generally fall within two to three-fold variation, though iron at 15 days shows a much greater variability (~21-fold). These controlled yet substantial gradients are particularly well suited for assessing model sensitivity and predictive stability.

3.4.2 Models for Nutrient Concentration Using Intact Foliage

The nutrient concentration models for intact foliage samples provide valuable insights into the prediction accuracy and reliability when using the portable NIR spectrometers DLP Nano and Microphazir. Figure 3.4 compares the performance of these models (based on R^2_{cv}) for all nutrients at 15 and 30 days after treatment.

The results show varying degrees of model performance for different nutrients, with some models exhibiting moderate to strong predictive accuracy, particularly for key macronutrients such as nitrogen, potassium, and calcium. The effectiveness of these models can differ by nutrient and developmental stage, indicating that predicting most nutrients accurately in intact samples may be more challenging.

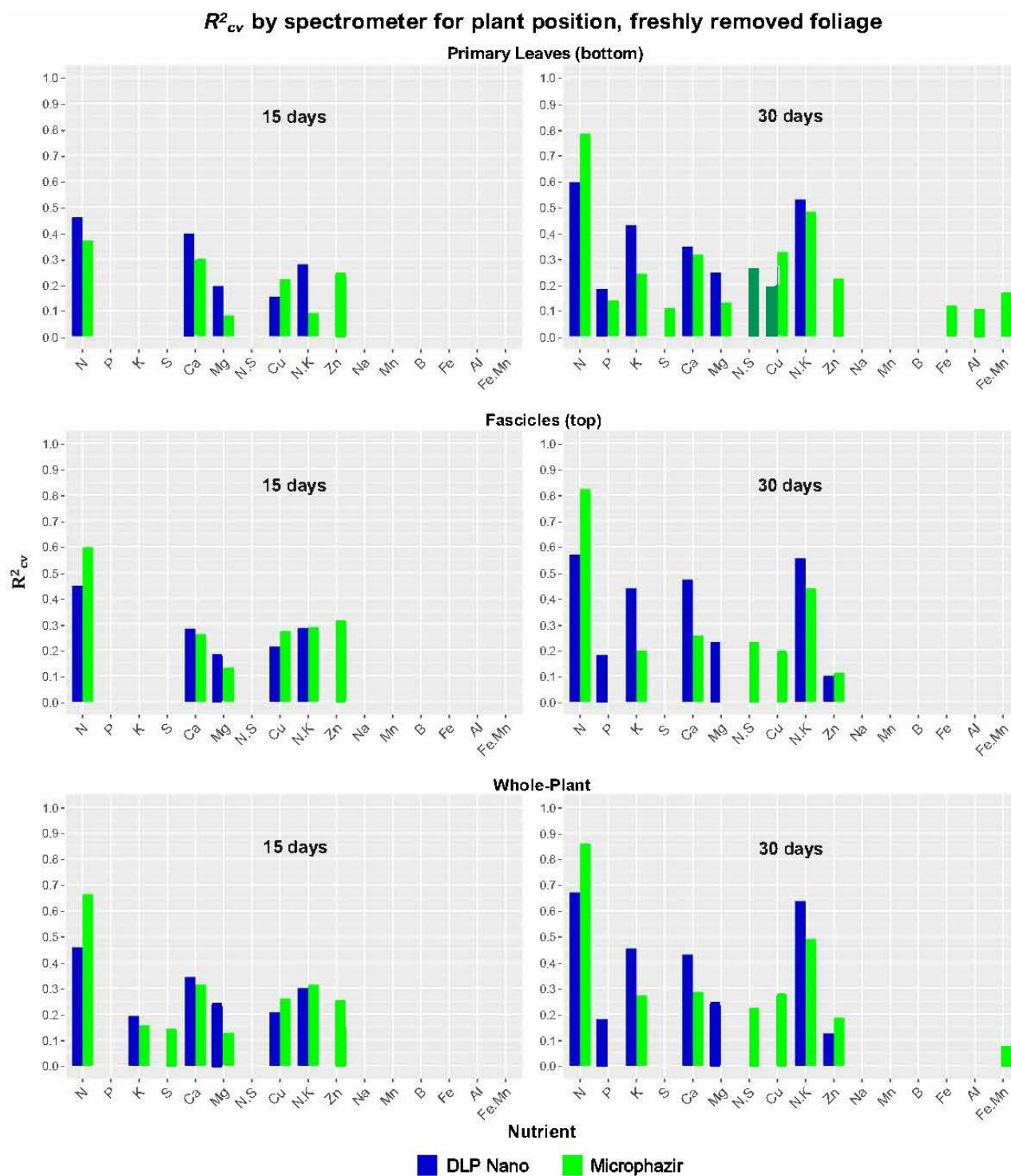


Figure 3.4 Bar charts comparing model performance comparison for all nutrients at 15- and 30-days post-treatment for the three datasets: Primary needles, Fascicles, and Whole-Plant, with spectra acquired using Microphazir and DLP Nano spectrometers.

3.4.2.1 Models at 15 Days Post-Treatment

At 15 days post-treatment, predictive performance varied considerably among nutrients and between spectrometers. The Microphazir spectrometer achieved moderately high predictive accuracy for nitrogen when whole-plant spectra were used ($R^2_{cv} = 0.66$), indicating fair predictability for nitrogen at this early growth stage. In contrast, nitrogen models developed with the DLP Nano exhibited weaker performance, with R^2_{cv} values below 0.50 across datasets. Predictability for potassium was low for both devices, with the DLP Nano reaching an R^2_{cv} of 0.19 for the whole-plant dataset and the Microphazir showing near-zero predictive accuracy.

Calcium models demonstrated moderately low predictive performance for both spectrometers, with R^2_{cv} values generally ranging between 0.30 and 0.40 across sampling positions. Similarly, the N:K ratio showed limited predictability, with R^2_{cv} values not exceeding 0.31 for either device. Most remaining nutrients, including phosphorus, magnesium, and trace elements such as iron and zinc, produced very low R^2_{cv} values (<0.30), indicating limited early-stage detectability under the conditions evaluated.

3.4.2.2 Models at 30 Days Post-Treatment

At 30 days post-treatment, model performance generally improved for several nutrients, particularly nitrogen. The Microphazir spectrometer achieved a substantially higher predictive accuracy for nitrogen using whole-plant spectra ($R^2_{cv} = 0.86$), indicating strong nitrogen detectability at this later growth stage. The DLP Nano also showed improved nitrogen performance, with R^2_{cv} increasing to 0.67, reflecting enhanced model accuracy as foliage matured.

Potassium prediction exhibited modest gains with the DLP Nano, reaching an R^2_{cv} of 0.45 for the whole-plant dataset, while potassium models developed with the Microphazir remained near zero. Calcium models showed slight improvement for the DLP Nano, with R^2_{cv} values increasing to 0.43, indicating moderate gains in predictive accuracy. The N:K ratio also demonstrated improved predictability at 30 days, with R^2_{cv} values of 0.49 for the Microphazir and 0.46 for the DLP Nano, suggesting better capture of nutrient balance in more developed foliage.

Despite these improvements, most other nutrients, including P, S, and micronutrients such as Zn and Mg, continued to exhibit low predictive accuracy, with R^2_{cv} values generally remaining below 0.30, indicating limited model performance for these constituents at this growth stage.

3.4.2.3 Comparison of Primary Needles, Fascicles, and Whole-Plant Spectral Datasets

For the 30-day models, the whole-plant (WP) dataset consistently produced higher R^2cv values than models developed using spectra from primary needles or fascicles alone, particularly for macronutrients such as nitrogen and potassium. Using the DLP Nano spectrometer, nitrogen predictability was strongest in the WP dataset ($R^2cv = 0.67$), whereas models based on primary needles and fascicles yielded R^2cv values below 0.50. Similarly, the Microphazir achieved its highest nitrogen performance using whole-plant spectra ($R^2cv = 0.86$), slightly outperforming models based on primary needles ($R^2cv = 0.78$) and fascicles ($R^2cv = 0.82$).

A comparable pattern was observed for potassium. The whole-plant dataset produced a modest improvement in potassium predictability using the DLP Nano ($R^2cv = 0.45$), while models based on primary needles and fascicles exhibited near-zero R^2cv values. For calcium, whole-plant spectra acquired with the DLP Nano also resulted in improved model performance ($R^2cv = 0.43$), compared with R^2cv values below 0.30 for the individual needle-position datasets. This suggests that aggregated spectral information better captures the overall nutrient status of the plant than localized needle measurements. The N:K ratio further benefited from spectral aggregation. Whole-plant models achieved R^2cv values of 0.46 for the DLP Nano and 0.49 for the Microphazir, both exceeding those obtained from primary needle and fascicle datasets, which remained below 0.35.

3.4.2.4 Comparison of Microphazir and DLP Nano Performance in Intact Foliage

Using the 30-day whole-plant dataset, the Microphazir spectrometer generally produced higher R^2cv values than the DLP Nano for several nutrients, most notably nitrogen. The Microphazir achieved a high R^2cv of 0.86 for nitrogen, indicating strong predictive performance at this growth stage. In comparison, the DLP Nano reached a moderate R^2cv of 0.67, reflecting improved nitrogen detectability relative to the 15-day models but not matching the performance of the Microphazir.

For potassium, the performance pattern differed between devices. The DLP Nano showed a modest improvement in whole-plant models, reaching an R^2cv of 0.45, whereas the Microphazir exhibited very low predictability for potassium across all sample locations, with R^2cv values near zero. Calcium models also favored the DLP Nano, which achieved a moderate R^2cv of 0.43 using whole-plant spectra, compared to a lower R^2cv of 0.31 for the Microphazir.

In contrast, the nitrogen-to-potassium (N:K) ratio was better predicted using the Microphazir, which achieved an R^2_{cv} of 0.49, slightly exceeding the DLP Nano value of 0.46.

3.4.3 Models for Nutrient Concentration in Dried and Ground Foliage

Models developed using dried and ground foliage exhibited higher predictive accuracy and greater consistency than those based on intact foliage. Figure 3.5 summarizes the performance of NIR models for all nutrients and nutrient ratios across the three spectrometers at both 15- and 30-days post-treatment. For key macronutrients, including nitrogen, phosphorus, and potassium, the resulting models achieved very good predictive performance, demonstrating the effectiveness of using dried samples for better nutrient determination.

3.4.3.1 Models at 15 Days Post-Treatment

At 15 days post-treatment, the Foss 6500 benchtop spectrometer produced the highest predictive accuracy across several key nutrients, consistently outperforming the two portable spectrometers, DLP Nano and Microphazir. Potassium exhibited the strongest model performance using the Foss 6500, achieving an R^2_{cv} of 0.84, followed by calcium with an R^2_{cv} of 0.80. Nitrogen also demonstrated promising predictability, with a moderately high R^2_{cv} of 0.78. Phosphorus showed moderate predictive capacity ($R^2_{cv} = 0.58$), while magnesium and sulfur achieved moderate accuracy with R^2_{cv} values of 0.72 and 0.65, respectively.

The portable spectrometers exhibited more limited predictive accuracy for most nutrients in the 15-day processed foliage models. For nitrogen, the DLP Nano achieved moderate predictability with an R^2_{cv} of 0.67, while the Microphazir showed comparable performance with an R^2_{cv} of 0.73. Calcium models developed using both portable devices exhibited moderately low accuracy, with R^2_{cv} values of 0.49 for the DLP Nano and 0.48 for the Microphazir. For the nitrogen-to-potassium (N:K) ratio, the Microphazir provided slightly better performance, achieving an R^2_{cv} of 0.41.

In contrast, most other nutrients, including potassium, magnesium, zinc, and sulfur, showed weak to very low predictive accuracy when modeled with the portable spectrometers, with R^2_{cv} values often below 0.30. Phosphorus and several trace elements, including aluminum, boron, iron, and manganese, exhibited no meaningful predictive capability at this stage, with R^2_{cv} values near zero.

3.4.3.2 Models at 30 Days Post-Treatment

At 30 days post-treatment, model performance improved, particularly for the Foss 6500 benchtop spectrometer, which achieved higher predictive accuracy across several key nutrients. Nitrogen showed the strongest performance, reaching an R^2_{cv} of 0.94, followed by potassium with an R^2_{cv} of 0.85 and phosphorus improving to 0.60. Calcium models also showed substantial improvement, with an R^2_{cv} of 0.74, while magnesium and sulfur maintained moderately reliable predictability.

The portable spectrometers demonstrated modest improvements at 30 days but remained less accurate than the Foss 6500. The DLP Nano nitrogen model increased to an R^2_{cv} of 0.67; however, predictions for potassium, phosphorus, and calcium remained weak, with R^2_{cv} values below 0.50. The Microphazir performed better for nitrogen, achieving an R^2_{cv} of 0.86, indicating improved detectability at this later stage. Despite this improvement, Microphazir models for phosphorus, potassium, and most micronutrients continued to show low predictive accuracy.

Figure 3.5 illustrates the comparison of model performance between 15- and 30-days post-treatment across all three spectrometers. While nutrient predictability improved at 30 days overall, the gains were most pronounced for the Foss 6500, particularly for nitrogen, phosphorus, potassium, and calcium. In contrast, the portable spectrometers showed limited improvement beyond nitrogen, highlighting continued challenges in predicting several nutrients in dried and ground foliage using handheld devices.

R^2_{cv} for Dried and Ground Foliage Samples (Processed)

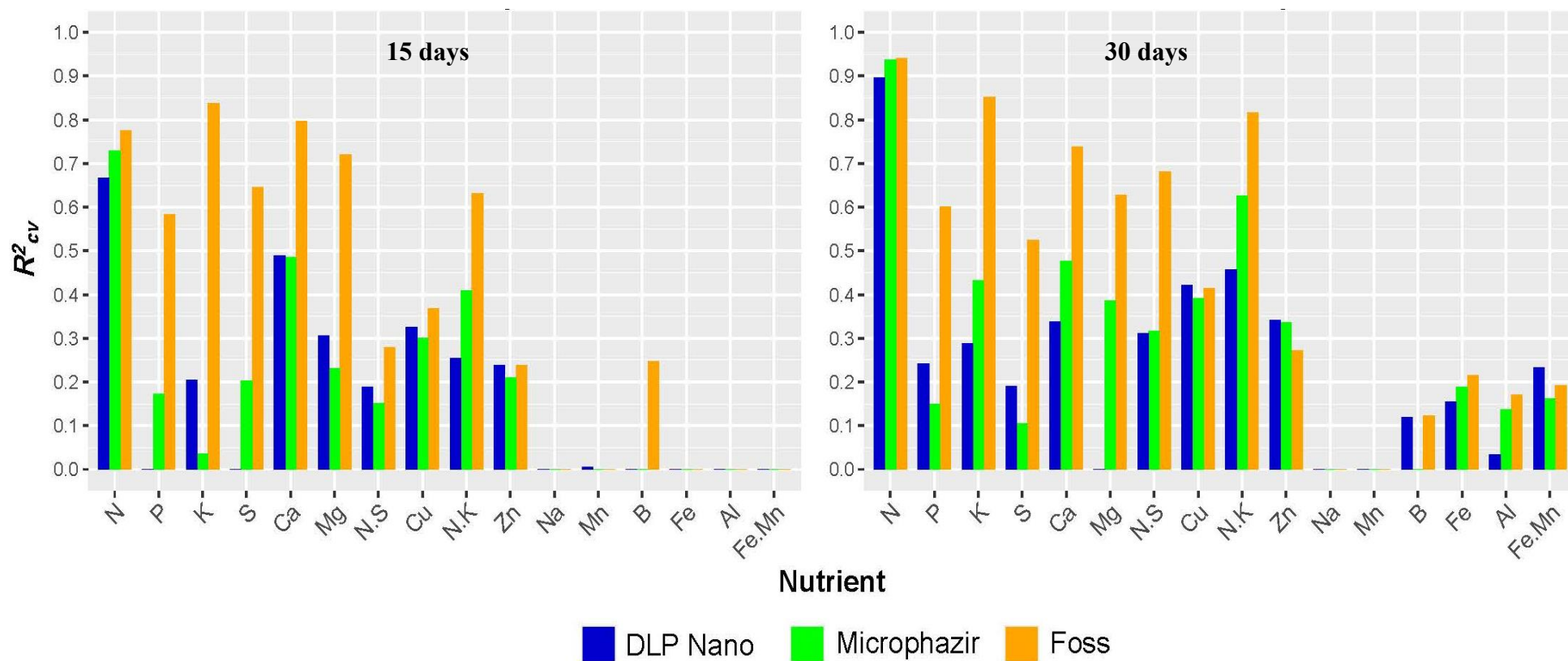


Figure 3.5 Bar charts displaying a model performance comparison for all nutrients at 15- and 30-days post-treatment of dried and ground samples with spectral data collected using Microphazir, DLP Nano spectrometers, and Foss 6500 spectrometers.

3.4.3.3 Comparison of Microphazir, DLP Nano, and Foss 6500 Performance

The Foss 6500 benchtop spectrometer consistently provided the highest predictive accuracy for nutrient concentration in dried and ground foliage samples, outperforming both portable spectrometers across most nutrients and growth stages. At 15 days post-treatment, Foss 6500 achieved moderate to strong predictive accuracy for nitrogen ($R^2_{cv} = 0.78$), potassium ($R^2_{cv} = 0.84$), and calcium ($R^2_{cv} = 0.80$). Magnesium ($R^2_{cv} = 0.72$) and sulfur ($R^2_{cv} = 0.65$) also showed moderate predictability. Model performance further improved at 30 days, with nitrogen reaching very high accuracy ($R^2_{cv} = 0.94$), potassium remaining high ($R^2_{cv} = 0.85$), and calcium maintaining strong predictability.

The portable spectrometers demonstrated moderate capability for nutrient prediction in processed foliage but were consistently less reliable than the Foss 6500. Nitrogen was the most reliably predicted nutrient using portable devices. At 15 days, DLP Nano achieved moderate nitrogen predictability ($R^2_{cv} = 0.67$), while Microphazir reached a moderately high R^2_{cv} of 0.73. By 30 days, nitrogen predictability improved further with the Microphazir, which achieved an R^2_{cv} of 0.86, indicating that nitrogen detection using portable spectrometers becomes more feasible as foliage matures.

For calcium, both DLP Nano and Microphazir showed moderately low predictive accuracy at 15 days, with R^2_{cv} values near 0.49, and only limited improvement at 30 days. Other nutrients, including potassium and the nitrogen-to-potassium (N:K) ratio, were predicted with weak to very low accuracy by the portable spectrometers, with R^2_{cv} values typically below 0.50 across both growth stages. These results highlight the superior performance of the benchtop spectrometer for processed samples, while also indicating that portable devices may be most effective for targeted nutrient prediction, particularly nitrogen, in later developmental stages.

3.4.3.4 Comparison of Portable Spectrometers: DLP Nano vs. Microphazir

The DLP Nano and Microphazir portable spectrometers demonstrated similar performance patterns across most nutrients. While the Microphazir occasionally achieved slightly higher predictive accuracy for selected nutrients, neither device consistently outperformed the other across all nutrient models. Overall, both spectrometers exhibited comparable strengths and shared similar limitations.

For nitrogen in dried and ground samples at 15 days post-treatment, both devices showed moderate predictive accuracy, with the DLP Nano achieving an R^2_{cv} of 0.67 and the Microphazir a slightly higher R^2_{cv} of 0.73. At 30 days, nitrogen predictability improved substantially for both spectrometers, with the Microphazir reaching an R^2_{cv} of 0.94 and the DLP Nano slightly lower at 0.90. These results indicate that both portable spectrometers are viable options for nitrogen detection in processed foliage, with the Microphazir showing marginally higher consistency, while the DLP Nano remains competitive.

For other nutrients, both spectrometers generally exhibited limited predictive accuracy. R^2_{cv} values for nutrients such as calcium, potassium, and magnesium were typically below moderate levels ($R^2_{cv} < 0.40$). The Microphazir showed slightly higher R^2_{cv} values for some elements, including calcium and copper, suggesting a minor advantage for these specific nutrients. However, both devices struggled to achieve strong predictive performance across a broader range of nutrients, particularly at the 15-day growth stage.

3.5 Discussion

Near-infrared spectroscopy (NIRS) has demonstrated strong potential as a rapid and accurate tool for real-time plant nutrient analysis (Prananto et al., 2021). Portable NIRS technology has emerged as a cost-effective alternative to conventional laboratory analyses, which are often labor-intensive, time-consuming, and expensive (García-Martínez et al., 2012; Azadnia et al., 2023). Previous studies have shown that portable NIR spectroscopy can be applied successfully to estimate macro- and micronutrient concentration in both fresh and detached leaves across a wide range of crops, including potato (Rawal et al., 2024), cotton (Prananto et al., 2021), cucumber (Zhang & Li, 2008), and apple trees (Azadnia et al., 2023).

For intact foliage, improved model performance was consistently achieved when spectra from both needle positions were combined to form whole-plant datasets. Models developed at the later growth stage, 30 days post-treatment, showed higher predictive accuracy than those developed at 15 days, for both intact foliage and dried and ground samples. In addition, the more intensive sample preparation associated with dried and ground foliage resulted in consistently higher predictive accuracy compared to intact foliage, reflecting reduced spectral noise and moisture-related interference. Across nutrients, the Foss 6500 benchtop spectrometer produced the most accurate and stable models, particularly for nitrogen, phosphorus, potassium, calcium, magnesium, and sulfur.

For nitrogen in intact foliage, high predictive accuracy was achieved using the Microphazir, with an R^2_{cv} of 0.86 and an $RMSEP_{cv}$ of 0.18. The DLP Nano also produced moderately accurate nitrogen models, with an R^2_{cv} of 0.67 and $RMSEP_{cv}$ of 0.28, indicating meaningful potential for nitrogen prediction using portable instrumentation. In contrast, phosphorus models derived from intact foliage were consistently weak for both portable spectrometers. This finding aligns with previous studies reporting strong NIR sensitivity to nitrogen-related absorbance features, particularly protein-related bands near 1490 nm and 1539 nm, while highlighting the persistent difficulty of predicting phosphorus using intact leaf spectra (McIlwee et al., 2001; Alwi et al., 2021).

For potassium, intact foliage spectra acquired with the DLP Nano produced moderately low predictive models ($R^2_{cv} = 0.45$, $RMSEP_{cv} = 0.26$), consistent with prior NIR studies

conducted on foliage from rice, corn, sesame, soybean, tea, grasses, and woody species using portable spectroradiometers (Zhai et al., 2013). While potassium prediction remained challenging, these results suggest that detectable spectral information is present, particularly when whole-plant datasets are used.

Previous work on hydroponically grown teak seedlings reported robust NIR models for nitrogen, phosphorus, and potassium using the Microphazir, with R^2_{cv} values exceeding 0.80 (Table 3.5). However, those authors also noted that reduced precision is expected when using portable devices on intact foliage due to increased environmental variability during spectral acquisition and the high-water content of fresh leaves (Whittier et al., 2021). These factors likely contributed to the lower and more variable performance observed in the present study for intact foliage models.

Both portable spectrometers produced moderate models for the nitrogen-to-potassium (N:K) ratio in intact foliage. The DLP Nano achieved an R^2_{cv} of 0.64 with an RMSEP_{cv} of 0.27, outperforming the Microphazir, which produced an R^2_{cv} of 0.49 and RMSEP_{cv} of 0.33. For calcium, the DLP Nano developed moderately low whole-plant models ($R^2_{cv} = 0.43$, RMSEP_{cv} = 0.07), suggesting limited but detectable sensitivity to this nutrient when aggregated spectra are used.}

Despite these successes, both portable spectrometers performed poorly for most remaining nutrients. Micronutrients such as aluminum, boron, copper, iron, magnesium, manganese, sodium, sulfur, and zinc are required by plants in relatively small concentrations, typically ranging from 0.1 to 100 mg kg⁻¹ of dry matter (Pandey, 2018). The low concentrations of these elements, combined with overlapping spectral features and high moisture content in intact foliage, likely constrained model development. As a result, predictive performance for individual micronutrients and ratios such as N:S and Fe:Mn varied considerably and remained generally low when using intact foliage spectra from portable devices.

Table 3.5 Comparison of NIRS fit statistics for nutrient levels of N, P, K, and Mg in teak (Whittier et al., 2021) and pine nursery material

Nutrient	<i>Teak</i>				<i>Pine</i>							
	Microphazir (¹ Intact)		Foss 6500 (² Processed)		Portable NIR (¹ Intact)				Foss 6500 (² Processed)			
					<i>15 days</i>		<i>30 days</i>		<i>15 days</i>		<i>30 days</i>	
	<i>R</i> ²	<i>RMSEP</i>	<i>R</i> ²	<i>RMSEP</i>	<i>R</i> ²	<i>RMSEP</i>	<i>R</i> ²	<i>RMSEP</i>	<i>R</i> ²	<i>RMSEP</i>	<i>R</i> ²	<i>RMSEP</i>
<i>N</i>	0.81	0.41	0.96	0.18	0.66	0.23	0.86	0.18	0.78	0.19	0.94	0.12
<i>P</i>	0.68	0.16	0.90	0.09	NA	NA	NA	NA	0.58	0.03	0.60	0.04
<i>K</i>	0.74	0.38	0.83	0.30	NA	NA	0.45	0.26	0.84	0.12	0.85	0.14
<i>Mg</i>	0.09	NA	0.51	NA	NA	NA	NA	NA	0.72	0.02	0.63	0.03

Spectra taken from ¹foliage (needles or leaves) still attached to the stem, and ² dried and ground foliage.

Most studies evaluating foliar nutrient concentration using NIR spectroscopy have focused on dried and ground leaf material, with comparatively fewer investigations using fresh leaves, whether intact or detached (Prananto et al., 2021). Several authors have reported that dried and ground samples generally yield better calibration performance than fresh foliage due to standardized moisture content and reduced particle-size variability. In addition, NIR spectroscopy conducted under laboratory conditions using benchtop instruments has been shown to outperform field-based measurements, largely due to reduced interference from external factors such as temperature fluctuations, moisture variability, solar radiation, and leaf orientation (Gillon et al., 1999; Whittier et al., 2021; Prananto et al., 2021).

The most accurate predictive models for nitrogen, phosphorus, and potassium were consistently derived from spectra collected 30 days post-treatment across all three spectrometers. In this study, spectra acquired using the Foss 6500 benchtop spectrometer produced the highest accuracy models for macronutrient prediction. Nitrogen models showed very high predictive performance, with an R^2_{cv} value of 0.94 and $RMSEP_{cv}$ of 0.12. Phosphorus models achieved moderate accuracy ($R^2_{cv} = 0.60$, $RMSEP_{cv} = 0.04$), while potassium models showed strong performance with an R^2_{cv} of 0.85 and $RMSEP_{cv}$ of 0.14. The strong nitrogen performance is consistent with findings reported by Gillon et al. (1999), who obtained highly accurate nitrogen models (R^2 ranging from 0.94 to 0.99) using *Pinus halepensis* needles collected from stands subjected to prescribed burning. However, while those authors also reported very strong phosphorus models ($R^2 \approx 0.95$), phosphorus prediction in the present study remained comparatively moderate. Potassium model performance aligns with results reported by Whittier et al. (2021) for teak foliage.

In contrast, the DLP Nano portable spectrometer produced a very strong nitrogen model in dried and ground foliage, achieving an R^2_{cv} of 0.90 and $RMSEP_{cv}$ of 0.16, indicating that portable instrumentation can effectively predict nitrogen under controlled laboratory conditions. However, the DLP Nano showed poor performance for phosphorus and potassium prediction, with weak models exhibiting R^2_{cv} values below 0.30.

The ability of both portable and benchtop NIR spectroscopy to predict nitrogen, phosphorus, and potassium using dried and ground foliage has been widely reported for several forest species, including teak (Whittier et al., 2021), *Eucalyptus pellita* (Alwi et al., 2021), *Populus*

spp. (Fernández-Martínez et al., 2017), and a broad range of hardwood and conifer species such as *Pinus halepensis*, *Pinus pinaster*, *Pinus pinea*, and *Pinus sylvestris* (Petisco et al., 2005; Gillon et al., 1999). Similar outcomes have also been reported for *Eucalyptus* species (McIlwee et al., 2001), reinforcing the robustness of NIRS for macronutrient prediction in processed foliage samples.

Analysis of dried and ground foliage further revealed that the Foss 6500 benchtop spectrometer produced reliable models for several micronutrients, including calcium, copper, magnesium, and sulfur, as well as nutrient ratios such as N:K and N:S, with predictive performance ranging from moderate to very strong. Using this instrument, the most reliable models for calcium, magnesium, and sulfur were obtained from spectra collected 15 days post-treatment. Calcium models achieved an R^2_{cv} of 0.80 with an RMSEP_{cv} of 0.03, magnesium models reached an R^2_{cv} of 0.72 with an RMSEP_{cv} of 0.02, and sulfur models achieved an R^2_{cv} of 0.65 with an RMSEP_{cv} of 0.04.

Despite these successes, suitable predictive models for the remaining micronutrients could not be developed using NIR spectra acquired with the Foss 6500, indicating the need for further investigation. This outcome is consistent with previous studies reporting limited predictive accuracy for many micronutrients, even when using high-resolution benchtop spectrometers (Whittier et al., 2021).

Spectral data collected using the Microphazir portable spectrometer produced moderately accurate calcium models in dried and ground foliage, with an R^2_{cv} of 0.48 and RMSEP_{cv} of 0.06. Similarly, spectra acquired with the DLP Nano produced moderate models for calcium, copper, and the N:S ratio. Calcium models yielded an R^2_{cv} of 0.49 with an RMSEP_{cv} of 0.05 using early-stage spectra, while copper and N:S ratio models achieved R^2_{cv} values of 0.42 and 0.46, respectively, with RMSEP_{cv} values of 0.91 and 0.34 using spectra collected 30 days post-treatment.

Near-infrared spectroscopy has inherent limitations in detecting analytes present at low concentrations, such as some micronutrients, due to low absorption coefficients and higher detection limits (Menezes et al., 2009). As a result, many models developed for micronutrients exhibited weak predictive performance, with most R^2_{cv} values below 0.30, and were therefore

excluded from further analysis. These limitations are well documented in NIR-based nutrient studies and are primarily attributed to low elemental concentrations in plant tissues and their minimal influence on NIR reflectance signals (Whittier et al., 2021; Prananto et al., 2021).

Additional challenges associated with NIRS, including low sensitivity, spectral noise, limited calibration ranges, interference from other chemical constituents, non-linearity, and matrix effects, further complicate the accurate detection of inorganic and organic compounds at low concentrations (Menezes et al., 2009). The small magnitude of spectral variation induced by micronutrients constrains model development and limits their practical applicability.

Despite these constraints, the fit statistics obtained for nitrogen, phosphorus, potassium, and magnesium in this study are comparable to, and in some cases exceed, those reported in previous NIRS investigations on hydroponically grown teak seedlings (Table 3.5), supporting the robustness of the developed models for key macronutrients.

3.6 Conclusion

In conclusion, Near-Infrared Spectroscopy (NIRS) technique emerges as a valuable tool capable of swiftly and accurately analyzing nitrogen levels in intact foliage of pine nursery seedlings by utilizing spectra collected with a portable spectrometer. However, for enhanced precision in predicting macronutrients such as nitrogen (N), phosphorus (P), potassium (K), calcium (Ca), magnesium (Mg), and the nitrogen-to-potassium (N:K) ratio, foliage samples from pine seedlings in advanced stages of nursery growth should undergo a process of drying and grinding, with spectra acquired using the laboratory-based Foss 6500 NIRSystems.

The decline in accuracy observed in models developed from intact foliage utilizing spectra collected with portable spectrometers underscores the existence of opportunities for refinement within this technique. Portable near-infrared spectroscopy, with its significant promise for *in situ* applications, serves as a valuable tool for guiding nutrient management decisions in nurseries, facilitating prompt and efficient nutrient analysis.

Future investigations should aim to establish a direct correlation between Near-Infrared Spectroscopy (NIRS) and nutrient management practices by developing models that leverage estimated plant nutrient status information to directly calculate fertilizer prescription rates tailored to the specific growth stage of pine seedlings. This targeted approach will not only contribute to advancing precision methodologies but also provide practical solutions for optimizing nutrient application in nursery environments.

3.7 References

- Acosta, J. J., Castillo, M. S., & Hodge, G. R. (2020). Comparison of benchtop and handheld near-infrared spectroscopy devices to determine forage nutritive value. *Crop Science*, *60*(6), 3410-3422. <https://doi-org.prox.lib.ncsu.edu/10.1002/csc2.20264>
- Alwi, A., Meder, R., Japarudin, Y., Hamid, H. A., Sanusi, R., & Mohd Yusoff, K. H. (2021). Near infrared spectroscopy of *Eucalyptus pellita* for foliar nutrients and the potential for real-time monitoring of trees in fertiliser trial plots. *Journal Of Near Infrared Spectroscopy*, *29*(3) 158 - 167. <https://doi-org.prox.lib.ncsu.edu/10.1177/09670335211007971>
- Azadnia, R., Rajabipour, A., Jamshidi, B., & Omid, M., (2023). New approach for rapid estimation of leaf nitrogen, phosphorus, and potassium contents in apple-trees using Vis/NIR spectroscopy based on wavelength selection coupled with machine learning. *Computers and Electronics in Agriculture*, *207*(1), 107746. <https://doi-org.prox.lib.ncsu.edu/10.1016/j.compag.2023.107746>
- Barnes, J., Whipker, B., McCall, I., & Frantz, J. (2012). Nutrient disorders of 'evolution' mealy-cup sage. *Hort Technology*, *22*(4), 502 - 508. <https://doi.org/10.21273/HORTTECH.22.4.502>
- Beć, K. B., Grabska, J., & Huck, C. W. (2021). Principles and Applications of Miniaturized Near-Infrared (NIR) Spectrometers. *Chemistry-A European Journal*, *27* (5) 1514-1532. <https://doi-org.prox.lib.ncsu.edu/10.1002/chem.202002838>
- Bhandari, N. (2018). Review: Techniques Used in Plant Tissue Analysis for Essential Elements on Horticultural Plants and Correlate with Nutrient. *North American Academic Research*, *1*(2), 94-113. <https://twasp.info/journal/Zq3423H/review-techniques-used-in-plant-tissue-analysis-for-essential-elements-on-horticultural-plants-and-correlate-with-nutrient-requirement>
- Breunig, M., Kriegel, H., Ng, R., & Sander, J. (2000). LOF: identifying density-based local outliers. *Sigmod Record*, *29*(2), 93-104. <https://doi-org.prox.lib.ncsu.edu/10.1145/335191.335388>
- Castillo, M. S., Acosta, J. J., Hodge, G. R., Vann, M. C., & Lewis, R. L. (2023). Analysis of alkaloids and reducing sugars in processed and unprocessed tobacco leaves using a handheld near infrared spectrometer. *Journal Of Near Infrared Spectroscopy*, *31*(2), 55 - 62. <https://doi-org.prox.lib.ncsu.edu/10.1177/09670335221148594>

- Castillo, M. S., Tiezzi, F., & Franzluebbers, A. J. (2020). Tree species effects on understory forage productivity and microclimate in a silvopasture of the Southeastern USA. *Agriculture, Ecosystems & Environment*, 295(1), 106917. <https://doi-org.prox.lib.ncsu.edu/10.1016/j.agee.2020.106917>
- Cen, H., & He, Y. (2007). Theory and application of near infrared reflectance spectroscopy in determination of food quality. *Trends in Food Science & Technology*, 18(2), 72 - 83. <https://doi-org.prox.lib.ncsu.edu/10.1016/j.tifs.2006.09.003>
- Diana, G., & Tommasi, C. (2002). Cross-validation methods in principal component analysis: A comparison. *Statistical Methods & Applications*, 11(1), 71-82. <https://doi.org/10.1007/BF02511446>
- Dvorak, W. S. (2000). Conservation & Testing of Tropical & Subtropical Forest Tree Species by the Camcore Cooperative. <https://www.camcore-ncsu.org/publications/#books>
- Fernández-Martínez, J., Joffre, R., Zacchini, M., Fernández-Marín, B., García-Plazaola, J. I., & Fleck, I. (2017). Near-infrared reflectance spectroscopy allows rapid and simultaneous evaluation of chloroplast pigments and antioxidants, carbon isotope discrimination and nitrogen content. *Forest Ecology And Management*, 399(1), 227 - 234. <https://doi-org.prox.lib.ncsu.edu/10.1016/j.foreco.2017.05.041>
- García-Martínez, S., Gálvez-Sola, L.N., Alonso, A., Agulló, E., Rubio, F., Ruiz, J. J., & Moral, R. (2012). Quality assessment of tomato landraces and virus-resistant breeding lines: quick estimation by near infrared reflectance spectroscopy. *Journal of the Science of Food and Agriculture*, 92(6), 1178-85. <https://doi.org/10.1002/jsfa.4661>
- Ge, S., Zhu, Z., Peng, L., Chen, Q., & Jiang, Y. (2018). Soil Nutrient Status and Leaf Nutrient Diagnosis in the Main Apple Producing Regions in China. *Horticultural Plant Journal*, 4(89-93), 89-93. <https://doi.org/10.1016/j.hpj.2018.03.009>
- Gillon, D., Houssard, C. & Joffre, R. (1999). Using Near-Infrared Reflectance Spectroscopy to Predict Carbon, Nitrogen and Phosphorus Content in Heterogeneous Plant Material. *Oecologia*, 118(2), 173-182.
- Grossnickle, S. C., & MacDonald, J. E. (2018). Why seedlings grow: influence of plant attributes. *New Forests*, 49(1), 1-34. <https://doi.org/10.1007/s11056-017-9606-4>

- Gullifa, G., Barone, L., Papa, E., Giuffrida, A., Materazzi, S., & Risoluti, R. (2023). Portable NIR spectroscopy: the route to green analytical chemistry. *Frontiers in Chemistry*, *11*(1), 1214825. <https://doi.org/10.3389/fchem.2023.1214825>
- Hoagland, D. R., & Arnon, D. I. (1950). The water-culture method for growing plants without soil. *Circular: California Agricultural Experiment Station*, *347*(1), 1-32. <https://archive.org/details/watercultureme3450hoag/page/n3/mode/2up>
- Hodge, G. R., Acosta, J. J., Unda, F., Woodbridge, W. C., & Mansfield, S. (2018). Global near infrared spectroscopy models to predict wood chemical properties of Eucalyptus. *Journal of Near Infrared Spectroscopy* *26*(2), 117-132. <https://doi-org.prox.lib.ncsu.edu/10.1177/0967033518770211>
- Hodge, G. R., & Dvorak, W. S. (2014). Breeding southern US and Mexican pines for increased value in a changing world. *New Forests*, *45*(3), 295–300. <https://doi.org/10.1007/s11056-014-9426-8>
- Hodge, G. R., & Dvorak, W. S. (2007). Variation in pitch canker resistance among provenances of *Pinus patula* and *Pinus tecunumanii* from Mexico and Central America. *New Forests*, *33*(2), 193–206. <https://doi.org/10.1007/s11056-006-9023-6>
- Kanzler, A., Nel, A., & Ford, C. (2014). Development and commercialization of the *Pinus patula* x *P. tecunumanii* hybrid in response to the threat of *Fusarium circinatum*. *New Forests*, *45*(3), 417-437. <https://doi.org/10.1007/s11056-014-9412-1>
- Landis, T. D. (2009). Nursery Practices . In F. T. Bonner& R. P. Karrfalt (Eds.), *The Woody Plant Seed Manual* (1st ed., pp. 125-145). U.S. Department of Agriculture, Forest Service.
- Leary, P. E., Crocombe, R. A., & Kammrath, B. W. (2021). Introduction to Portable Spectroscopy. In R. A. Crocombe, P. E. Leary, B. W. Kammrath, H. C. Lee, R. A. Crocombe, & P. E. Leary (Eds.), *Portable Spectroscopy and Spectrometry 1*, (1st ed., pp 1-13). Wiley.
- Mbinga, J. M., Omondi, S. F., & Onyango, A. A. (2019). Conifers: Species diversity and improvement status in Kenya. In A. C. Gonçalves & T. Fonseca (Eds.) *Conifers-Recent Advances*, (1st ed., 1-242). IntechOpen.

- McIlwee, A. M., Lawler, I. R., Cork, S. J., & Foley, W. J. (2001). Marsupials, Coping with Chemical Complexity in Mammal-Plant Interactions: Near-Infrared Spectroscopy as a Predictor of *Eucalyptus* Foliar Nutrients and of the Feeding Rates of Folivorous. *Oecologia*, 128(4), 539-548.
- Menezes, J. C., Ferreira, A. P., Rodrigues L. O., Brás, L. P., & Alves, T. P. (2009). Chemometrics Role within the PAT Context: Examples from Primary Pharmaceutical Manufacturing. In S. D. Brown, R. Tauler & W. Beata (Eds.), *Comprehensive Chemometrics* (1st ed. pp. 313-355). Elsevier. <https://doi-org.prox.lib.ncsu.edu/10.1016/B978-044452701-1.00012-0>
- Mevik, B. & Wehrens, R. (2016). Introduction to the pls Package. *The Comprehensive R Archive Network*. <https://cran.r-project.org/web/packages/pls/vignettes/pls-manual.pdf>
- Pandey, N. (2018). Role of Plant Nutrients in Plant Growth and Physiology. In: *Plant Nutrients and Abiotic Stress Tolerance*. Singapur: Springer Singapore (1st ed. pp. 51-93. https://doi.org/10.1007/978-981-10-9044-8_2
- Perez, I. M., Cruz-Tirado, L. J., Badaro, A. T., de Oliveira, M. M., & Barbin, D. F. (2019). Present and future of portable/handheld near-infrared spectroscopy in chicken meat industry. *NIR News*, 30(5-6), 26-29. <https://doi.org/10.1177/0960336019861476>
- Petisco, C., García-Criado, B., Vázquez de Aldana, B. R., Zabalgoceazcoa, I., Mediavilla, S., & Garcia-Ciudad, A. (2005). Use of near-infrared reflectance spectroscopy in predicting nitrogen, phosphorus and calcium contents in heterogeneous woody plant species. *Analytical And Bioanalytical Chemistry*, 382(1) 458-465.
- Pimstein, A., Karnieli, A., Bansal, S. K., & Bonfil, D. J. (2011). Exploring Remotely Sensed Technologies for Monitoring Wheat Potassium and Phosphorus Using Field Spectroscopy. *Field Crops Research*, 121(1), 125-135. <https://doi-org.prox.lib.ncsu.edu/10.1016/j.fcr.2010.12.001>
- Prananto, J. A., Minasny, B., & Weaver, T. (2021). Rapid and cost-effective nutrient content analysis of cotton leaves using near-infrared spectroscopy (NIRS). *PeerJ*, 9(1), <https://doi.org/10.7717/peerj.11042>

- Rawal, A., Hartemink, A., Zhang, Y., Wang, Y., Lankau, R. A., & Ruark, M. D. (2024). Visible and near-infrared spectroscopy predicted leaf nitrogen contents of potato varieties under different growth and management conditions. *Precision Agriculture*, 25(2), 751-770. <https://doi.org/10.1007/s11119-023-10091-z>
- Whittier, W. A., Hodge, G. R., Lopez, J., Saravitz, C., & Acosta, J. J. (2021). Near Infrared Spectroscopy Studies of Teak Grown Under Varying Levels of Nitrogen, Phosphorus and Potassium. *Journal Of Near Infrared Spectroscopy*, 29(5) 301-310. <https://doi-org.prox.lib.ncsu.edu/10.1177/09670335211025649>
- Zhai, Y., Cui, L., Zhou, X., Gao, Y., Fei, T., & Gao, W. (2013). Estimation of nitrogen, phosphorus, and potassium contents in the leaves of different plants using laboratory-based visible and nearinfrared reflectance spectroscopy: comparison of partial least-square regression and support vector machine regression meth. *International Journal of Remote Sensing*, 34(7), 2502–2518. <https://doi-org.prox.lib.ncsu.edu/10.1080/01431161.2012.746484>
- Zhang, W., Kasun, L. C., Wang, Q. J., Zheng, Y., & Lin, Z. (2022). A Review of Machine Learning for Near-Infrared Spectroscopy. *Sensors*, 22(24), 9764. <https://doi.org/10.3390/s22249764>
- Zhang, X. & Li, M. (2008). Analysis and Estimation of the Phosphorus Content in Cucumber Leaf in Greenhouse by Spectroscopy. *Spectroscopy and Spectral Analysis*, 10(1), 2404-2408. <https://pubmed.ncbi.nlm.nih.gov/19123417/>

CHAPTER 4

Thesis Conclusions

4.1 Scope

The primary goal of this study was to evaluate the potential of Near-Infrared Spectroscopy (NIRS) for predicting macronutrient and micronutrient concentrations in nursery-grown pine and eucalypt seedlings. Specifically, the study aimed to develop and assess predictive models using NIR spectra acquired with portable spectrometers, including the Microphazir (Thermo Fisher Scientific) and the DLP NIRscan Nano EVM (Texas Instruments), as well as a laboratory-based benchtop spectrometer, the Foss NIRSystems 6500 (Foss).

The research was conducted using nursery stock material of *Pinus tecunumanii* and *Eucalyptus urophylla* × *Eucalyptus grandis* grown hydroponically under controlled greenhouse conditions at North Carolina State University. Seedlings were subjected to five nutrient regimes that primarily varied nitrogen, phosphorus, and potassium concentrations, while maintaining a complete solution containing essential micronutrients.

NIR spectra were collected from intact and freshly removed foliage using the two portable spectrometers. Following spectral acquisition from intact pine needles, the entire foliage of each seedling was harvested, dried, and ground to a fine particle size. A second set of NIR spectra was then collected from the processed samples using the Foss 6500 benchtop spectrometer. In addition, spectra from the dried and ground samples were also acquired through the glass covers of the Foss spinning-sample module cups using the two portable spectrometers. Spectral data were collected at two growth stages, 15 and 30 days after treatment initiation. After each spectral acquisition, all foliage samples, both fresh and processed, were labeled and submitted to the North Carolina Department of Agriculture & Consumer Services (NCDA&CS) for standard laboratory nutrient analysis.

Raw NIR spectra were pre-processed using a range of mathematical transformations to reduce noise and account for variation associated with leaf structure and measurement conditions. Outliers were identified and removed from each dataset prior to model development. Partial Least Squares (PLS) regression was used to develop predictive models relating spectral data to observed nutrient concentrations obtained from standard laboratory analysis. Model performance was

evaluated using cross-validated coefficients of determination (R^2_{cv}) and cross-validated root mean squared error of prediction (RMSEP_{cv}), providing a consistent framework for assessing predictive accuracy across species, growth stages, sample preparation methods, and spectrometer types.

4.2 Key Findings

Across both species and experimental conditions, combining spectra from multiple plant locations improved predictive accuracy. Whole-plant spectral datasets consistently produced stronger and more stable models than spectra collected from individual plant sections, supporting the objective of establishing effective protocols for NIR spectral acquisition that capture spatial variability in nutrient distribution.

4.2.1 Freshly removed leaves of eucalypt seedlings

Consistent with the objective of evaluating portable NIR spectrometers for rapid nutrient assessment, Chapter 2 demonstrated that both the Microphazir and DLP Nano can be used to predict selected nutrients in freshly removed eucalypt foliage, with clear differences in performance between devices.

The Microphazir produced highly accurate nitrogen models at both time points. At 15 days post-treatment, the nitrogen model achieved an R^2_{cv} of 0.91, with a slight reduction to 0.82 at 30 days. These results demonstrate that the Microphazir can reliably track nitrogen status across developmental stages, supporting its use for real-time nutrient assessment in nursery systems. The DLP Nano generated lower, but still useful, nitrogen models, with R^2_{cv} values of 0.73 at 15 days and 0.59 at 30 days, indicating acceptable performance for early-stage nitrogen monitoring.

Phosphorus prediction with the Microphazir improved at the later growth stage, reaching an R^2_{cv} of 0.64 at 30 days, whereas potassium prediction remained weak ($R^2_{cv} = 0.25$). The DLP Nano exhibited reduced predictive capability for phosphorus ($R^2_{cv} = 0.40$ at 30 days) and consistently low accuracy for potassium at both stages, indicating limited suitability for these nutrients using either device.

The Microphazir also demonstrated good predictive capability for sulfur, calcium, and magnesium at 15 days post-treatment, with R^2_{cv} values of 0.74, 0.63, and 0.62, respectively. The DLP Nano produced moderately lower R^2_{cv} values for the same nutrients (0.61 for sulfur, 0.54 for

calcium, and 0.57 for magnesium), suggesting that while usable models can be developed, performance remains inferior to that of the Microphazir.

The Microphazir consistently produced stronger nutrient models for freshly removed eucalypt leaves, particularly for nitrogen and selected secondary macronutrients. The DLP Nano provided moderate predictability for nitrogen and sulfur but showed limited utility for phosphorus, potassium, and most micronutrients.

4.2.2 Intact needles of pine seedlings

In alignment with the objective of evaluating non-destructive, in situ nutrient assessment, Chapter 3 focused on nutrient prediction using NIR spectra collected from intact, still-attached pine needles.

The Microphazir demonstrated stronger nitrogen predictability across both growth stages. At 15 days, nitrogen models achieved an R^2_{cv} of 0.66, increasing substantially to 0.86 at 30 days. This improvement indicates enhanced nitrogen detectability as seedlings matured and highlights the effectiveness of the Microphazir for in situ nitrogen assessment.

Nitrogen models developed with the DLP Nano were weaker at 15 days ($R^2_{cv} = 0.46$) but improved at 30 days ($R^2_{cv} = 0.67$). Although these results indicate increasing predictability with plant development, nitrogen models generated with the DLP Nano remained less accurate than those produced with the Microphazir.

Both spectrometers showed limited performance for potassium and other nutrients in intact foliage. For the Microphazir, potassium models yielded R^2_{cv} values below 0.30 at both time points. The DLP Nano exhibited negligible potassium predictability at 15 days, with modest improvement at 30 days ($R^2_{cv} = 0.45$), though accuracy remained insufficient for practical application.

These results highlight the suitability of the Microphazir for non-destructive nitrogen monitoring in pine seedlings, particularly at later growth stages. While phosphorus and potassium prediction remains challenging in intact foliage, nitrogen models demonstrate that portable NIR spectroscopy can support operational nutrient monitoring where rapid and repeated measurements are required.

4.2.3 Dried and ground needles of pine seedlings

To address the objective of comparing sample preparation methods and instrument types, Chapter 3 also evaluated nutrient prediction using dried and ground pine needles analyzed with portable and benchtop spectrometers.

The Microphazir demonstrated strong nitrogen predictability in processed samples, achieving an R^2_{cv} of 0.73 at 15 days and 0.94 at 30 days. The DLP Nano also produced high nitrogen models at 30 days ($R^2_{cv} = 0.90$), though with lower accuracy at 15 days ($R^2_{cv} = 0.67$).

These results confirm that portable spectrometers can reliably predict nitrogen when sample moisture and particle size are standardized.

The Foss 6500 benchtop spectrometer produced the most accurate nitrogen models, achieving R^2_{cv} values of 0.78 at 15 days and 0.94 at 30 days. These results confirm the advantage of benchtop instrumentation for nitrogen prediction in processed foliage.

For phosphorus and potassium, both portable spectrometers showed limited predictive capability. The Microphazir produced a moderately accurate potassium model at 30 days ($R^2_{cv} = 0.43$), while the DLP Nano generated weak models for both nutrients ($R^2_{cv} < 0.30$). In contrast, the Foss 6500 produced substantially stronger models, with R^2_{cv} values of 0.84 and 0.85 for potassium at 15 and 30 days, and R^2_{cv} values of 0.58 and 0.60 for phosphorus.

Calcium and magnesium models followed a similar pattern. Portable devices yielded moderately low accuracy ($R^2_{cv} \approx 0.48$ – 0.49), whereas the Foss 6500 achieved R^2_{cv} values exceeding 0.70 for both nutrients, indicating greater reliability across a wider nutrient range..

From an applied perspective, the Microphazir emerged as the most effective portable option for nitrogen monitoring in both fresh and processed foliage. The Foss 6500 remains the preferred instrument for detailed nutrient profiling across multiple elements, while the DLP Nano may be suitable for basic nitrogen assessments where simplicity and cost are prioritized.

4.3 Significance of the Results and Implications for Nursery Operations

This study demonstrates that portable Near-Infrared Spectroscopy (NIRS) has clear potential as a practical tool for nursery operations, offering a rapid and non-destructive approach

for monitoring foliar nutrient status in forestry seedlings. In particular, portable NIR spectrometers showed strong capability for assessing nitrogen and provided useful predictive performance for phosphorus, calcium, magnesium, and sulfur, supporting their application in operational nutrient monitoring within nursery environments.

The ability to acquire spectra directly from intact or freshly removed foliage enables in situ assessment of nutrient status, reducing reliance on time-consuming and costly laboratory analyses. This approach allows nursery managers to monitor nutrient dynamics more frequently and adjust fertilization practices in a timely manner, potentially improving nutrient-use efficiency and reducing fertilizer inputs and associated costs. Given the strong agreement observed between NIR-based nitrogen models and standard laboratory measurements, portable NIRS offers a reliable alternative for repeated nitrogen assessments during the seedling production cycle.

Importantly, this study highlights that accurate NIR-based nutrient prediction depends on appropriate sampling strategies. Combining spectra from multiple sections of the plant to generate whole-plant datasets consistently improved model performance compared to spectra collected from individual leaf pairs or needle positions. This finding has direct operational relevance, as it provides clear guidance on how spectra should be collected to maximize predictive accuracy while minimizing destructive sampling.

Together, these results indicate that portable NIR spectrometers can support more informed, data-driven nutrient management in nursery operations. By enabling rapid, non-invasive monitoring across growth stages, NIRS has the potential to enhance decision-making, improve seedling nutritional quality, and support more efficient and sustainable nursery management practices.

4.4 Limitations of the Results and Implications

This study demonstrates the practical potential of Near-Infrared Spectroscopy (NIRS) for real-time, non-destructive assessment of foliar nutrient status in forestry seedlings. The central premise—that portable NIR spectrometers can provide operationally useful predictions for key nutrients, particularly nitrogen—was supported. However, the results also reveal important limitations that constrain the broader applicability of the technique, especially for micronutrient prediction.

Several factors limited model performance across nutrients. These include restricted spectral sensitivity for certain analytes, low signal strength associated with nutrients present at low concentrations, increased spectral noise during data acquisition, and spectral interference from other foliar components. In addition, the relatively narrow concentration ranges observed for some nutrients, particularly at later growth stages, reduced the ability of calibration models to resolve meaningful variation. Together, these factors limited the predictability of several target nutrients despite consistent modeling approaches.

The inability to develop useful models for micronutrients such as sodium, iron, manganese, zinc, copper, boron, aluminum, and the Fe:Mn ratio highlights a key limitation of NIRS in this context. These elements occur at low concentrations and contribute weakly to near-infrared absorbance, making them difficult to detect reliably using standard portable NIR instrumentation. Improving predictability for these nutrients may require enhanced spectral preprocessing, alternative mathematical transformations, expanded calibration datasets with greater concentration variability, or the application of different modeling techniques beyond conventional PLS regression.

These limitations have important implications for operational use. While portable NIR spectrometers show clear value for monitoring macronutrients and selected secondary nutrients, particularly nitrogen, they should not be viewed as replacements for laboratory analysis when comprehensive micronutrient profiling is required. Instead, NIRS is best positioned as a complementary tool, supporting rapid screening and targeted decision-making, while laboratory analyses remain necessary for nutrients that fall below the effective detection limits of current NIR systems.

4.5 Recommendations

This study indicates that Near-Infrared Spectroscopy (NIRS) shows strong potential as a decision-support tool for nutrient monitoring in nursery production systems, particularly for nitrogen and selected secondary nutrients. Portable NIR spectrometers may be effectively integrated into nursery operations to support rapid, non-destructive assessments of seedling nutrient status, enabling more timely adjustments to fertilization practices and reducing reliance on repeated laboratory analyses for macronutrient monitoring.

For operational use, emphasis should be placed on collecting spectra that represents the whole plant rather than isolated foliage segments, as whole-plant datasets consistently yielded stronger and more stable predictive models. In addition, NIR-based assessments are most effective when applied at growth stages characterized by greater nutrient variability, where spectral differences are more pronounced and model sensitivity is enhanced.

Future research should focus on improving model performance for nutrients that exhibited weak predictability, particularly micronutrients. This may include exploring advanced spectral pre-processing strategies, refining calibration datasets to better capture physiological variation, and evaluating alternative regression and machine-learning approaches that may improve sensitivity to low-concentration analytes. Further validation under operational nursery and field conditions would also strengthen confidence in the transferability and robustness of portable NIR applications beyond controlled environments.

Together, these efforts can help position NIRS as a practical and complementary tool for nursery nutrient management, supporting more efficient, responsive, and data-informed fertilization strategies in forestry production systems.

APPENDICES

Appendix A. Fit Statistics for PLS Regression Models Predicting Foliar Nutrient Concentration in Freshly Removed Eucalypt Leaves

Stage	Location	Spectrometer	Nutrient	Transformation	Factors	R ² cal	RMSEPCal	R ² cv	RMSEPCv	ExpVarY	ExpVarX
15	P1	Microphazir	N	DT	5	0.86	0.39	0.81	0.45	85.56	97.49
15	P1	Microphazir	P	SNV	5	0.00	0.00	0.13	0.06	0.00	0.00
15	P1	Microphazir	K	SNV	3	0.00	0.00	0.07	0.32	0.00	0.00
15	P2	Microphazir	N	SNV	8	0.94	0.25	0.88	0.35	94.08	98.72
15	P2	Microphazir	P	SG7	2	0.00	0.00	0.13	0.06	0.00	0.00
15	P2	Microphazir	K	DT	1	0.22	0.29	0.16	0.30	22.47	40.56
15	P3	Microphazir	N	SNV_SG7	4	0.87	0.37	0.81	0.45	86.84	95.83
15	P3	Microphazir	P	NIR	8	0.00	0.00	0.15	0.06	0.00	0.00
15	P3	Microphazir	K	SNV	1	0.29	0.28	0.24	0.28	28.95	52.67
15	P4	Microphazir	N	NIR	7	0.85	0.40	0.79	0.47	85.00	99.86
15	P4	Microphazir	P	MSC_DT	5	0.00	0.00	0.12	0.06	0.00	0.00
15	P4	Microphazir	K	DT	1	0.26	0.28	0.21	0.29	26.13	48.03
15	G12	Microphazir	N	SNV	7	0.94	0.25	0.90	0.33	93.87	98.98
15	G12	Microphazir	P	MSC	5	0.00	0.00	0.13	0.06	0.00	0.00
15	G12	Microphazir	K	DT	1	0.14	0.30	0.10	0.31	14.30	59.16
15	G23	Microphazir	N	SNV_SG7	4	0.87	0.37	0.81	0.45	86.84	95.83
15	G23	Microphazir	P	NIR	6	0.00	0.00	0.13	0.06	0.00	0.00
15	G23	Microphazir	K	SNV	1	0.29	0.28	0.24	0.28	28.95	52.67
15	G34	Microphazir	N	NIR	7	0.85	0.40	0.79	0.47	85.00	99.86
15	G34	Microphazir	P	MSC_DT	5	0.00	0.00	0.12	0.06	0.00	0.00
15	G34	Microphazir	K	DT	1	0.26	0.28	0.21	0.29	26.13	48.03
15	G123	Microphazir	N	SNV	8	0.95	0.22	0.92	0.29	95.39	99.23
15	G123	Microphazir	P	MSC	1	0.12	0.06	0.09	0.06	11.96	96.90
15	G123	Microphazir	K	DT	1	0.28	0.28	0.23	0.29	28.23	39.98
15	G234	Microphazir	N	SG7	5	0.93	0.28	0.89	0.34	92.53	97.62
15	G234	Microphazir	P	MSC_DT	4	0.00	0.00	0.12	0.06	0.00	0.00
15	G234	Microphazir	K	DT	1	0.30	0.27	0.25	0.28	30.03	52.79
15	WP	Microphazir	N	SNV_SG7	4	0.93	0.27	0.91	0.30	93.27	96.23
15	WP	Microphazir	K	DT	1	0.30	0.27	0.25	0.28	30.24	45.65
15	WP	Microphazir	P	MSC	1	0.13	0.06	0.10	0.06	13.20	96.96

Appendix A. Fit Statistics for PLS Regression Models Predicting Foliar Nutrient Concentration in Freshly Removed Eucalypt Leaves (*continued*)

Stage	Location	Spectrometer	Nutrient	Transformation	Factors	R ² cal	RMSEPCal	R ² cv	RMSEPCv	ExpVarY	ExpVarX
15	P1	DLP_Nano	N	MSC	6	0.74	0.53	0.60	0.65	73.93	98.31
15	P1	DLP_Nano	P	NIR	4	0.00	0.00	0.00	0.06	0.00	0.00
15	P1	DLP_Nano	K	NIR	7	0.00	0.00	0.08	0.32	0.00	0.00
15	P2	DLP_Nano	N	MSC	4	0.70	0.57	0.64	0.62	69.69	96.16
15	P2	DLP_Nano	P	SNV	2	0.00	0.00	0.18	0.06	0.00	0.00
15	P2	DLP_Nano	K	SNV	1	0.10	0.31	0.06	0.32	10.41	69.37
15	P3	DLP_Nano	N	DT	4	0.72	0.54	0.64	0.62	71.99	94.62
15	P3	DLP_Nano	P	MSC_DT	5	0.00	0.00	0.07	0.06	0.00	0.00
15	P3	DLP_Nano	K	DT	1	0.28	0.28	0.24	0.29	27.61	51.92
15	P4	DLP_Nano	N	NIR	6	0.75	0.51	0.64	0.62	75.27	99.87
15	P4	DLP_Nano	P	MSC_DT	14	0.00	0.00	0.02	0.06	0.00	0.00
15	P4	DLP_Nano	K	DT	1	0.20	0.29	0.17	0.30	20.21	53.04
15	G12	DLP_Nano	N	DT	4	0.75	0.52	0.68	0.58	74.86	91.84
15	G12	DLP_Nano	P	MSC_DT	4	0.00	0.00	0.10	0.06	0.00	0.00
15	G12	DLP_Nano	K	SNV	2	0.17	0.30	0.08	0.31	16.62	87.11
15	G23	DLP_Nano	N	DT	4	0.72	0.54	0.64	0.62	71.99	94.62
15	G23	DLP_Nano	P	MSC_DT	5	0.00	0.00	0.07	0.06	0.00	0.00
15	G23	DLP_Nano	K	DT	1	0.28	0.28	0.24	0.29	27.61	51.92
15	G34	DLP_Nano	N	NIR	6	0.75	0.51	0.64	0.62	75.27	99.87
15	G34	DLP_Nano	P	MSC_DT	14	0.00	0.00	0.02	0.06	0.00	0.00
15	G34	DLP_Nano	K	DT	1	0.20	0.29	0.17	0.30	20.21	53.04
15	G123	DLP_Nano	N	NIR	7	0.79	0.47	0.72	0.55	79.21	99.96
15	G123	DLP_Nano	P	MSC_DT	5	0.00	0.00	0.08	0.06	0.00	0.00
15	G123	DLP_Nano	K	DT	1	0.27	0.28	0.21	0.29	27.10	24.58
15	G234	DLP_Nano	N	SNV	4	0.76	0.50	0.71	0.55	76.08	97.98
15	G234	DLP_Nano	P	DT	5	0.00	0.00	0.12	0.06	0.00	0.00
15	G234	DLP_Nano	K	DT	1	0.26	0.28	0.22	0.29	26.04	43.81
15	WP	DLP_Nano	N	DT	4	0.79	0.47	0.73	0.53	78.82	96.18
15	WP	DLP_Nano	K	DT	1	0.27	0.28	0.22	0.29	26.59	32.49
15	WP	DLP_Nano	P	MSC	4	0.00	0.00	0.05	0.06	0.00	0.00

Appendix A. Fit Statistics for PLS Regression Models Predicting Foliar Nutrient Concentration in Freshly Removed Eucalypt Leaves (*continued*)

Stage	Location	Spectrometer	Nutrient	Transformation	Factors	R ² cal	RMSEPCal	R ² cv	RMSEPCv	ExpVarY	ExpVarX
30	P1	Microphazir	N	MSC_SG7	5	0.77	0.25	0.53	0.36	77.39	96.19
30	P1	Microphazir	P	DT	5	0.52	0.04	0.26	0.05	52.18	93.31
30	P1	Microphazir	K	MSC_SG5	1	0.00	0.00	0.00	0.41	0.00	0.00
30	P2	Microphazir	N	SNV	7	0.79	0.24	0.71	0.29	79.16	99.28
30	P2	Microphazir	P	DT	4	0.64	0.04	0.59	0.04	64.36	95.98
30	P2	Microphazir	K	DT	4	0.00	0.00	0.00	0.41	0.00	0.00
30	P3	Microphazir	N	MSC_SG7	5	0.81	0.23	0.74	0.27	81.34	97.09
30	P3	Microphazir	P	NIR	8	0.73	0.03	0.61	0.04	72.53	99.96
30	P3	Microphazir	K	SG5	1	0.00	0.00	0.00	0.41	0.00	0.00
30	P4	Microphazir	N	SNV	7	0.83	0.22	0.74	0.27	82.77	99.18
30	P4	Microphazir	P	MSC	5	0.41	0.05	0.28	0.05	40.76	98.34
30	P4	Microphazir	K	SNV	2	0.00	0.00	0.00	0.40	0.00	0.00
30	G12	Microphazir	N	SNV	7	0.79	0.24	0.72	0.28	79.46	99.36
30	G12	Microphazir	P	MSC	6	0.63	0.04	0.53	0.04	62.60	99.27
30	G12	Microphazir	K	MSC_DT	2	0.00	0.00	0.00	0.41	0.00	0.00
30	G23	Microphazir	N	MSC_SG7	5	0.81	0.23	0.74	0.27	81.34	97.09
30	G23	Microphazir	P	NIR	8	0.73	0.03	0.61	0.04	72.53	99.96
30	G23	Microphazir	K	SG5	1	0.00	0.00	0.00	0.41	0.00	0.00
30	G34	Microphazir	N	SNV	7	0.83	0.22	0.74	0.27	82.77	99.18
30	G34	Microphazir	P	MSC	5	0.41	0.05	0.28	0.05	40.76	98.34
30	G34	Microphazir	K	SNV	2	0.00	0.00	0.00	0.40	0.00	0.00
30	G123	Microphazir	N	SNV	7	0.85	0.21	0.79	0.24	84.59	99.35
30	G123	Microphazir	P	NIR	8	0.73	0.03	0.64	0.04	72.82	99.98
30	G123	Microphazir	K	MSC_DT	2	0.00	0.00	0.00	0.41	0.00	0.00
30	G234	Microphazir	N	DT	7	0.86	0.20	0.80	0.24	86.10	98.80
30	G234	Microphazir	P	NIR	8	0.73	0.03	0.64	0.04	72.68	99.97
30	G234	Microphazir	K	SNV_SG5	1	0.00	0.00	0.00	0.41	0.00	0.00
30	WP	Microphazir	N	MSC_SG7	5	0.87	0.19	0.82	0.22	86.95	95.99
30	WP	Microphazir	P	NIR	8	0.72	0.03	0.64	0.04	71.54	99.98
30	WP	Microphazir	K	DT	2	0.00	0.00	0.01	0.40	0.00	0.00

Appendix A. Fit Statistics for PLS Regression Models Predicting Foliar Nutrient Concentration in Freshly Removed Eucalypt Leaves (*continued*)

Stage	Location	Spectrometer	Nutrient	Transformation	Factors	R ² cal	RMSEPCal	R ² cv	RMSEPCv	ExpVarY	ExpVarX
30	P1	DLP_Nano	N	NIR	1	0.14	0.49	0.05	0.52	14.39	49.70
30	P1	DLP_Nano	P	MSC_DT	5	0.00	0.00	0.13	0.06	0.00	0.00
30	P1	DLP_Nano	K	MSC	2	0.00	0.00	0.00	0.41	0.00	0.00
30	P2	DLP_Nano	N	SNV	9	0.86	0.20	0.36	0.42	85.64	98.75
30	P2	DLP_Nano	P	NIR	5	0.43	0.04	0.27	0.05	42.99	99.78
30	P2	DLP_Nano	K	DT_SG5	2	0.00	0.00	0.07	0.39	0.00	0.00
30	P3	DLP_Nano	N	SNV	10	0.90	0.17	0.43	0.40	89.54	99.02
30	P3	DLP_Nano	P	DT	4	0.33	0.05	0.20	0.05	32.78	90.68
30	P3	DLP_Nano	K	MSC	1	0.00	0.00	0.00	0.41	0.00	0.00
30	P4	DLP_Nano	N	NIR	3	0.47	0.38	0.42	0.40	47.32	98.83
30	P4	DLP_Nano	P	NIR	11	0.00	0.00	0.07	0.06	0.00	0.00
30	P4	DLP_Nano	K	NIR	1	0.00	0.00	0.00	0.41	0.00	0.00
30	G12	DLP_Nano	N	SNV	6	0.53	0.36	0.26	0.45	52.98	98.51
30	G12	DLP_Nano	P	DT	6	0.59	0.04	0.35	0.05	59.14	97.76
30	G12	DLP_Nano	K	NIR	1	0.00	0.00	0.00	0.41	0.00	0.00
30	G23	DLP_Nano	N	SNV	10	0.90	0.17	0.43	0.40	89.54	99.02
30	G23	DLP_Nano	P	DT	4	0.33	0.05	0.20	0.05	32.78	90.68
30	G23	DLP_Nano	K	MSC	1	0.00	0.00	0.00	0.41	0.00	0.00
30	G34	DLP_Nano	N	NIR	3	0.47	0.38	0.42	0.40	47.32	98.83
30	G34	DLP_Nano	P	NIR	11	0.00	0.00	0.07	0.06	0.00	0.00
30	G34	DLP_Nano	K	NIR	1	0.00	0.00	0.00	0.41	0.00	0.00
30	G123	DLP_Nano	N	MSC	10	0.88	0.18	0.48	0.38	88.38	99.55
30	G123	DLP_Nano	P	DT	6	0.60	0.04	0.40	0.05	59.55	98.38
30	G123	DLP_Nano	K	MSC	2	0.00	0.00	0.00	0.41	0.00	0.00
30	G234	DLP_Nano	N	SNV	8	0.83	0.22	0.56	0.35	83.34	99.47
30	G234	DLP_Nano	P	NIR	10	0.76	0.03	0.38	0.05	76.08	99.97
30	G234	DLP_Nano	K	MSC	2	0.00	0.00	0.00	0.41	0.00	0.00
30	WP	DLP_Nano	N	SNV	10	0.89	0.18	0.59	0.34	88.73	99.62
30	WP	DLP_Nano	P	SNV	8	0.74	0.03	0.39	0.05	74.41	99.51
30	WP	DLP_Nano	K	SNV	2	0.00	0.00	0.00	0.41	0.00	0.00

Appendix A. Fit Statistics for PLS Regression Models Predicting Foliar Nutrient Concentration in Freshly Removed Eucalypt Leaves (*continued*)

Stage	Location	Spectrometer	Nutrient	Transformation	Factors	R ² cal	RMSEPCal	R ² cv	RMSEPCv	ExpVarY	ExpVarX
15	WP	Microphazir	S	SG7	4	0.79	0.02	0.74	0.02	79.21	97.18
15	WP	Microphazir	Ca	MSC_SG7	3	0.69	0.13	0.63	0.15	68.63	98.38
15	WP	Microphazir	Mg	MSC_SG7	3	0.67	0.03	0.62	0.04	66.85	98.41
15	WP	Microphazir	N.S	MSC_SG7	3	0.65	1.53	0.58	1.67	65.19	98.44
15	WP	Microphazir	Cu	SG7	4	0.63	2.83	0.55	3.12	63.24	97.17
15	WP	Microphazir	N.K	SG7	4	0.60	0.50	0.52	0.55	60.49	97.14
15	WP	Microphazir	Zn	DT	1	0.30	4.95	0.26	5.08	29.50	46.48
15	WP	Microphazir	Na	DT_SG7	2	0.29	0.08	0.23	0.08	28.97	93.43
15	WP	Microphazir	Fe	MSC_SG5	1	0.22	16.20	0.19	16.56	22.33	67.57
15	WP	Microphazir	B	SNV	1	0.18	5.18	0.12	5.38	18.17	29.94
15	WP	Microphazir	Al	MSC	4	0.00	0.00	0.14	4.82	0.00	0.00
15	WP	Microphazir	Fe.Mn	NIR	1	0.00	0.00	0.06	0.15	0.00	0.00
15	WP	Microphazir	Mn	DT_SG5	1	0.00	0.00	0.05	36.97	0.00	0.00
15	WP	DLP_Nano	S	MSC	4	0.68	0.03	0.61	0.03	68.12	98.01
15	WP	DLP_Nano	Mg	NIR	4	0.61	0.04	0.57	0.04	60.77	99.67
15	WP	DLP_Nano	Ca	NIR	4	0.59	0.15	0.54	0.16	58.79	99.68
15	WP	DLP_Nano	N.S	SG7	2	0.65	1.54	0.51	1.81	64.58	38.17
15	WP	DLP_Nano	Cu	DT	4	0.49	3.34	0.38	3.68	48.88	96.39
15	WP	DLP_Nano	Zn	DT	1	0.26	5.08	0.21	5.23	25.73	35.36
15	WP	DLP_Nano	N.K	DT	1	0.22	0.70	0.18	0.71	22.25	36.66
15	WP	DLP_Nano	Na	SNV	1	0.21	0.08	0.16	0.09	20.76	70.61
15	WP	DLP_Nano	Al	MSC_DT	3	0.00	0.00	0.03	5.13	0.00	0.00
15	WP	DLP_Nano	B	NIR	4	0.00	0.00	0.14	5.31	0.00	0.00
15	WP	DLP_Nano	Fe	SNV	2	0.00	0.00	0.15	16.91	0.00	0.00
15	WP	DLP_Nano	Fe.Mn	NIR	2	0.00	0.00	0.00	0.15	0.00	0.00
15	WP	DLP_Nano	Mn	SNV	1	0.00	0.00	-0.01	38.11	0.00	0.00

Appendix A. Fit Statistics for PLS Regression Models Predicting Foliar Nutrient Concentration in Freshly Removed Eucalypt Leaves (*continued*)

Stage	Location	Spectrometer	Nutrient	Transformation	Factors	R ² cal	RMSEPCal	R ² cv	RMSEPCv	ExpVarY	ExpVarX
30	WP	Microphazir	S	DT	4	0.60	0.03	0.57	0.03	59.84	89.02
30	WP	Microphazir	Ca	SG7	3	0.48	0.13	0.43	0.14	48.11	96.24
30	WP	Microphazir	Mg	NIR	3	0.42	0.04	0.38	0.04	41.64	94.89
30	WP	Microphazir	N.S	DT	5	0.42	1.75	0.31	1.91	42.43	97.84
30	WP	Microphazir	Mn	DT_SG7	3	0.44	35.21	0.30	39.32	43.90	92.23
30	WP	Microphazir	Na	DT	1	0.25	0.15	0.20	0.15	24.60	53.64
30	WP	Microphazir	Zn	DT	1	0.23	4.62	0.18	4.78	22.98	46.24
30	WP	Microphazir	N.K	DT	1	0.13	0.93	0.07	0.95	12.74	53.42
30	WP	Microphazir	Cu	MSC_SG7	1	0.09	2.84	0.05	2.90	8.63	82.47
30	WP	Microphazir	Al	MSC_DT	7	0.00	0.00	0.10	5.08	0.00	0.00
30	WP	Microphazir	B	MSC_DT	2	0.00	0.00	0.03	5.19	0.00	0.00
30	WP	Microphazir	Fe	DT_SG7	4	0.00	0.00	0.11	20.94	0.00	0.00
30	WP	Microphazir	Fe.Mn	SG7	2	0.00	0.00	0.10	0.20	0.00	0.00
30	WP	DLP_Nano	Ca	SNV	2	0.44	0.14	0.40	0.14	43.66	91.60
30	WP	DLP_Nano	S	SNV	2	0.39	0.03	0.35	0.03	38.71	91.82
30	WP	DLP_Nano	Mg	SNV	2	0.34	0.05	0.30	0.05	34.36	91.69
30	WP	DLP_Nano	Na	DT	1	0.18	0.16	0.12	0.16	17.51	46.45
30	WP	DLP_Nano	N.S	DT	1	0.08	2.22	-0.01	2.32	7.54	29.21
30	WP	DLP_Nano	Al	MSC	1	0.00	0.00	-0.02	6.01	0.00	0.00
30	WP	DLP_Nano	B	MSC	2	0.00	0.00	-0.01	6.40	0.00	0.00
30	WP	DLP_Nano	Cu	MSC_DT	3	0.00	0.00	0.08	2.85	0.00	0.00
30	WP	DLP_Nano	Fe	MSC_DT	2	0.00	0.00	0.05	21.61	0.00	0.00
30	WP	DLP_Nano	Fe.Mn	SNV	4	0.00	0.00	0.09	0.19	0.00	0.00
30	WP	DLP_Nano	Mn	NIR	4	0.00	0.00	0.01	46.85	0.00	0.00
30	WP	DLP_Nano	N.K	SNV	2	0.00	0.00	0.05	0.96	0.00	0.00
30	WP	DLP_Nano	Zn	NIR	18	0.00	0.00	0.17	4.79	0.00	0.00

Appendix B(a). Standard laboratory foliar nutrient concentrations for the **complete HNS regime** at **15 days post-treatment**.

Treatments	N	P	K	Ca	Mg	S	Fe	Mn	Zn	Cu	B	Na	Al	N:S	N:K	Fe:Mn
Complete	3.47	0.22	1.45	1.26	0.41	0.24	82.6	176	31.8	19	33	0.51	8.51	14.4	2.39	0.47
Complete	3.3	0.21	1.67	1.29	0.4	0.2	89.8	115	30.7	15.3	25.6	0.29	12.4	16.2	1.97	0.78
Complete	3.64	0.25	1.85	1.6	0.44	0.25	94.9	115	38.4	21.4	31.3	0.31	6.96	14.7	1.97	0.83
Complete	4.16	0.27	1.86	1.6	0.5	0.28	98.1	157	35.1	24.9	31.5	0.42	4.45	14.7	2.23	0.62
Complete	3.82	0.23	1.84	1.26	0.43	0.29	83.4	92.7	35.1	21	38.2	0.37	11.7	13.1	2.07	0.9
Complete	4.2	0.27	1.85	1.25	0.42	0.26	111	157	38	24.2	25.4	0.31	5.03	15.9	2.27	0.71
Complete	3.62	0.23	1.95	1.38	0.44	0.24	73.1	101	29.7	18.1	24.6	0.37	4.05	15	1.85	0.72
Complete	3.66	0.23	1.77	1.26	0.38	0.27	81.9	145	33.7	20	33.8	0.32	5.16	13.4	2.07	0.57
Complete	4.04	0.22	1.78	1.32	0.38	0.24	83.2	159	34.1	19.7	30.3	0.28	7.22	17.2	2.27	0.52
Complete	4.12	0.27	1.62	1.24	0.37	0.28	100	167	36	19.1	20.4	0.46	8.52	14.5	2.54	0.6
Complete	3.37	0.22	1.79	1.33	0.43	0.23	112	158	32.7	16.6	34.5	0.41	22.5	15	1.88	0.71
Complete	4.08	0.25	1.86	1.55	0.45	0.24	80.1	182	30	19.6	31.9	0.31	6.9	16.8	2.19	0.44
Complete	4.81	0.32	2.43	1.27	0.37	0.27	95.4	119	35	16.1	22.4	0.33	4.76	18	1.98	0.8
Complete	3.28	0.2	1.79	1.19	0.37	0.23	73.8	156	24	17.7	26.2	0.4	6.29	14.1	1.83	0.47
Complete	4.11	0.26	1.61	1.36	0.38	0.26	82.3	128	36.7	17	21.6	0.5	3.94	15.5	2.55	0.64
Complete	4.64	0.25	1.76	1.48	0.41	0.24	106	166	37.7	23.9	39.8	0.33	3.66	19.3	2.64	0.64
Complete	4.28	0.27	1.72	1.44	0.41	0.25	104	190	30.3	14.2	28.5	0.42	8.49	17.2	2.49	0.55
Complete	4.21	0.23	2.02	1.09	0.38	0.24	74.6	157	29.2	18.9	23.5	0.26	4.79	17.7	2.08	0.48
Complete	4.19	0.22	2.21	1.24	0.34	0.2	133	145	34	21.2	30.5	0.5	6.89	20.6	1.89	0.92
Complete	3.51	0.24	1.53	1.42	0.39	0.26	136	173	26.1	20.2	28.2	0.46	22.6	13.7	2.29	0.79

Appendix B(b). Standard laboratory foliar nutrient concentrations for the **50% NPK HNS regime** at **15 days post-treatment**.

Treatments	N	P	K	Ca	Mg	S	Fe	Mn	Zn	Cu	B	Na	Al	N:S	N:K	Fe:Mn
50%NPK	2.9	0.22	1.83	1.41	0.48	0.19	139	227	39.2	10.2	25.9	0.35	17.9	15.4	1.58	0.61
50%NPK	2.64	0.16	1.84	0.95	0.33	0.17	107	150	35.4	10.8	22.6	0.34	9.55	15.4	1.43	0.71
50%NPK	3.25	0.2	2.03	1.44	0.37	0.24	112	219	42.3	9.63	35.7	0.15	5.34	13.7	1.6	0.51
50%NPK	3	0.22	1.84	1.43	0.4	0.22	104	224	31.5	12.5	22.9	0.44	10.7	13.8	1.63	0.47
50%NPK	2.7	0.23	1.69	1.21	0.42	0.21	91.8	206	30.7	11.8	19.9	0.31	4.88	13.1	1.6	0.45
50%NPK	3.55	0.21	1.79	1.36	0.39	0.22	113	120	36.4	7.26	33.1	0.52	12.6	15.8	1.99	0.95
50%NPK	2.91	0.2	1.37	1.32	0.35	0.17	99.5	206	34.4	11.6	24.5	0.35	12.1	16.9	2.12	0.48
50%NPK	2.77	0.19	1.43	1.2	0.34	0.18	95.8	175	35.6	12.2	24.9	0.24	5.89	15.1	1.94	0.55
50%NPK	2.83	0.24	1.67	1.58	0.43	0.22	133	260	42.3	11.3	32.3	0.38	9.91	13.1	1.7	0.51
50%NPK	2.75	0.19	1.76	1.09	0.32	0.19	104	150	31.5	8.25	22.2	0.34	4.4	14.3	1.56	0.69
50%NPK	2.35	0.19	1.69	1.38	0.42	0.16	68.8	176	25	7.8	26	0.24	10.8	15.1	1.39	0.39
50%NPK	2.15	0.16	1.69	1.21	0.35	0.16	74.3	133	33.6	9.46	25.8	0.29	17.7	13.3	1.28	0.56
50%NPK	1.95	0.13	1.26	1	0.26	0.16	107	166	22.9	8.03	28.3	0.37	30.9	12	1.54	0.64
50%NPK	2.9	0.2	1.86	1.35	0.4	0.2	116	146	35.4	13.9	33	0.33	7.69	14.2	1.56	0.79
50%NPK	2.94	0.2	1.99	1.04	0.36	0.21	94.4	224	32.2	10.1	20.7	0.38	7.45	14.1	1.48	0.42
50%NPK	2.83	0.21	1.61	1.27	0.38	0.18	121	215	30.2	10	21.5	0.36	7.93	16.1	1.76	0.56
50%NPK	3.13	0.23	2.03	1.4	0.41	0.23	113	236	28.8	11.7	25	0.33	12.8	13.5	1.54	0.48
50%NPK	2.68	0.22	1.79	1.17	0.37	0.21	149	242	38.7	11.9	32.5	0.4	20.2	13	1.5	0.62
50%NPK	3.26	0.26	1.96	1.37	0.46	0.26	123	265	53.4	13.9	21.1	0.39	7.04	12.6	1.66	0.46
50%NPK	3.95	0.27	1.76	1.33	0.4	0.28	127	230	43.5	12.6	26.8	0.39	6.38	14.3	2.25	0.55

Appendix B(c). Standard laboratory foliar nutrient concentrations for the **10% N HNS regime** at **15 days post-treatment**.

Treatments	N	P	K	Ca	Mg	S	Fe	Mn	Zn	Cu	B	Na	Al	N:S	N:K	Fe:Mn
10%N	1.34	0.17	1.42	0.66	0.26	0.16	72.2	177	28	6.77	26.7	0.24	19.2	8.51	0.94	0.41
10%N	1.76	0.24	1.19	0.77	0.3	0.16	113	185	28.7	10.9	18.7	0.3	7.21	11	1.48	0.61
10%N	1.63	0.25	1.46	1.04	0.36	0.15	78.8	179	28.8	9.59	21.5	0.26	15.6	10.6	1.12	0.44
10%N	1.48	0.21	1.14	0.88	0.33	0.14	62.7	186	24.7	7.36	19.5	0.24	7.6	10.5	1.3	0.34
10%N	1.92	0.26	1.44	0.96	0.35	0.19	95.6	134	31.3	12.1	17.9	0.25	6.04	10.3	1.33	0.71
10%N	1.4	0.17	1.01	0.67	0.25	0.2	62.9	168	22.4	7.38	29.3	0.39	10.6	7.16	1.39	0.38
10%N	1.75	0.26	1.28	0.82	0.32	0.16	91.9	207	28.7	9.53	19.1	0.33	3.86	10.7	1.37	0.44
10%N	1.71	0.23	1.1	0.8	0.31	0.16	69.6	180	28	11.8	18.1	0.31	7.8	10.9	1.56	0.39
10%N	1.2	0.12	1.01	0.64	0.25	0.15	66.5	152	23.2	7	29	0.24	18.7	7.91	1.19	0.44
10%N	1.52	0.2	1.41	0.89	0.34	0.16	70.7	163	36.7	12.4	28.2	0.25	14.5	9.48	1.08	0.43
10%N	1.7	0.29	1.59	1.02	0.34	0.13	92.9	189	29.1	10.6	19.3	0.19	5.29	12.6	1.07	0.49
10%N	1.89	0.28	1.46	0.92	0.34	0.14	80.4	172	33.3	11.8	22.9	0.25	6.92	13.2	1.29	0.47
10%N	2.05	0.32	1.89	1.28	0.44	0.16	80.4	226	32.2	13.4	28.6	0.2	9.06	13.2	1.09	0.36
10%N	1.8	0.26	1.3	0.94	0.3	0.19	83.8	209	28.7	11.5	25.1	0.34	2.94	9.67	1.38	0.4
10%N	2.49	0.32	1.46	1	0.38	0.19	67.9	141	35.8	13.5	30.1	0.38	7.42	13.3	1.71	0.48
10%N	1.85	0.29	1.62	0.92	0.36	0.19	76.1	199	31.5	11.6	22.9	0.3	3.83	9.51	1.14	0.38
10%N	1.48	0.2	1.1	0.72	0.28	0.14	123	101	25.6	6.93	19.1	0.26	6.13	10.9	1.34	1.22
10%N	1.16	0.1	1	0.43	0.2	0.11	54.2	114	19.8	6.21	23.8	0.19	14.7	10.4	1.17	0.47
10%N	1.58	0.21	1.47	0.81	0.31	0.14	66.2	198	27.5	11	22.3	0.2	5.19	11	1.08	0.33
10%N	1.75	0.23	1.47	0.9	0.35	0.15	59.2	166	24.5	12	21	0.21	5.82	11.8	1.2	0.36

Appendix B(d). Standard laboratory foliar nutrient concentrations for the **10% P HNS regime** at **15 days post-treatment**.

Treatments	N	P	K	Ca	Mg	S	Fe	Mn	Zn	Cu	B	Na	Al	N:S	N:K	Fe:Mn
10%P	3.54	0.16	1.65	0.97	0.4	0.21	72.2	143	26.7	14.6	37.8	0.32	14.3	16.6	2.14	0.5
10%P	3.15	0.1	1.39	1.23	0.43	0.19	70.6	188	30.3	13	29.9	0.26	13.3	16.4	2.27	0.38
10%P	3.6	0.14	1.78	1.21	0.5	0.23	100	241	39	15.9	29	0.29	6.92	15.6	2.02	0.42
10%P	3.49	0.15	1.44	1.27	0.44	0.23	79.3	187	34.3	19.2	32	0.56	5.59	15.4	2.43	0.42
10%P	3.43	0.14	2.01	1.21	0.36	0.23	92.9	238	35.8	17.8	27.3	0.24	6.24	15.1	1.71	0.39
10%P	3.5	0.15	2.1	1.27	0.44	0.23	86.7	215	42.3	20.1	28.9	0.35	10.7	15.1	1.66	0.4
10%P	3.69	0.12	1.76	1.22	0.43	0.22	84.1	197	40.6	16	34.3	0.29	9.32	16.7	2.1	0.43
10%P	2.55	0.08	1.42	0.82	0.3	0.17	87.5	154	24.1	9.39	32.7	0.49	16.9	14.6	1.8	0.57
10%P	3.67	0.15	1.98	1.31	0.45	0.26	91.9	249	42.8	20.5	29.9	0.36	15.2	14.2	1.85	0.37
10%P	4.08	0.15	1.63	1.36	0.42	0.24	83	267	31.6	15.9	27.2	0.32	5.03	17.1	2.5	0.31
10%P	4.12	0.14	1.95	1.17	0.43	0.22	83.5	167	34.6	13.2	38.7	0.29	6.88	18.7	2.12	0.5
10%P	3.9	0.15	1.77	1.07	0.39	0.23	83.9	183	30	15.6	27.5	0.35	7.5	16.8	2.21	0.46
10%P	4.06	0.17	1.81	1.16	0.35	0.25	89.1	186	38.4	19.5	31.1	0.26	5.22	16.5	2.24	0.48
10%P	4.13	0.18	2.17	1.02	0.37	0.28	87.9	189	36.6	19	31.4	0.29	3.58	14.8	1.9	0.47
10%P	3.45	0.15	1.9	1.37	0.42	0.22	105	136	34.4	16.1	28.4	0.37	7.56	15.5	1.82	0.77
10%P	3.32	0.12	1.58	1.07	0.42	0.19	77.9	185	26.9	10.4	36.6	0.34	7.69	17.2	2.11	0.42
10%P	3.81	0.19	2.2	1.26	0.44	0.29	99.9	275	38.3	15.7	30.8	0.31	5.88	13.1	1.73	0.36
10%P	3.89	0.16	2.17	1.47	0.5	0.26	105	126	43.6	16.9	34.9	0.34	6.72	14.7	1.8	0.83
10%P	3.69	0.15	2.39	1.13	0.42	0.25	81.8	218	41.2	16.7	43.9	0.26	4.63	14.8	1.54	0.37
10%P	3.26	0.12	1.69	1.19	0.41	0.22	84.4	201	36.7	16	48.3	0.38	18.3	14.9	1.93	0.42

Appendix B(e). Standard laboratory foliar nutrient concentrations for the **10% K HNS regime at 15 days post-treatment.**

Treatments	N	P	K	Ca	Mg	S	Fe	Mn	Zn	Cu	B	Na	Al	N:S	N:K	Fe:Mn
10%K	3.86	0.22	1.02	1.41	0.39	0.23	77.4	174	28.3	15.1	32.6	0.31	10.1	17	3.77	0.45
10%K	4.6	0.3	1.12	1.48	0.47	0.3	108	189	36.9	20.2	29.2	0.5	7.1	15.2	4.12	0.57
10%K	4.94	0.36	1.14	1.69	0.5	0.28	91.3	210	53	24.4	32.9	0.34	5.9	17.3	4.35	0.43
10%K	4.14	0.28	1.19	1.38	0.47	0.28	95.8	189	35.5	16.9	25.3	0.46	8.09	15	3.48	0.51
10%K	4.35	0.3	1.34	1.2	0.38	0.27	80.9	204	25.9	13.4	24.2	0.38	3.7	15.9	3.23	0.4
10%K	3.63	0.23	1.15	1.34	0.41	0.23	82.4	171	33.3	18	30.7	0.46	4.24	15.8	3.15	0.48
10%K	5.07	0.33	1.35	1.17	0.42	0.29	92.2	182	30.9	18.7	23.3	0.57	2.88	17.2	3.75	0.51
10%K	4.27	0.27	1.31	1.21	0.44	0.24	95.1	190	33	19	26.2	0.42	3.97	17.6	3.26	0.5
10%K	4.45	0.32	1.57	1.12	0.42	0.26	96	198	34.6	21.1	28.5	0.37	7.97	16.8	2.84	0.48
10%K	3.91	0.25	1.34	1.55	0.47	0.26	99.8	174	34.6	20.6	31.4	0.36	9.73	15.1	2.92	0.57
10%K	4.17	0.24	1.38	1.21	0.36	0.25	83.2	180	28.5	16.8	27.5	0.36	1.79	17	3.02	0.46
10%K	5.08	0.34	1.39	1.13	0.35	0.28	94.2	176	37.2	18.7	25.6	0.56	4.53	18.4	3.66	0.53
10%K	4.45	0.28	1.29	1.38	0.44	0.28	85.5	172	31	17.9	35.6	0.48	2.07	16.1	3.46	0.5
10%K	4.69	0.33	1.32	1.34	0.41	0.3	87.3	153	34.4	20.7	24.2	0.49	2.58	15.8	3.57	0.57
10%K	4.88	0.3	1.51	1.33	0.42	0.26	87.7	197	30.9	15.9	24.8	0.39	3.59	18.8	3.22	0.45
10%K	4.97	0.37	1.53	1.52	0.47	0.28	86.4	170	40.9	26.5	30.9	0.46	5.2	17.5	3.24	0.51
10%K	4.41	0.26	1.46	0.95	0.38	0.27	79.6	173	30.9	17	26	0.44	4.94	16.6	3.03	0.46
10%K	3.88	0.23	0.97	1.28	0.41	0.22	71.8	131	29.3	13.5	32	0.48	3.21	17.6	4	0.55
10%K	4.02	0.26	1.15	1.23	0.4	0.24	83.7	143	30.7	12.4	34.9	0.54	5.28	16.5	3.49	0.59
10%K	4.07	0.3	1.14	1.51	0.47	0.29	76.1	159	39.2	18	24.2	0.62	2.39	13.8	3.58	0.48

Appendix B(f). Standard laboratory foliar nutrient concentrations for the **complete HNS regime** at **30 days post-treatment**.

Treatments	N	P	K	Ca	Mg	S	Fe	Mn	Zn	Cu	B	Na	Al	N:S	N:K	Fe:Mn
Complete	2.28	0.13	1.69	1.23	0.38	0.2	76.7	138	21.3	12	26.2	0.26	6.59	11.6	1.35	0.56
Complete	2.18	0.12	1.55	1.15	0.36	0.25	70.2	76.5	22.9	10.7	35.7	0.43	11.1	8.82	1.41	0.92
Complete	2.15	0.13	1.5	0.94	0.31	0.18	61.5	74.9	25.3	10.5	25.9	0.4	5.11	11.7	1.43	0.82
Complete	2.13	0.14	1.47	1.09	0.34	0.18	78.4	133	31.2	11.2	26.4	0.47	6.27	11.7	1.44	0.59
Complete	2.08	0.11	1.76	0.97	0.32	0.17	66.2	121	27.1	12	25	0.31	2.88	12	1.18	0.55
Complete	2.2	0.13	1.58	1.08	0.35	0.21	75.8	142	25.1	9.83	26	0.33	7.46	10.6	1.39	0.53
Complete	2.78	0.17	2.19	1.25	0.33	0.23	79	93.3	37.6	16.5	22.8	0.15	1.56	12.1	1.27	0.85
Complete	2.08	0.13	1.59	0.83	0.27	0.18	61.2	124	22.5	9.55	27.5	0.29	4.31	11.8	1.31	0.49
Complete	1.67	0.13	1.82	1.32	0.34	0.16	85.7	132	23.9	12.6	25.8	0.34	9.83	10.4	0.92	0.65
Complete	1.8	0.14	1.68	1.64	0.44	0.22	75.7	135	25.5	14.2	32.3	0.2	12.4	8.31	1.08	0.56
Complete	1.62	0.12	1.89	0.99	0.32	0.17	56.2	78.7	26	13	28.6	0.28	2.43	9.77	0.86	0.71
Complete	1.92	0.15	1.84	1.04	0.27	0.16	62	118	26	12.6	22.5	0.27	1.7	12.1	1.05	0.52
Complete	3.25	0.2	1.89	1.18	0.37	0.22	83.6	86.2	34.2	14.5	26.8	0.31	3.66	14.6	1.72	0.97
Complete	2.17	0.13	1.49	0.97	0.29	0.19	57.1	71.6	23.6	10.3	21.2	0.48	1.65	11.4	1.46	0.8
Complete	1.81	0.11	1.79	1.11	0.3	0.17	66.7	101	30.3	10.7	28.2	0.39	4.62	10.8	1.01	0.66
Complete	2.6	0.16	2.1	1.1	0.3	0.17	56.1	94.2	24.2	10.7	23.8	0.34	1.43	15.4	1.24	0.6
Complete	2.2	0.12	1.83	1.16	0.34	0.2	60.7	92.8	21.4	12.3	26.9	0.32	3.01	11.2	1.2	0.65
Complete	3.37	0.2	1.75	1.12	0.4	0.27	89.7	85.7	30.6	8.54	27.5	0.49	2.05	12.7	1.93	1.05
Complete	1.8	0.11	1.79	1.1	0.26	0.19	68.8	86.6	21.1	9.84	28.5	0.39	7.35	9.61	1.01	0.79
Complete	2.75	0.15	1.84	1.13	0.36	0.23	88.1	82.9	31.9	9.13	26.8	0.43	6.52	12	1.49	1.06

Appendix B(g). Standard laboratory foliar nutrient concentrations for the **50% NPK HNS regime at 30 days post-treatment.**

Treatments	N	P	K	Ca	Mg	S	Fe	Mn	Zn	Cu	B	Na	Al	N:S	N:K	Fe:Mn
50%NPK	1.99	0.15	1.29	1.29	0.42	0.16	108	174	33.4	5.31	39.5	0.5	20.8	12.2	1.54	0.62
50%NPK	1.78	0.12	1.25	1.23	0.35	0.15	72.7	190	33.5	5.88	27.4	0.31	16.2	11.8	1.42	0.38
50%NPK	1.82	0.13	1.65	1.35	0.37	0.15	162	207	38.4	7.33	26.7	0.39	23.4	12.4	1.1	0.78
50%NPK	1.56	0.11	1.28	0.96	0.26	0.12	86.5	105	24.3	4.7	18.9	0.31	9.68	12.8	1.22	0.82
50%NPK	1.51	0.1	1.15	0.9	0.23	0.12	75.8	171	28.3	5.77	26.4	0.4	6.54	12.4	1.31	0.44
50%NPK	1.48	0.11	1.42	1.13	0.32	0.14	80.9	109	26.4	6.87	26.4	0.34	11.6	10.3	1.05	0.74
50%NPK	1.64	0.12	1.51	1.21	0.37	0.14	92.9	216	39	6.58	22.1	0.26	10.1	11.9	1.08	0.43
50%NPK	1.86	0.13	1.25	0.85	0.28	0.14	140	171	26.7	4.02	30.8	0.26	8.68	13.2	1.49	0.82
50%NPK	1.45	0.11	1.43	0.95	0.34	0.13	86.6	175	25.9	4.57	33.5	0.27	14.3	10.9	1.01	0.49
50%NPK	1.68	0.12	1.16	1.04	0.31	0.14	84.9	204	26.2	5.73	25	0.33	7.83	12.1	1.44	0.42
50%NPK	1.43	0.11	1.27	1.05	0.32	0.16	96.7	112	28.1	6.79	34.3	0.33	16.5	8.84	1.12	0.86
50%NPK	1.32	0.1	1.44	0.79	0.23	0.13	79.3	163	27	7	31.8	0.31	11	10.5	0.92	0.49
50%NPK	1.67	0.12	1.55	1.21	0.35	0.14	84.1	193	29.2	5.89	31.9	0.32	13.4	11.5	1.08	0.44
50%NPK	1.52	0.12	1.54	1.19	0.34	0.15	118	136	22.3	4.7	25.5	0.33	26	10.2	0.99	0.87
50%NPK	1.52	0.12	1.07	1.02	0.3	0.14	78.3	185	26.8	5.01	26.6	0.35	7.27	10.8	1.42	0.42
50%NPK	1.95	0.14	1.71	1.19	0.34	0.15	153	209	40.5	6.21	25.3	0.29	6.48	13	1.14	0.73
50%NPK	1.37	0.1	1.62	1.01	0.33	0.15	105	133	29.4	6.39	38.4	0.26	27.1	9.34	0.84	0.79
50%NPK	1.81	0.12	1.07	0.86	0.29	0.14	84.4	91.7	32.2	3.7	21	0.3	14.3	12.7	1.68	0.92
50%NPK	1.65	0.12	1.45	0.93	0.28	0.16	78	161	27.7	4.97	25.9	0.25	8.46	10.4	1.13	0.49
50%NPK	1.51	0.1	1.31	0.87	0.28	0.17	81.2	164	32.7	6.08	29.9	0.3	7.52	8.87	1.15	0.49

Appendix B(h). Standard laboratory foliar nutrient concentrations for the **10% N HNS regime at 30 days post-treatment.**

Treatments	N	P	K	Ca	Mg	S	Fe	Mn	Zn	Cu	B	Na	Al	N:S	N:K	Fe:Mn
10%N	1.11	0.24	1.45	1.04	0.37	0.18	68.6	134	38.5	10.5	36.3	0.23	15.6	6.04	0.76	0.51
10%N	1.06	0.21	1.47	1	0.37	0.11	59.7	120	32.3	8.37	37.4	0.2	11	9.69	0.72	0.5
10%N	1.1	0.22	1.59	0.99	0.37	0.16	100	220	26.3	7.94	37.2	0.26	16.2	6.83	0.69	0.46
10%N	1	0.21	1.34	0.7	0.25	0.11	83.5	199	34.3	9.6	28.7	0.31	7.4	8.77	0.75	0.42
10%N	1.28	0.25	1.58	0.96	0.36	0.14	65.4	236	35.3	10.1	31.6	0.39	13.1	8.85	0.81	0.28
10%N	1.03	0.19	1.35	0.82	0.26	0.11	141	208	25	10.6	23.2	0.18	6.67	9.42	0.76	0.68
10%N	1.13	0.25	1.47	1.03	0.35	0.14	53.8	192	25.1	11	35.6	0.22	10	8.37	0.77	0.28
10%N	1.19	0.24	1.26	0.94	0.28	0.22	99.4	220	32.1	9.65	26.4	0.31	8.14	5.52	0.95	0.45
10%N	1.37	0.26	1.22	0.94	0.35	0.12	42.1	189	21.9	11.1	30.6	0.3	8.83	11	1.12	0.22
10%N	1.05	0.25	1.37	0.9	0.33	0.13	58.4	231	28.8	9.86	32.1	0.25	20.1	8.35	0.77	0.25
10%N	1.19	0.26	1.89	1.02	0.34	0.14	68.3	132	32.8	11.6	26.5	0.18	10.9	8.38	0.63	0.52
10%N	1.5	0.29	1.66	1.21	0.46	0.16	64.8	216	48.2	12	33.2	0.3	11.6	9.16	0.9	0.3
10%N	1.05	0.2	1.02	0.85	0.29	0.13	114	112	27.5	9.09	28.4	0.21	9.3	7.78	1.03	1.01
10%N	1.26	0.24	1.8	0.95	0.34	0.12	70.6	216	28.9	12.5	25	0.2	11	10.3	0.7	0.33
10%N	0.84	0.14	0.92	0.63	0.23	0.11	52.2	67.4	23.7	6.65	26.7	0.19	16.1	7.61	0.92	0.77
10%N	0.94	0.19	1.37	0.76	0.25	0.09	36	110	17.6	6.32	21.8	0.13	3.74	10.6	0.69	0.33
10%N	1.27	0.26	1.54	1.1	0.35	0.15	89.7	248	29.4	10.8	33.2	0.41	16.3	8.25	0.82	0.36
10%N	1.23	0.26	1.43	1	0.31	0.12	50	267	30	12	23.7	0.26	10	9.96	0.86	0.19
10%N	0.98	0.17	1.29	0.79	0.26	0.13	37.7	155	20.6	6.9	25.3	0.19	5.54	7.4	0.75	0.24
10%N	1.19	0.23	1.55	0.92	0.28	0.1	56.3	214	32.4	11	21	0.21	8.21	11.7	0.77	0.26

Appendix B(i). Standard laboratory foliar nutrient concentrations for the **10% P HNS regime** at **30 days post-treatment**.

Treatments	N	P	K	Ca	Mg	S	Fe	Mn	Zn	Cu	B	Na	Al	N:S	N:K	Fe:Mn
10%P	1.84	0.05	1.5	1.05	0.39	0.12	67.1	163	20.3	8.09	29.7	0.21	20.2	15.1	1.22	0.41
10%P	1.74	0.05	1.26	1.08	0.29	0.13	58.1	76	20.4	11.8	30.6	0.25	7.2	13.7	1.38	0.77
10%P	2.58	0.07	1.74	0.9	0.29	0.15	70.3	86.5	31.4	13.4	25.5	0.23	8.81	16.9	1.49	0.81
10%P	1.85	0.05	1.41	0.7	0.25	0.13	55.5	82.6	26	12.4	28.6	0.21	10.3	14.1	1.31	0.67
10%P	1.94	0.05	1.35	0.8	0.26	0.12	50.8	120	19.6	7.21	24	0.22	4.54	16.5	1.44	0.42
10%P	1.83	0.06	1.81	0.86	0.29	0.14	45.9	156	24	17.3	24.8	0.2	3.28	13.2	1.01	0.29
10%P	1.78	0.06	1.43	0.84	0.29	0.13	53.7	124	22.6	12.9	20.3	0.18	3.45	13.8	1.24	0.43
10%P	1.8	0.07	1.48	0.97	0.31	0.14	63.3	144	23.9	12.8	24	0.2	3.33	12.6	1.21	0.44
10%P	1.96	0.06	1.43	0.8	0.25	0.15	52	78.1	25.3	12.6	19.8	0.26	1.94	13.5	1.37	0.67
10%P	2.41	0.06	1.44	0.99	0.3	0.17	66.1	147	23.2	15.2	38.2	0.26	4.17	14.5	1.67	0.45
10%P	2.05	0.06	1.46	1.05	0.31	0.14	58.8	157	22.5	10.2	24	0.29	4.39	14.9	1.4	0.38
10%P	1.84	0.06	1.41	1.08	0.34	0.13	56.4	136	24.8	12.3	37	0.24	6.21	14.2	1.31	0.41
10%P	2.28	0.07	1.51	0.99	0.28	0.16	69.3	157	23.6	12.3	37.3	0.28	14	14.6	1.51	0.44
10%P	1.6	0.06	1.3	0.7	0.24	0.16	44.6	75.4	18.8	11.3	28.4	0.28	2.09	10	1.24	0.59
10%P	2.25	0.06	1.56	0.93	0.37	0.14	70.2	213	23.3	18.1	24.7	0.24	9.11	15.7	1.44	0.33
10%P	2.02	0.05	1.37	0.73	0.23	0.13	54.9	121	22.6	11.2	29.6	0.26	3.68	15.5	1.48	0.46
10%P	1.69	0.05	1.28	0.9	0.28	0.13	60	131	22.8	10.8	29.3	0.23	9.9	12.9	1.32	0.46
10%P	1.78	0.06	0.97	0.7	0.29	0.13	61.1	138	23.3	15	30.3	0.18	3.99	13.7	1.84	0.44
10%P	1.83	0.05	1.32	0.97	0.3	0.12	45.3	163	18.6	9.01	32.3	0.22	7.42	15.7	1.39	0.28
10%P	2.21	0.06	1.79	0.78	0.29	0.16	51.1	130	27	9.89	21.5	0.18	2.62	13.5	1.24	0.39

Appendix B(j). Standard laboratory foliar nutrient concentrations for the **10% K HNS regime at 30 days post-treatment.**

Treatments	N	P	K	Ca	Mg	S	Fe	Mn	Zn	Cu	B	Na	Al	N:S	N:K	Fe:Mn
10%K	2.43	0.15	0.57	1.07	0.33	0.2	78.1	108	30.3	10.2	27.2	0.76	8.91	12.1	4.28	0.72
10%K	2.15	0.13	0.61	1.12	0.38	0.21	70.5	93.6	27.8	10.7	33	0.71	10.4	10.1	3.51	0.75
10%K	2.42	0.14	0.56	0.96	0.32	0.21	79.1	155	31.1	10.2	26.9	0.62	8.92	11.3	4.29	0.51
10%K	2.41	0.14	0.65	1.23	0.38	0.22	73.3	124	28.4	10.4	36.6	0.68	10.3	11.2	3.72	0.59
10%K	2.41	0.15	0.69	1.5	0.53	0.21	86.4	158	32.7	14.5	44.2	0.72	15.1	11.7	3.5	0.55
10%K	1.93	0.12	0.63	1.08	0.35	0.22	77.2	124	29.1	11.4	31.2	0.65	6.54	8.6	3.07	0.62
10%K	2.55	0.13	0.76	1.2	0.4	0.24	76.6	119	27.7	11.9	30.6	0.72	4.3	10.8	3.37	0.64
10%K	3.04	0.19	0.73	1.05	0.33	0.23	77.3	147	24.8	9.15	37.6	0.8	3.69	13.5	4.18	0.52
10%K	2.36	0.15	0.61	1.32	0.45	0.25	72	125	28.5	12.9	35.2	0.8	8.85	9.64	3.89	0.57
10%K	2.72	0.17	0.72	1.24	0.4	0.21	73.5	82.5	21.4	8.8	35.9	0.6	3.2	12.9	3.75	0.89
10%K	1.85	0.1	0.64	0.92	0.27	0.17	55.9	112	19.4	8.24	21.6	0.36	14.6	11.2	2.91	0.5
10%K	2.07	0.1	0.65	1.02	0.36	0.16	61	118	23.5	10.9	25.1	0.6	4.33	13	3.21	0.52
10%K	2.25	0.13	0.67	1.03	0.36	0.21	64.3	102	22.2	9.76	29.2	0.46	5.34	10.9	3.34	0.63
10%K	2.6	0.16	0.72	1.23	0.37	0.21	85.3	139	29.8	11.3	36.6	0.66	7.57	12.6	3.6	0.61
10%K	2.04	0.12	0.65	0.93	0.35	0.19	63.7	121	29.1	10.6	27.8	0.52	6.57	10.9	3.14	0.53
10%K	2.86	0.19	0.75	1.56	0.49	0.25	89.1	95.1	29.7	13.5	39.3	0.73	5.74	11.5	3.81	0.94
10%K	1.9	0.13	0.67	1.3	0.38	0.23	67.6	83.2	30	9.66	36.3	0.74	6.29	8.27	2.83	0.81
10%K	1.82	0.12	0.68	1.14	0.35	0.18	54.1	72.9	26.1	8.64	24.1	0.68	3.45	10.4	2.69	0.74
10%K	1.76	0.12	0.49	1.11	0.31	0.2	88.7	105	21.8	8.57	35.3	0.63	6.3	8.69	3.58	0.84
10%K	2.4	0.12	0.7	1.25	0.35	0.2	76.3	121	27.5	11.5	32.5	0.72	11.6	12.1	3.42	0.63

Appendix C. Fit Statistics for PLS Regression Models Predicting Foliar Nutrient Concentration in pine needles.

Stage	Location	Spectrometer	Nutrient	Transformation	Factors	R ² cal	RMSEPCal	R ² cv	RMSEPcv	ExpVarY	ExpVarX
15	Bottom	Microphazir	N	SG7	4	0.60	0.25	0.37	0.32	60.46	97.54
15	Bottom	Microphazir	Ca	MSC	2	0.37	0.06	0.30	0.06	36.91	78.68
15	Bottom	Microphazir	Zn	DT	3	0.39	4.90	0.25	5.44	39.26	89.98
15	Bottom	Microphazir	Cu	SNV	2	0.30	1.20	0.22	1.26	29.87	67.16
15	Bottom	Microphazir	N.K	NIR	3	0.20	0.23	0.09	0.24	19.90	99.63
15	Bottom	Microphazir	Mg	SNV	1	0.12	0.03	0.08	0.04	11.82	67.98
15	Bottom	Microphazir	Al	SNV	0	0.00	0.00	0.00	0.00	0.00	0.00
15	Bottom	Microphazir	B	SNV	0	0.00	0.00	0.00	0.00	0.00	0.00
15	Bottom	Microphazir	Fe	SNV	0	0.00	0.00	0.00	0.00	0.00	0.00
15	Bottom	Microphazir	Fe.Mn	SNV	0	0.00	0.00	0.00	0.00	0.00	0.00
15	Bottom	Microphazir	K	SNV	0	0.00	0.00	0.00	0.00	0.00	0.00
15	Bottom	Microphazir	Mn	SNV	0	0.00	0.00	0.00	0.00	0.00	0.00
15	Bottom	Microphazir	N.S	SNV	0	0.00	0.00	0.00	0.00	0.00	0.00
15	Bottom	Microphazir	Na	SNV	0	0.00	0.00	0.00	0.00	0.00	0.00
15	Bottom	Microphazir	P	SNV	0	0.00	0.00	0.00	0.00	0.00	0.00
15	Bottom	Microphazir	S	SNV	0	0.00	0.00	0.00	0.00	0.00	0.00
15	Bottom	DLP Nano	N	MSC_SG7	1	0.53	0.27	0.46	0.29	53.31	16.20
15	Bottom	DLP Nano	Ca	DT	2	0.47	0.06	0.40	0.06	46.66	65.67
15	Bottom	DLP Nano	N.K	MSC_SG7	1	0.38	0.20	0.28	0.22	37.63	16.12
15	Bottom	DLP Nano	Mg	DT	1	0.24	0.03	0.19	0.03	24.48	41.07
15	Bottom	DLP Nano	Cu	SNV	2	0.28	1.22	0.15	1.32	27.71	75.74
15	Bottom	DLP Nano	Al	SNV	0	0.00	0.00	0.00	0.00	0.00	0.00
15	Bottom	DLP Nano	B	SNV	0	0.00	0.00	0.00	0.00	0.00	0.00
15	Bottom	DLP Nano	Fe	SNV	0	0.00	0.00	0.00	0.00	0.00	0.00
15	Bottom	DLP Nano	Fe.Mn	SNV	0	0.00	0.00	0.00	0.00	0.00	0.00
15	Bottom	DLP Nano	K	SNV	0	0.00	0.00	0.00	0.00	0.00	0.00
15	Bottom	DLP Nano	Mn	SNV	0	0.00	0.00	0.00	0.00	0.00	0.00
15	Bottom	DLP Nano	N.S	SNV	0	0.00	0.00	0.00	0.00	0.00	0.00
15	Bottom	DLP Nano	Na	SNV	0	0.00	0.00	0.00	0.00	0.00	0.00
15	Bottom	DLP Nano	P	SNV	0	0.00	0.00	0.00	0.00	0.00	0.00
15	Bottom	DLP Nano	S	SNV	0	0.00	0.00	0.00	0.00	0.00	0.00
15	Bottom	DLP Nano	Zn	SNV	0	0.00	0.00	0.00	0.00	0.00	0.00

Appendix C. Fit Statistics for PLS Regression Models Predicting Foliar Nutrient Concentration in pine needles (*continued*)

Stage	Location	Spectrometer	Nutrient	Transformation	Factors	R ² cal	RMSEPCal	R ² cv	RMSEPcv	ExpVarY	ExpVarX
15	Dry	Foss	K	MSC	15	0.93	0.08	0.84	0.12	92.91	99.85
15	Dry	Foss	Ca	SNV_SG7	7	0.93	0.02	0.80	0.03	93.17	84.50
15	Dry	Foss	N	DT	3	0.80	0.18	0.78	0.19	80.12	91.49
15	Dry	Foss	Mg	DT	12	0.84	0.01	0.72	0.02	84.20	99.74
15	Dry	Foss	S	SNV	18	0.90	0.02	0.65	0.04	90.24	99.92
15	Dry	Foss	N.K	DT	6	0.70	0.14	0.63	0.16	70.19	97.20
15	Dry	Foss	P	DT	13	0.80	0.02	0.58	0.03	79.83	99.78
15	Dry	Foss	Cu	SG5	1	0.42	1.09	0.37	1.14	42.29	31.20
15	Dry	Foss	N.S	DT	3	0.36	1.16	0.28	1.23	35.64	92.50
15	Dry	Foss	B	MSC_SG7	4	0.56	4.29	0.25	5.58	55.77	65.81
15	Dry	Foss	Zn	SNV_SG5	1	0.31	5.22	0.24	5.48	30.99	27.23
15	Dry	Foss	Al	SNV	0	0.00	0.00	0.00	0.00	0.00	0.00
15	Dry	Foss	Fe	SNV	0	0.00	0.00	0.00	0.00	0.00	0.00
15	Dry	Foss	Fe.Mn	SNV	0	0.00	0.00	0.00	0.00	0.00	0.00
15	Dry	Foss	Mn	SNV	0	0.00	0.00	0.00	0.00	0.00	0.00
15	Dry	Foss	Na	SNV	0	0.00	0.00	0.00	0.00	0.00	0.00
15	Dry	Microphazir	N	DT	2	0.75	0.20	0.73	0.21	75.32	66.42
15	Dry	Microphazir	Ca	SG7	2	0.56	0.05	0.48	0.05	56.41	46.48
15	Dry	Microphazir	N.K	DT	2	0.45	0.19	0.41	0.20	44.91	38.14
15	Dry	Microphazir	Cu	SG7	1	0.35	1.16	0.30	1.20	35.22	32.77
15	Dry	Microphazir	Mg	DT	6	0.56	0.02	0.23	0.03	56.37	93.14
15	Dry	Microphazir	Zn	MSC_SG7	1	0.29	5.33	0.21	5.60	28.62	26.85
15	Dry	Microphazir	S	DT	1	0.26	0.07	0.20	0.07	25.60	44.24
15	Dry	Microphazir	P	SG7	4	0.51	0.03	0.17	0.04	51.07	58.22
15	Dry	Microphazir	N.S	SNV	1	0.23	1.27	0.15	1.34	22.75	31.20
15	Dry	Microphazir	K	DT	1	0.11	0.27	0.03	0.29	11.36	30.14
15	Dry	Microphazir	Al	SNV	0	0.00	0.00	0.00	0.00	0.00	0.00
15	Dry	Microphazir	B	SNV	0	0.00	0.00	0.00	0.00	0.00	0.00
15	Dry	Microphazir	Fe	SNV	0	0.00	0.00	0.00	0.00	0.00	0.00
15	Dry	Microphazir	Fe.Mn	SNV	0	0.00	0.00	0.00	0.00	0.00	0.00
15	Dry	Microphazir	Mn	SNV	0	0.00	0.00	0.00	0.00	0.00	0.00
15	Dry	Microphazir	Na	SNV	0	0.00	0.00	0.00	0.00	0.00	0.00

Appendix C. Fit Statistics for PLS Regression Models Predicting Foliar Nutrient Concentration in pine needles (*continued*)

Stage	Location	Spectrometer	Nutrient	Transformation	Factors	R ² cal	RMSEPCal	R ² cv	RMSEPcv	ExpVarY	ExpVarX
15	Dry	DLP Nano	N	DT	5	0.77	0.19	0.67	0.23	76.85	94.37
15	Dry	DLP Nano	Ca	SNV	4	0.60	0.05	0.49	0.05	60.00	82.56
15	Dry	DLP Nano	Cu	SNV	5	0.49	1.02	0.32	1.18	48.92	94.71
15	Dry	DLP Nano	Mg	SNV	4	0.39	0.03	0.31	0.03	38.64	86.69
15	Dry	DLP Nano	N.K	SG7	1	0.31	0.21	0.25	0.22	31.00	32.27
15	Dry	DLP Nano	Zn	MSC	5	0.46	4.62	0.24	5.49	45.91	94.61
15	Dry	DLP Nano	K	SNV	5	0.43	0.22	0.20	0.26	42.89	93.72
15	Dry	DLP Nano	N.S	SG7	1	0.24	1.26	0.19	1.30	24.40	34.61
15	Dry	DLP Nano	Mn	NIR	2	0.07	40.40	0.01	41.78	6.98	99.94
15	Dry	DLP Nano	Al	SNV	0	0.00	0.00	0.00	0.00	0.00	0.00
15	Dry	DLP Nano	B	SNV	0	0.00	0.00	0.00	0.00	0.00	0.00
15	Dry	DLP Nano	Fe	SNV	0	0.00	0.00	0.00	0.00	0.00	0.00
15	Dry	DLP Nano	Fe.Mn	SNV	0	0.00	0.00	0.00	0.00	0.00	0.00
15	Dry	DLP Nano	Na	SNV	0	0.00	0.00	0.00	0.00	0.00	0.00
15	Dry	DLP Nano	P	SNV	0	0.00	0.00	0.00	0.00	0.00	0.00
15	Dry	DLP Nano	S	SNV	0	0.00	0.00	0.00	0.00	0.00	0.00
15	Top	Microphazir	N	MSC_SG7	4	0.74	0.20	0.60	0.25	73.89	96.80
15	Top	Microphazir	Zn	NIR	4	0.41	4.85	0.32	5.18	40.53	99.87
15	Top	Microphazir	N.K	DT_SG7	3	0.42	0.19	0.29	0.22	42.41	95.93
15	Top	Microphazir	Cu	NIR	3	0.37	1.13	0.27	1.22	37.29	99.55
15	Top	Microphazir	Ca	MSC	2	0.33	0.06	0.26	0.07	32.71	89.40
15	Top	Microphazir	Mg	NIR	1	0.18	0.03	0.13	0.03	17.51	89.91
15	Top	Microphazir	K	NIR	1	0.03	0.29	0.00	0.29	3.04	66.54
15	Top	Microphazir	Al	SNV	0	0.00	0.00	0.00	0.00	0.00	0.00
15	Top	Microphazir	B	SNV	0	0.00	0.00	0.00	0.00	0.00	0.00
15	Top	Microphazir	Fe	SNV	0	0.00	0.00	0.00	0.00	0.00	0.00
15	Top	Microphazir	Fe.Mn	SNV	0	0.00	0.00	0.00	0.00	0.00	0.00
15	Top	Microphazir	Mn	SNV	0	0.00	0.00	0.00	0.00	0.00	0.00
15	Top	Microphazir	N.S	SNV	0	0.00	0.00	0.00	0.00	0.00	0.00
15	Top	Microphazir	Na	SNV	0	0.00	0.00	0.00	0.00	0.00	0.00
15	Top	Microphazir	P	SNV	0	0.00	0.00	0.00	0.00	0.00	0.00
15	Top	Microphazir	S	SNV	0	0.00	0.00	0.00	0.00	0.00	0.00

Appendix C. Fit Statistics for PLS Regression Models Predicting Foliar Nutrient Concentration in pine needles (*continued*)

Stage	Location	Spectrometer	Nutrient	Transformation	Factors	R ² cal	RMSEPCal	R ² cv	RMSEPCv	ExpVarY	ExpVarX
15	Top	DLP Nano	N	MSC	3	0.58	0.26	0.45	0.29	58.03	70.45
15	Top	DLP Nano	N.K	MSC_SG7	1	0.37	0.20	0.28	0.22	36.62	17.88
15	Top	DLP Nano	Ca	SG7	1	0.38	0.06	0.28	0.06	38.01	16.27
15	Top	DLP Nano	Cu	SG7	1	0.32	1.18	0.21	1.27	31.74	16.91
15	Top	DLP Nano	Mg	SG7	1	0.32	0.03	0.19	0.03	32.03	14.50
15	Top	DLP Nano	Al	SNV	0	0.00	0.00	0.00	0.00	0.00	0.00
15	Top	DLP Nano	B	SNV	0	0.00	0.00	0.00	0.00	0.00	0.00
15	Top	DLP Nano	Fe	SNV	0	0.00	0.00	0.00	0.00	0.00	0.00
15	Top	DLP Nano	Fe.Mn	SNV	0	0.00	0.00	0.00	0.00	0.00	0.00
15	Top	DLP Nano	K	SNV	0	0.00	0.00	0.00	0.00	0.00	0.00
15	Top	DLP Nano	Mn	SNV	0	0.00	0.00	0.00	0.00	0.00	0.00
15	Top	DLP Nano	N.S	SNV	0	0.00	0.00	0.00	0.00	0.00	0.00
15	Top	DLP Nano	Na	SNV	0	0.00	0.00	0.00	0.00	0.00	0.00
15	Top	DLP Nano	P	SNV	0	0.00	0.00	0.00	0.00	0.00	0.00
15	Top	DLP Nano	S	SNV	0	0.00	0.00	0.00	0.00	0.00	0.00
15	Top	DLP Nano	Zn	SNV	0	0.00	0.00	0.00	0.00	0.00	0.00
15	WP	Microphazir	N	DT	7	0.80	0.18	0.66	0.23	79.51	98.71
15	WP	Microphazir	Ca	MSC	2	0.37	0.06	0.31	0.06	37.42	86.15
15	WP	Microphazir	N.K	MSC_SG7	3	0.45	0.19	0.31	0.21	45.13	95.56
15	WP	Microphazir	Cu	NIR	3	0.38	1.13	0.26	1.23	37.50	99.46
15	WP	Microphazir	Zn	SNV	2	0.32	5.20	0.26	5.42	31.51	87.27
15	WP	Microphazir	K	NIR	3	0.26	0.25	0.16	0.27	26.14	99.49
15	WP	Microphazir	S	NIR	3	0.26	0.06	0.15	0.07	26.02	99.46
15	WP	Microphazir	Mg	DT	1	0.17	0.03	0.13	0.03	17.46	73.77
15	WP	Microphazir	Al	SNV	0	0.00	0.00	0.00	0.00	0.00	0.00
15	WP	Microphazir	B	SNV	0	0.00	0.00	0.00	0.00	0.00	0.00
15	WP	Microphazir	Fe	SNV	0	0.00	0.00	0.00	0.00	0.00	0.00
15	WP	Microphazir	Fe.Mn	SNV	0	0.00	0.00	0.00	0.00	0.00	0.00
15	WP	Microphazir	Mn	SNV	0	0.00	0.00	0.00	0.00	0.00	0.00
15	WP	Microphazir	N.S	SNV	0	0.00	0.00	0.00	0.00	0.00	0.00
15	WP	Microphazir	Na	SNV	0	0.00	0.00	0.00	0.00	0.00	0.00
15	WP	Microphazir	P	SNV	0	0.00	0.00	0.00	0.00	0.00	0.00

Appendix C. Fit Statistics for PLS Regression Models Predicting Foliar Nutrient Concentration in pine needles (*continued*)

Stage	Location	Spectrometer	Nutrient	Transformation	Factors	R ² cal	RMSEPCal	R ² cv	RMSEPCv	ExpVarY	ExpVarX
15	WP	DLP Nano	N	MSC_SG7	1	0.50	0.28	0.46	0.29	50.17	27.19
15	WP	DLP Nano	Ca	DT	1	0.39	0.06	0.34	0.06	39.32	37.66
15	WP	DLP Nano	N.K	MSC_SG7	1	0.36	0.21	0.30	0.21	35.73	27.02
15	WP	DLP Nano	Mg	DT	1	0.30	0.03	0.25	0.03	29.67	38.95
15	WP	DLP Nano	Cu	SG7	1	0.29	1.20	0.21	1.27	28.97	25.93
15	WP	DLP Nano	K	SNV	2	0.28	0.25	0.19	0.26	27.57	20.28
15	WP	DLP Nano	Al	SNV	0	0.00	0.00	0.00	0.00	0.00	0.00
15	WP	DLP Nano	B	SNV	0	0.00	0.00	0.00	0.00	0.00	0.00
15	WP	DLP Nano	Fe	SNV	0	0.00	0.00	0.00	0.00	0.00	0.00
15	WP	DLP Nano	Fe.Mn	SNV	0	0.00	0.00	0.00	0.00	0.00	0.00
15	WP	DLP Nano	Mn	SNV	0	0.00	0.00	0.00	0.00	0.00	0.00
15	WP	DLP Nano	N.S	SNV	0	0.00	0.00	0.00	0.00	0.00	0.00
15	WP	DLP Nano	Na	SNV	0	0.00	0.00	0.00	0.00	0.00	0.00
15	WP	DLP Nano	P	SNV	0	0.00	0.00	0.00	0.00	0.00	0.00
15	WP	DLP Nano	S	SNV	0	0.00	0.00	0.00	0.00	0.00	0.00
15	WP	DLP Nano	Zn	SNV	0	0.00	0.00	0.00	0.00	0.00	0.00
30	Bottom	Microphazir	N	SG7	6	0.82	0.21	0.78	0.23	81.73	98.11
30	Bottom	Microphazir	N.K	NIR	8	0.54	0.31	0.48	0.33	54.37	99.97
30	Bottom	Microphazir	Cu	NIR	6	0.37	0.95	0.33	0.98	37.06	99.95
30	Bottom	Microphazir	Ca	SG7	3	0.39	0.07	0.32	0.07	38.53	97.29
30	Bottom	Microphazir	N.S	SG7	3	0.32	1.15	0.27	1.19	31.54	97.41
30	Bottom	Microphazir	K	NIR	7	0.32	0.29	0.24	0.31	31.50	99.97
30	Bottom	Microphazir	Zn	DT	3	0.25	5.41	0.22	5.51	25.19	91.20
30	Bottom	Microphazir	Fe.Mn	SG7	3	0.23	0.06	0.17	0.07	22.57	97.40
30	Bottom	Microphazir	P	DT	3	0.18	0.05	0.14	0.05	17.56	90.72
30	Bottom	Microphazir	Mg	SG7	3	0.20	0.04	0.13	0.04	20.22	97.39
30	Bottom	Microphazir	Fe	DT	2	0.14	15.03	0.12	15.16	13.74	88.13
30	Bottom	Microphazir	S	SG7	3	0.19	0.08	0.11	0.08	19.06	97.36
30	Bottom	Microphazir	Al	DT	2	0.13	2.31	0.11	2.33	12.80	87.90
30	Bottom	Microphazir	B	SNV	0	0.00	0.00	0.00	0.00	0.00	0.00
30	Bottom	Microphazir	Mn	SNV	0	0.00	0.00	0.00	0.00	0.00	0.00
30	Bottom	Microphazir	Na	SNV	0	0.00	0.00	0.00	0.00	0.00	0.00

Appendix C. Fit Statistics for PLS Regression Models Predicting Foliar Nutrient Concentration in pine needles (*continued*)

Stage	Location	Spectrometer	Nutrient	Transformation	Factors	R ² cal	RMSEPCal	R ² cv	RMSEPCv	ExpVarY	ExpVarX
30	Bottom	DLP Nano	N	DT	4	0.64	0.29	0.60	0.31	64.13	86.39
30	Bottom	DLP Nano	N.K	NIR	5	0.59	0.29	0.53	0.31	59.44	99.52
30	Bottom	DLP Nano	K	SG5	2	0.52	0.25	0.43	0.27	52.11	59.93
30	Bottom	DLP Nano	Ca	SNV	3	0.42	0.07	0.35	0.07	42.01	84.33
30	Bottom	DLP Nano	Mg	SG7	1	0.31	0.04	0.25	0.04	30.77	27.82
30	Bottom	DLP Nano	Cu	SNV	2	0.27	1.02	0.20	1.07	27.32	33.80
30	Bottom	DLP Nano	P	MSC_SG7	1	0.23	0.05	0.18	0.05	22.70	45.17
30	Bottom	DLP Nano	Al	SNV	0	0.00	0.00	0.00	0.00	0.00	0.00
30	Bottom	DLP Nano	B	SNV	0	0.00	0.00	0.00	0.00	0.00	0.00
30	Bottom	DLP Nano	Fe	SNV	0	0.00	0.00	0.00	0.00	0.00	0.00
30	Bottom	DLP Nano	Fe.Mn	SNV	0	0.00	0.00	0.00	0.00	0.00	0.00
30	Bottom	DLP Nano	Mn	SNV	0	0.00	0.00	0.00	0.00	0.00	0.00
30	Bottom	DLP Nano	N.S	SNV	0	0.00	0.00	0.00	0.00	0.00	0.00
30	Bottom	DLP Nano	Na	SNV	0	0.00	0.00	0.00	0.00	0.00	0.00
30	Bottom	DLP Nano	S	SNV	0	0.00	0.00	0.00	0.00	0.00	0.00
30	Bottom	DLP Nano	Zn	SNV	0	0.00	0.00	0.00	0.00	0.00	0.00
30	Dry	Foss	N	SNV	4	0.95	0.11	0.94	0.12	95.04	98.31
30	Dry	Foss	K	DT	14	0.93	0.09	0.85	0.14	93.16	99.92
30	Dry	Foss	N.K	MSC	13	0.91	0.13	0.82	0.19	91.32	99.92
30	Dry	Foss	Ca	DT	16	0.88	0.03	0.74	0.05	88.08	99.96
30	Dry	Foss	N.S	DT	7	0.78	0.66	0.68	0.78	77.57	99.38
30	Dry	Foss	Mg	MSC	8	0.74	0.02	0.63	0.03	74.04	99.66
30	Dry	Foss	P	DT	11	0.78	0.03	0.60	0.04	77.53	99.87
30	Dry	Foss	S	SNV	7	0.66	0.05	0.52	0.06	65.71	99.36
30	Dry	Foss	Cu	SG5	2	0.49	0.85	0.41	0.92	49.25	69.05
30	Dry	Foss	Zn	DT_SG5	2	0.40	4.86	0.27	5.34	39.68	67.14
30	Dry	Foss	Fe	SG7	1	0.25	14.01	0.21	14.34	25.07	68.53
30	Dry	Foss	Fe.Mn	SG7	1	0.23	0.06	0.19	0.06	22.93	68.30
30	Dry	Foss	Al	SNV_SG5	1	0.21	2.20	0.17	2.25	21.15	59.70
30	Dry	Foss	B	NIR	1	0.19	6.68	0.12	6.96	19.21	41.75
30	Dry	Foss	Mn	SNV	0	0.00	0.00	0.00	0.00	0.00	0.00
30	Dry	Foss	Na	SNV	0	0.00	0.00	0.00	0.00	0.00	0.00

Appendix C. Fit Statistics for PLS Regression Models Predicting Foliar Nutrient Concentration in pine needles (*continued*)

Stage	Location	Spectrometer	Nutrient	Transformation	Factors	R ² cal	RMSEPCal	R ² cv	RMSEPCv	ExpVarY	ExpVarX
30	Dry	Microphazir	N	SNV_SG5	4	0.96	0.09	0.94	0.12	96.35	67.88
30	Dry	Microphazir	N.K	SG7	4	0.74	0.23	0.63	0.28	74.28	84.62
30	Dry	Microphazir	Ca	DT	4	0.58	0.06	0.48	0.06	58.45	98.01
30	Dry	Microphazir	K	SG7	4	0.63	0.22	0.43	0.27	62.56	84.33
30	Dry	Microphazir	Cu	SG5	2	0.58	0.78	0.39	0.93	57.77	54.38
30	Dry	Microphazir	Mg	MSC	6	0.66	0.02	0.39	0.03	65.88	98.71
30	Dry	Microphazir	Zn	SNV	2	0.40	4.85	0.34	5.10	40.06	89.95
30	Dry	Microphazir	N.S	SNV	2	0.39	1.09	0.32	1.15	38.66	94.19
30	Dry	Microphazir	Fe	SNV_SG5	1	0.23	14.19	0.19	14.57	23.09	52.72
30	Dry	Microphazir	Fe.Mn	SG7	1	0.20	0.06	0.16	0.07	19.89	69.21
30	Dry	Microphazir	P	MSC_SG7	2	0.29	0.05	0.15	0.05	28.63	78.45
30	Dry	Microphazir	Al	SNV_SG5	1	0.18	2.23	0.14	2.30	18.27	52.13
30	Dry	Microphazir	S	SG7	1	0.15	0.08	0.11	0.08	14.68	69.30
30	Dry	Microphazir	B	SNV	0	0.00	0.00	0.00	0.00	0.00	0.00
30	Dry	Microphazir	Mn	SNV	0	0.00	0.00	0.00	0.00	0.00	0.00
30	Dry	Microphazir	Na	SNV	0	0.00	0.00	0.00	0.00	0.00	0.00
30	Dry	DLP Nano	N	DT	6	0.94	0.12	0.90	0.16	93.92	96.96
30	Dry	DLP Nano	N.K	NIR	2	0.49	0.33	0.46	0.34	49.02	99.96
30	Dry	DLP Nano	Cu	NIR	2	0.46	0.88	0.42	0.91	45.80	99.96
30	Dry	DLP Nano	Zn	NIR	2	0.39	4.90	0.34	5.08	38.68	99.96
30	Dry	DLP Nano	Ca	NIR	1	0.37	0.07	0.34	0.07	36.60	99.88
30	Dry	DLP Nano	N.S	MSC	8	0.76	0.68	0.31	1.15	76.32	97.86
30	Dry	DLP Nano	K	NIR	2	0.34	0.29	0.29	0.30	34.10	99.96
30	Dry	DLP Nano	P	SNV	1	0.28	0.05	0.24	0.05	27.97	66.40
30	Dry	DLP Nano	Fe.Mn	NIR	2	0.28	0.06	0.23	0.06	28.20	99.96
30	Dry	DLP Nano	S	NIR	2	0.24	0.08	0.19	0.08	23.82	99.96
30	Dry	DLP Nano	Fe	NIR	2	0.21	14.40	0.15	14.88	20.82	99.96
30	Dry	DLP Nano	B	MSC	1	0.17	6.81	0.12	7.02	17.06	68.26
30	Dry	DLP Nano	Al	DT	1	0.08	2.37	0.03	2.43	8.10	71.67
30	Dry	DLP Nano	Mg	SNV	0	0.00	0.00	0.00	0.00	0.00	0.00
30	Dry	DLP Nano	Mn	SNV	0	0.00	0.00	0.00	0.00	0.00	0.00
30	Dry	DLP Nano	Na	SNV	0	0.00	0.00	0.00	0.00	0.00	0.00

Appendix C. Fit Statistics for PLS Regression Models Predicting Foliar Nutrient Concentration in pine needles (*continued*)

Stage	Location	Spectrometer	Nutrient	Transformation	Factors	R ² cal	RMSEPCal	R ² cv	RMSEPCv	ExpVarY	ExpVarX
30	Top	Microphazir	N	SG7	5	0.90	0.15	0.82	0.20	90.22	99.04
30	Top	Microphazir	N.K	NIR	6	0.56	0.30	0.44	0.34	56.16	99.97
30	Top	Microphazir	Ca	MSC_SG7	2	0.36	0.07	0.26	0.08	36.00	93.82
30	Top	Microphazir	N.S	MSC_SG7	2	0.36	1.12	0.23	1.22	35.57	93.94
30	Top	Microphazir	Cu	NIR	3	0.30	1.00	0.20	1.07	30.11	99.54
30	Top	Microphazir	K	NIR	3	0.26	0.31	0.20	0.32	26.23	99.80
30	Top	Microphazir	Zn	NIR	1	0.18	5.68	0.11	5.89	17.62	27.28
30	Top	Microphazir	Al	SNV	0	0.00	0.00	0.00	0.00	0.00	0.00
30	Top	Microphazir	B	SNV	0	0.00	0.00	0.00	0.00	0.00	0.00
30	Top	Microphazir	Fe	SNV	0	0.00	0.00	0.00	0.00	0.00	0.00
30	Top	Microphazir	Fe.Mn	SNV	0	0.00	0.00	0.00	0.00	0.00	0.00
30	Top	Microphazir	Mg	SNV	0	0.00	0.00	0.00	0.00	0.00	0.00
30	Top	Microphazir	Mn	SNV	0	0.00	0.00	0.00	0.00	0.00	0.00
30	Top	Microphazir	Na	SNV	0	0.00	0.00	0.00	0.00	0.00	0.00
30	Top	Microphazir	P	SNV	0	0.00	0.00	0.00	0.00	0.00	0.00
30	Top	Microphazir	S	SNV	0	0.00	0.00	0.00	0.00	0.00	0.00
30	Top	DLP Nano	N	DT	7	0.75	0.24	0.57	0.32	75.07	96.43
30	Top	DLP Nano	N.K	SG7	2	0.60	0.29	0.55	0.30	59.71	67.37
30	Top	DLP Nano	Ca	DT	3	0.52	0.06	0.47	0.06	51.66	64.92
30	Top	DLP Nano	K	SG7	1	0.48	0.26	0.44	0.27	48.39	29.10
30	Top	DLP Nano	Mg	SG7	1	0.30	0.04	0.24	0.04	29.74	29.50
30	Top	DLP Nano	P	MSC_SG7	1	0.22	0.05	0.18	0.05	22.44	48.11
30	Top	DLP Nano	Zn	SNV	1	0.14	5.80	0.10	5.94	14.03	52.01
30	Top	DLP Nano	Al	SNV	0	0.00	0.00	0.00	0.00	0.00	0.00
30	Top	DLP Nano	B	SNV	0	0.00	0.00	0.00	0.00	0.00	0.00
30	Top	DLP Nano	Cu	SNV	0	0.00	0.00	0.00	0.00	0.00	0.00
30	Top	DLP Nano	Fe	SNV	0	0.00	0.00	0.00	0.00	0.00	0.00
30	Top	DLP Nano	Fe.Mn	SNV	0	0.00	0.00	0.00	0.00	0.00	0.00
30	Top	DLP Nano	Mn	SNV	0	0.00	0.00	0.00	0.00	0.00	0.00
30	Top	DLP Nano	N.S	SNV	0	0.00	0.00	0.00	0.00	0.00	0.00
30	Top	DLP Nano	Na	SNV	0	0.00	0.00	0.00	0.00	0.00	0.00
30	Top	DLP Nano	S	SNV	0	0.00	0.00	0.00	0.00	0.00	0.00

Appendix C. Fit Statistics for PLS Regression Models Predicting Foliar Nutrient Concentration in pine needles (*continued*)

Stage	Location	Spectrometer	Nutrient	Transformation	Factors	R ² cal	RMSEPCal	R ² cv	RMSEPCv	ExpVarY	ExpVarX
30	WP	Microphazir	N	SNV_SG7	6	0.93	0.13	0.86	0.18	92.99	98.07
30	WP	Microphazir	N.K	NIR	7	0.64	0.27	0.49	0.33	64.20	99.98
30	WP	Microphazir	Ca	MSC_SG5	2	0.40	0.07	0.28	0.07	40.50	89.43
30	WP	Microphazir	Cu	SNV	3	0.35	0.97	0.28	1.02	34.94	94.77
30	WP	Microphazir	K	NIR	7	0.51	0.25	0.27	0.30	50.98	99.98
30	WP	Microphazir	N.S	SG7	2	0.28	1.18	0.23	1.22	27.53	98.87
30	WP	Microphazir	Zn	MSC_SG7	2	0.27	5.33	0.19	5.64	27.48	94.68
30	WP	Microphazir	Fe.Mn	SNV	1	0.14	0.07	0.08	0.07	14.00	45.22
30	WP	Microphazir	Al	SNV	0	0.00	0.00	0.00	0.00	0.00	0.00
30	WP	Microphazir	B	SNV	0	0.00	0.00	0.00	0.00	0.00	0.00
30	WP	Microphazir	Fe	SNV	0	0.00	0.00	0.00	0.00	0.00	0.00
30	WP	Microphazir	Mg	SNV	0	0.00	0.00	0.00	0.00	0.00	0.00
30	WP	Microphazir	Mn	SNV	0	0.00	0.00	0.00	0.00	0.00	0.00
30	WP	Microphazir	Na	SNV	0	0.00	0.00	0.00	0.00	0.00	0.00
30	WP	Microphazir	P	SNV	0	0.00	0.00	0.00	0.00	0.00	0.00
30	WP	Microphazir	S	SNV	0	0.00	0.00	0.00	0.00	0.00	0.00
30	WP	DLP Nano	N	DT	6	0.76	0.24	0.67	0.28	76.21	96.96
30	WP	DLP Nano	N.K	SG7	3	0.70	0.25	0.64	0.27	70.35	82.54
30	WP	DLP Nano	K	SG5	2	0.52	0.25	0.45	0.26	52.03	74.07
30	WP	DLP Nano	Ca	NIR	4	0.47	0.06	0.43	0.07	47.17	98.83
30	WP	DLP Nano	Mg	SG7	1	0.30	0.04	0.25	0.04	30.36	33.51
30	WP	DLP Nano	P	MSC_SG7	1	0.22	0.05	0.19	0.05	22.26	55.07
30	WP	DLP Nano	Zn	DT_SG5	1	0.17	5.70	0.13	5.85	17.09	60.35
30	WP	DLP Nano	Al	SNV	0	0.00	0.00	0.00	0.00	0.00	0.00
30	WP	DLP Nano	B	SNV	0	0.00	0.00	0.00	0.00	0.00	0.00
30	WP	DLP Nano	Cu	SNV	0	0.00	0.00	0.00	0.00	0.00	0.00
30	WP	DLP Nano	Fe	SNV	0	0.00	0.00	0.00	0.00	0.00	0.00
30	WP	DLP Nano	Fe.Mn	SNV	0	0.00	0.00	0.00	0.00	0.00	0.00
30	WP	DLP Nano	Mn	SNV	0	0.00	0.00	0.00	0.00	0.00	0.00
30	WP	DLP Nano	N.S	SNV	0	0.00	0.00	0.00	0.00	0.00	0.00
30	WP	DLP Nano	Na	SNV	0	0.00	0.00	0.00	0.00	0.00	0.00
30	WP	DLP Nano	S	SNV	0	0.00	0.00	0.00	0.00	0.00	0.00

Appendix D(a). Standard laboratory foliar nutrient concentrations for the **complete HNS regime** at **15 days post-treatment**.

Treatments	N	P	K	Ca	Mg	S	Fe	Mn	Zn	Cu	B	Na	Al	N:S	N:K	Fe:Mn
Complete	2.06	0.28	2	0.33	0.19	0.33	263	234	22.1	7.17	41.8	0.11	11.5	6.19	1.03	1.13
Complete	2.28	0.3	2.18	0.39	0.19	0.52	632	323	26.4	8.2	44.1	0.06	10.9	4.34	1.05	1.96
Complete	2.58	0.33	1.81	0.4	0.21	0.32	42.8	273	23.1	6.66	55	0.05	9.94	8.18	1.43	0.16
Complete	2.18	0.24	1.66	0.44	0.22	0.32	39	281	20.1	6.81	54.9	0.08	4.47	6.79	1.31	0.14
Complete	2.15	0.31	2.3	0.46	0.26	0.46	157	209	30.9	7.84	51	0.11	7.34	4.72	0.93	0.75
Complete	1.93	0.28	1.64	0.45	0.23	0.35	62.5	274	29.5	7.42	46.5	0.13	4.05	5.54	1.18	0.23
Complete	2.34	0.31	1.93	0.37	0.22	0.39	52.8	303	26.6	7.86	55.1	0.06	2.94	5.92	1.21	0.17
Complete	1.82	0.28	1.55	0.44	0.23	0.29	58.6	230	26.3	6.85	52.4	0.1	3.52	6.3	1.18	0.25
Complete	2.21	0.24	1.8	0.44	0.23	0.27	32.8	178	19.2	6.38	44.2	0.05	2.52	8.18	1.23	0.18
Complete	2.31	0.3	1.75	0.42	0.2	0.39	36.4	302	21.6	7.41	49.4	0.05	3.84	5.98	1.32	0.12
Complete	2.34	0.28	2.11	0.48	0.24	0.39	36.8	250	22.3	7	54.1	0.04	2.65	6.07	1.11	0.15
Complete	2.21	0.3	1.64	0.48	0.24	0.38	39.8	290	31.8	6.73	52.9	0.06	7.69	5.79	1.35	0.14
Complete	2.01	0.29	2.16	0.36	0.21	0.39	37.6	236	26.8	6.74	39.8	0.09	2.75	5.21	0.93	0.16
Complete	2.51	0.27	1.65	0.32	0.18	0.34	34.3	273	26	6.48	38.5	0.08	4.29	7.34	1.52	0.13
Complete	2.08	0.28	1.57	0.43	0.2	0.31	44.5	325	33.3	7.19	52.9	0.11	6.39	6.76	1.32	0.14
Complete	2	0.26	1.65	0.39	0.21	0.3	45.8	174	41	7.42	47.5	0.06	7.33	6.69	1.21	0.26
Complete	2.05	0.28	1.76	0.37	0.18	0.26	47.9	235	19.6	6.59	46	0.08	5.84	7.99	1.17	0.2
Complete	2.18	0.25	1.87	0.38	0.23	0.33	38.4	270	22.9	6.31	49.8	0.06	3.46	6.63	1.17	0.14
Complete	2.17	0.29	1.78	0.41	0.21	0.41	38.1	237	24.6	6.28	53.9	0.04	4.78	5.34	1.21	0.16
Complete	1.79	0.31	1.9	0.42	0.22	0.31	34.5	264	27.5	6.96	48.9	0.08	3.56	5.76	0.94	0.13

Appendix D(b). Standard laboratory foliar nutrient concentrations for the **50% NPK HNS regime at 15 days post-treatment.**

Treatments	N	P	K	Ca	Mg	S	Fe	Mn	Zn	Cu	B	Na	Al	N:S	N:K	Fe:Mn
50%NPK	1.87	0.24	1.52	0.32	0.19	0.33	32.7	211	18.3	5.93	38.9	0.04	4.09	5.76	1.23	0.15
50%NPK	1.94	0.23	2.3	0.4	0.21	0.36	30.2	258	19.5	6.38	46.9	0.05	3.76	5.37	0.84	0.12
50%NPK	1.58	0.19	1.55	0.33	0.17	0.25	35.8	204	17	7	29.4	0.1	7.34	6.38	1.02	0.18
50%NPK	2.8	0.26	1.61	0.47	0.27	0.36	44.3	186	32.5	7.73	49.6	0.13	4.97	7.7	1.74	0.24
50%NPK	2.68	0.26	1.58	0.42	0.2	0.21	35.1	297	21.7	7.63	45	0.11	6.7	12.6	1.7	0.12
50%NPK	1.9	0.23	1.66	0.36	0.23	0.36	36.3	195	21.9	7.52	40.1	0.09	4.33	5.3	1.14	0.19
50%NPK	2.03	0.24	1.68	0.35	0.23	0.44	41.6	292	22.5	6.69	47.3	0.07	5.51	4.61	1.2	0.14
50%NPK	2.79	0.21	1.63	0.36	0.2	0.29	36.5	219	15.8	7.51	45.8	0.09	3.47	9.53	1.71	0.17
50%NPK	1.74	0.2	2.11	0.49	0.28	0.39	41.2	241	22.4	8.27	41.8	0.11	4.58	4.48	0.83	0.17
50%NPK	1.86	0.21	1.65	0.45	0.24	0.28	34.1	237	18	5.63	41.4	0.1	2.87	6.71	1.12	0.14
50%NPK	2.33	0.28	2.06	0.39	0.24	0.38	33.7	292	26.6	7.2	51.4	0.12	2.99	6.17	1.13	0.12
50%NPK	2.22	0.27	1.95	0.44	0.25	0.41	44.1	272	28.9	7.93	54.5	0.11	4.06	5.38	1.14	0.16
50%NPK	2.03	0.27	2.04	0.46	0.27	0.38	49.1	310	27.6	7.01	54.9	0.07	3.2	5.34	1	0.16
50%NPK	2.28	0.23	1.51	0.46	0.25	0.4	47.7	228	20.1	6.75	45.3	0.11	4	5.78	1.51	0.21
50%NPK	2.08	0.24	1.53	0.37	0.23	0.41	36.7	274	21.9	7.27	37.6	0.11	3.02	5.08	1.36	0.13
50%NPK	2.06	0.23	1.86	0.33	0.2	0.41	39.7	205	26.1	7.21	43.8	0.07	4.68	4.97	1.11	0.19
50%NPK	1.92	0.22	1.64	0.38	0.21	0.32	39.2	243	19.1	5.89	48.4	0.06	3.08	5.93	1.17	0.16
50%NPK	2.12	0.25	1.93	0.38	0.21	0.38	35.3	289	20.7	6.22	43.9	0.07	6.6	5.57	1.1	0.12
50%NPK	2.05	0.27	1.47	0.45	0.25	0.38	39	261	36.6	6.88	48.2	0.08	3.07	5.35	1.4	0.15
50%NPK	2.04	0.27	1.68	0.44	0.27	0.35	41	294	30.6	7.58	54.2	0.13	2.92	5.83	1.21	0.14

Appendix D(c). Standard laboratory foliar nutrient concentrations for the **0% N HNS regime** at **15 days post-treatment**.

Treatments	N	P	K	Ca	Mg	S	Fe	Mn	Zn	Cu	B	Na	Al	N:S	N:K	Fe:Mn
0%N	1.26	0.35	1.53	0.38	0.25	0.29	61	302	33.9	6.32	49.7	0.05	5.2	4.4	0.83	0.2
0%N	1.22	0.25	1.52	0.35	0.21	0.31	54.2	214	33.9	6.43	40.1	0.11	4.93	3.99	0.8	0.25
0%N	1.26	0.29	1.92	0.45	0.24	0.44	93.2	259	20.8	7.02	42.7	0.11	14.4	2.9	0.66	0.36
0%N	1.28	0.29	1.43	0.34	0.23	0.33	57.7	271	25.6	5.49	41.9	0.07	4.3	3.93	0.89	0.21
0%N	1.44	0.33	1.53	0.36	0.23	0.27	97.2	269	18.2	6.12	48.8	0.07	6.73	5.28	0.94	0.36
0%N	1.34	0.32	1.55	0.39	0.27	0.25	48.8	239	18.3	5.35	62.5	0.13	6.16	5.27	0.86	0.2
0%N	1.23	0.26	2.02	0.36	0.22	0.34	72.7	213	16.7	6.03	46.9	0.11	15.9	3.6	0.61	0.34
0%N	1.07	0.27	1.41	0.31	0.2	0.22	45.6	184	15.5	4.8	37.2	0.11	11.3	4.78	0.76	0.25
0%N	1.24	0.26	1.64	0.37	0.22	0.22	91.7	229	14.4	5.83	51.4	0.05	5.62	5.59	0.76	0.4
0%N	1.4	0.3	1.64	0.34	0.23	0.41	90	248	26.4	6.84	42.1	0.11	6.39	3.38	0.85	0.36
0%N	1.3	0.26	1.46	0.41	0.23	0.35	52.6	281	20.4	5.77	51.1	0.11	7.98	3.69	0.89	0.19
0%N	1.29	0.31	1.94	0.39	0.22	0.36	103	269	23	5.69	57.3	0.06	7.33	3.58	0.67	0.38
0%N	1.29	0.34	1.81	0.4	0.23	0.37	91.4	269	26.9	6.41	54.4	0.07	7.65	3.53	0.71	0.34
0%N	1.24	0.25	1.53	0.3	0.21	0.33	78.1	253	19.2	5.97	46.2	0.1	4.69	3.75	0.81	0.31
0%N	1.29	0.32	1.75	0.32	0.2	0.35	54.1	233	19	5.22	46.3	0.08	5.1	3.7	0.74	0.23
0%N	1.13	0.33	1.38	0.3	0.19	0.23	58.6	174	14.3	5.23	50.2	0.15	6.1	5	0.82	0.34
0%N	1.37	0.32	1.73	0.39	0.21	0.35	83.6	300	20.5	5.62	52.1	0.12	4.68	3.88	0.79	0.28
0%N	1.32	0.35	1.57	0.31	0.22	0.25	51.9	250	23.8	4.72	53.3	0.07	5.59	5.31	0.84	0.21
0%N	1.35	0.27	1.41	0.36	0.2	0.34	67.8	248	28.3	6.07	48.9	0.07	7.56	3.96	0.96	0.27
0%N	1.5	0.35	2.05	0.37	0.24	0.45	56.7	292	24.5	7.46	51.8	0.1	5.1	3.3	0.73	0.19

Appendix D(d). Standard laboratory foliar nutrient concentrations for the **0% P HNS regime at 15 days post-treatment.**

Treatments	N	P	K	Ca	Mg	S	Fe	Mn	Zn	Cu	B	Na	Al	N:S	N:K	Fe:Mn
0%P	1.96	0.25	1.97	0.36	0.2	0.35	40.8	299	35.7	8.25	47.3	0.05	11.7	5.52	0.99	0.14
0%P	2.33	0.25	1.69	0.4	0.21	0.34	39.7	291	29.9	7.79	41.5	0.09	4.29	6.88	1.37	0.14
0%P	2	0.21	2.08	0.34	0.19	0.41	37.8	280	28.5	6.86	36.6	0.09	4.05	4.89	0.96	0.13
0%P	2.14	0.25	1.81	0.38	0.21	0.46	48.6	302	37.1	8.07	42.3	0.12	4.81	4.7	1.18	0.16
0%P	1.67	0.19	1.76	0.38	0.23	0.26	35.5	226	25	6.01	41.7	0.07	5.72	6.48	0.95	0.16
0%P	2.1	0.23	1.75	0.41	0.24	0.36	44.2	325	32.2	7.33	57	0.1	3.98	5.85	1.2	0.14
0%P	2.06	0.26	2.01	0.55	0.24	0.47	46.5	321	36.6	7.95	60.5	0.17	9.8	4.36	1.02	0.14
0%P	2.44	0.3	2.19	0.57	0.32	0.48	45	387	37.5	8.72	55.6	0.12	4.16	5.11	1.11	0.12
0%P	2.56	0.25	2.29	0.41	0.27	0.5	41.3	295	29	9.07	48.6	0.08	4.32	5.15	1.12	0.14
0%P	2.58	0.29	2.43	0.54	0.28	0.52	41.6	368	37.1	9.44	54.4	0.1	3.48	4.95	1.06	0.11
0%P	2.24	0.19	2.15	0.47	0.28	0.45	47.8	218	30.2	8.13	44.9	0.12	5.67	5	1.04	0.22
0%P	1.9	0.29	2.93	0.45	0.24	0.33	36.9	167	35	9.32	41.3	0.07	11.1	5.77	0.65	0.22
0%P	2.25	0.26	2.06	0.45	0.25	0.46	47.9	288	28.8	7.65	47.7	0.11	19.6	4.92	1.09	0.17
0%P	1.71	0.2	2.3	0.47	0.3	0.46	41.2	268	32.3	7.69	41.9	0.06	3.95	3.68	0.74	0.15
0%P	2.16	0.21	1.91	0.51	0.26	0.28	50.7	280	32.1	7.23	51	0.1	10.2	7.72	1.13	0.18
0%P	2.05	0.24	2.06	0.5	0.24	0.37	48.9	289	36.8	15.8	46.4	0.12	178	5.5	1	0.17
0%P	2.06	0.24	2.01	0.5	0.24	0.44	174	283	28.8	7.98	48.7	0.07	9.46	4.69	1.03	0.62
0%P	2.11	0.26	2.27	0.45	0.24	0.48	56.7	235	30.8	9.23	44.2	0.15	8.42	4.39	0.93	0.24
0%P	2.03	0.25	1.76	0.42	0.21	0.35	49	292	32.6	7.93	54.3	0.15	6.65	5.83	1.15	0.17
0%P	2.22	0.24	2.14	0.4	0.2	0.43	62.5	258	40.7	7.25	48.5	0.04	6.2	5.1	1.04	0.24

Appendix D(e). Standard laboratory foliar nutrient concentrations for the **0% K HNS regime** at **15 days post-treatment**.

Treatments	N	P	K	Ca	Mg	S	Fe	Mn	Zn	Cu	B	Na	Al	N:S	N:K	Fe:Mn
0%K	2.13	0.31	1.45	0.52	0.24	0.28	41.9	305	35.8	8.62	60.9	0.11	4.32	7.57	1.47	0.14
0%K	2.15	0.35	1.5	0.55	0.32	0.52	454	293	33.7	10.1	54.4	0.21	6.33	4.15	1.43	1.55
0%K	1.92	0.26	1.53	0.52	0.27	0.42	38.2	249	28.1	8.05	50.7	0.08	2.93	4.6	1.25	0.15
0%K	2.57	0.34	1.95	0.52	0.29	0.43	34.7	306	33.8	8.29	61.5	0.04	1.85	5.92	1.32	0.11
0%K	2.07	0.31	1.41	0.44	0.25	0.3	38.9	279	24.7	7.71	57.2	0.11	5.28	6.92	1.47	0.14
0%K	1.97	0.27	1.53	0.49	0.25	0.4	57.7	259	26.4	6.61	45.5	0.12	11	4.95	1.29	0.22
0%K	2.07	0.29	1.43	0.61	0.33	0.47	34.8	280	30.6	9.6	51.3	0.11	4.26	4.38	1.45	0.12
0%K	1.81	0.3	1.39	0.45	0.25	0.35	44.4	267	24.2	7.23	38.9	0.11	5.98	5.13	1.3	0.17
0%K	2.1	0.31	1.45	0.68	0.36	0.27	41	278	27.2	7.85	66.2	0.11	1.56	7.76	1.45	0.15
0%K	2.12	0.25	1.49	0.49	0.28	0.38	40.3	276	22.8	7.37	46.8	0.09	6.2	5.53	1.42	0.15
0%K	2	0.29	1.69	0.48	0.3	0.49	41.6	237	24.3	8.7	49.1	0.09	15.5	4.09	1.18	0.18
0%K	1.89	0.28	1.66	0.52	0.32	0.4	59.8	213	20.9	8.26	49.2	0.17	8.44	4.73	1.14	0.28
0%K	2.17	0.3	1.73	0.49	0.28	0.35	39.1	244	27.4	7.36	55.2	0.06	3.62	6.16	1.26	0.16
0%K	2.18	0.33	1.62	0.6	0.32	0.49	34.1	356	29.7	8.63	58.6	0.04	3.2	4.48	1.35	0.1
0%K	1.99	0.27	1.17	0.48	0.24	0.27	35.3	273	23.3	5.43	48.7	0.09	2.82	7.33	1.7	0.13
0%K	2.34	0.37	1.74	0.55	0.29	0.35	39.2	303	34.6	9.66	53.2	0.08	3.82	6.72	1.35	0.13
0%K	2.03	0.3	1.35	0.54	0.28	0.42	34.8	311	27.1	6.75	48.6	0.08	2.69	4.81	1.5	0.11
0%K	2.1	0.3	1.42	0.51	0.26	0.27	34.3	212	22.2	6.49	57.2	0.06	2.15	7.76	1.48	0.16
0%K	2.29	0.34	1.96	0.6	0.29	0.52	35.5	296	37.2	10.5	60.6	0.07	57.2	4.36	1.17	0.12
0%K	1.85	0.24	1.45	0.44	0.24	0.32	32.2	214	22	7.37	47.4	0.14	15	5.85	1.27	0.15

Appendix D(f). Standard laboratory foliar nutrient concentrations for the **complete HNS regime** at **30 days post-treatment**.

Treatments	N	P	K	Ca	Mg	S	Fe	Mn	Zn	Cu	B	Na	Al	N:S	N:K	Fe:Mn
Complete	2.03	0.33	1.81	0.48	0.25	0.51	85.4	387	36.2	8.37	52	0.1	4.41	3.94	1.12	0.22
Complete	2.24	0.3	1.68	0.45	0.21	0.35	59.4	278	26.5	5.86	56.1	0.15	5.72	6.46	1.33	0.21
Complete	1.97	0.28	1.82	0.4	0.22	0.35	50.1	169	26	6.77	42.5	0.1	4.4	5.67	1.08	0.3
Complete	2.15	0.3	1.95	0.45	0.19	0.39	49.5	310	23.3	7.08	56	0.09	4.06	5.5	1.1	0.16
Complete	2.38	0.3	2.23	0.49	0.22	0.39	55.4	358	26.5	7.53	54.3	0.11	5.51	6.1	1.07	0.15
Complete	2.45	0.38	1.99	0.51	0.27	0.5	57.6	301	32.6	7.96	55.9	0.1	6.67	4.87	1.23	0.19
Complete	2.35	0.32	2.21	0.45	0.24	0.39	41.6	322	26.5	6.54	51.4	0.06	4.1	5.95	1.06	0.13
Complete	2.29	0.3	1.77	0.41	0.25	0.4	49.3	289	26.3	7.82	45.1	0.11	5.5	5.75	1.3	0.17
Complete	2.31	0.36	2.35	0.43	0.24	0.45	50	330	21	7.82	42.8	0.07	5.27	5.13	0.98	0.15
Complete	2.17	0.31	1.71	0.48	0.22	0.3	42.4	266	26.8	6.98	62	0.06	3.06	7.29	1.27	0.16
Complete	2.18	0.29	1.51	0.49	0.28	0.56	51.8	485	30.9	8.21	50.1	0.08	4.88	3.87	1.44	0.11
Complete	2.22	0.37	1.93	0.39	0.23	0.39	54.5	331	27.1	7.98	43.9	0.07	4.7	5.68	1.15	0.16
Complete	2.17	0.32	1.73	0.44	0.23	0.36	47.7	264	26.5	8.01	41.9	0.1	8.64	6	1.26	0.18
Complete	2.51	0.37	1.9	0.5	0.26	0.42	48.6	396	25.1	8.3	47.5	0.12	4.56	5.93	1.32	0.12
Complete	2.23	0.32	1.69	0.47	0.21	0.42	43.6	346	29.3	6.6	45	0.07	7.72	5.29	1.32	0.13
Complete	2.43	0.36	1.88	0.46	0.24	0.49	66.7	321	23	6.62	47.2	0.12	8.28	5.01	1.29	0.21
Complete	2.23	0.33	2.28	0.5	0.23	0.46	51.5	332	24.1	7.56	47.5	0.1	4.4	4.87	0.98	0.16
Complete	2.08	0.31	1.84	0.45	0.23	0.46	48.8	225	27	7.19	50.5	0.11	4.04	4.5	1.13	0.22
Complete	2.34	0.33	1.76	0.38	0.22	0.36	42.6	355	30.8	7.32	47.2	0.06	3.65	6.54	1.33	0.12
Complete	2.14	0.31	1.67	0.41	0.22	0.32	42.7	330	31	7.71	52.4	0.07	4.16	6.69	1.28	0.13

Appendix D(g). Standard laboratory foliar nutrient concentrations for the **50% NPK HNS regime at 30 days post-treatment.**

Treatments	N	P	K	Ca	Mg	S	Fe	Mn	Zn	Cu	B	Na	Al	N:S	N:K	Fe:Mn
50%NPK	2.23	0.26	1.85	0.41	0.26	0.46	53.1	348	25.7	6.96	51.8	0.1	3.74	4.84	1.2	0.15
50%NPK	2.1	0.28	1.44	0.46	0.29	0.51	65.3	337	22.3	7.25	47	0.14	5.58	4.14	1.46	0.19
50%NPK	2.28	0.3	1.85	0.35	0.23	0.36	52.5	334	30.6	7.47	47.2	0.13	5.09	6.33	1.23	0.16
50%NPK	2.32	0.28	1.89	0.35	0.24	0.42	51.5	312	30.2	8.96	49.7	0.07	4.26	5.54	1.23	0.17
50%NPK	2.04	0.28	1.95	0.47	0.28	0.5	39.3	309	26.9	7.57	45.3	0.11	2.67	4.11	1.05	0.13
50%NPK	2.07	0.22	1.92	0.33	0.23	0.32	40.9	147	23.9	6.68	39.4	0.09	12.8	6.41	1.08	0.28
50%NPK	1.98	0.23	1.59	0.37	0.25	0.36	53.6	280	24	6.76	43.8	0.09	4.93	5.42	1.24	0.19
50%NPK	2.31	0.33	1.78	0.41	0.26	0.5	58.1	362	27.3	8.76	44.5	0.12	4.37	4.6	1.3	0.16
50%NPK	2.35	0.28	1.63	0.44	0.27	0.48	51.6	356	32.1	9.67	53.4	0.11	5.04	4.92	1.44	0.14
50%NPK	2.21	0.28	1.54	0.32	0.21	0.22	68.4	199	22.3	7.74	47.5	0.12	9.6	10.1	1.43	0.34
50%NPK	2.26	0.3	2.21	0.55	0.36	0.47	54.9	426	33.4	8.96	52.5	0.04	2.99	4.86	1.02	0.13
50%NPK	2	0.25	1.58	0.44	0.29	0.5	56.1	336	32.7	8.38	58.2	0.04	4.31	4.01	1.26	0.17
50%NPK	2.11	0.25	2.14	0.44	0.26	0.62	49.8	340	31	8.98	57.5	0.12	3.68	3.42	0.99	0.15
50%NPK	1.99	0.26	1.84	0.49	0.32	0.38	51.2	332	23	7.58	53.3	0.06	4.85	5.19	1.08	0.15
50%NPK	1.99	0.24	1.65	0.34	0.19	0.28	46.4	304	20.7	5.58	50.3	0.06	4.51	7.16	1.2	0.15
50%NPK	1.99	0.22	1.44	0.38	0.26	0.34	54.2	319	22.2	6.68	45.1	0.04	4.91	5.8	1.38	0.17
50%NPK	2.41	0.28	1.47	0.44	0.25	0.48	57.2	394	23.4	7.39	53.5	0.1	4.62	5.01	1.64	0.15
50%NPK	2.16	0.27	1.82	0.46	0.25	0.4	62.1	253	23.7	6.87	46.1	0.15	5.73	5.38	1.18	0.25
50%NPK	2.2	0.25	1.52	0.39	0.24	0.34	65.7	341	29.5	7.19	46.1	0.1	5.26	6.54	1.44	0.19
50%NPK	2.14	0.24	1.95	0.43	0.27	0.38	41	363	25.3	8.47	71.5	0.04	3.86	5.6	1.1	0.11

Appendix D(h). Standard laboratory foliar nutrient concentrations for the **0% N HNS regime at 30 days post-treatment.**

Treatments	N	P	K	Ca	Mg	S	Fe	Mn	Zn	Cu	B	Na	Al	N:S	N:K	Fe:Mn
0%N	0.81	0.3	1.57	0.25	0.19	0.22	66.6	178	20.3	5.08	40.5	0.08	7.34	3.73	0.51	0.37
0%N	1.14	0.32	1.42	0.42	0.29	0.45	90.9	333	24.7	6.6	56.5	0.15	7.19	2.54	0.8	0.27
0%N	0.88	0.33	1.64	0.33	0.21	0.29	74.8	267	19.4	5.62	46.4	0.08	6.62	3.04	0.54	0.28
0%N	1.1	0.39	1.72	0.38	0.25	0.3	93.9	359	24.5	7.1	62.4	0.13	9.95	3.67	0.64	0.26
0%N	0.95	0.38	1.69	0.34	0.23	0.31	80.3	257	19.8	6.07	53.7	0.13	7.31	3.07	0.56	0.31
0%N	1.25	0.37	1.43	0.44	0.29	0.34	58.3	332	17	6.4	61.8	0.12	7.99	3.67	0.87	0.18
0%N	1.09	0.38	1.92	0.44	0.24	0.49	104	323	26.2	6.97	61.6	0.13	10.4	2.22	0.57	0.32
0%N	1.09	0.38	1.58	0.45	0.28	0.36	80.1	360	28.2	7.69	64.6	0.12	12.3	3.05	0.69	0.22
0%N	1.08	0.39	1.47	0.36	0.25	0.34	84.1	373	23.2	5.76	50.7	0.04	9.1	3.18	0.74	0.23
0%N	0.87	0.3	1.16	0.27	0.18	0.22	52.8	236	17.5	5.1	37	0.1	8.27	3.99	0.74	0.22
0%N	0.87	0.31	1.24	0.34	0.22	0.29	65.2	268	20.3	4.85	47.1	0.12	9.77	3.04	0.7	0.24
0%N	1.11	0.36	1.59	0.39	0.26	0.42	65.9	352	27.6	7.28	65.7	0.04	7.06	2.61	0.7	0.19
0%N	1.04	0.4	1.89	0.39	0.22	0.36	93.6	310	20.1	5.77	56.5	0.12	8.79	2.93	0.55	0.3
0%N	0.89	0.34	1.65	0.39	0.21	0.28	88.2	252	20	5.53	38.2	0.1	8.81	3.19	0.54	0.35
0%N	0.98	0.33	1.33	0.3	0.21	0.24	60.5	218	19.6	4.97	50.2	0.09	8.21	4	0.73	0.28
0%N	1.16	0.31	1.49	0.35	0.19	0.37	78.1	344	21.9	5.75	50.3	0.09	9.79	3.14	0.78	0.23
0%N	1.14	0.49	1.85	0.48	0.31	0.58	86.7	339	29.4	6.48	56.6	0.08	8.96	1.97	0.61	0.26
0%N	0.99	0.33	1.45	0.33	0.19	0.32	86.9	332	25.2	6.32	55.8	0.1	10.3	3.06	0.68	0.26
0%N	1.09	0.39	1.7	0.41	0.23	0.34	78	428	27.8	7.1	63.8	0.11	10.2	3.2	0.64	0.18
0%N	1.09	0.36	1.5	0.51	0.29	0.28	73.1	183	22.3	5.52	74.7	0.08	6.31	3.88	0.72	0.4

Appendix D(i). Standard laboratory foliar nutrient concentrations for the **0% P HNS regime at 30 days post-treatment.**

Treatments	N	P	K	Ca	Mg	S	Fe	Mn	Zn	Cu	B	Na	Al	N:S	N:K	Fe:Mn
0%P	2.19	0.2	1.65	0.46	0.22	0.31	58	290	37.7	7.6	50.7	0.12	10.4	7.07	1.32	0.2
0%P	2.4	0.23	1.73	0.59	0.26	0.46	51.7	327	35.1	10.1	50.7	0.14	5.26	5.22	1.38	0.16
0%P	2.11	0.24	1.63	0.39	0.21	0.32	58.8	289	38.1	7.24	41.8	0.05	4.56	6.6	1.29	0.2
0%P	2.03	0.22	1.81	0.45	0.26	0.41	85.1	272	28.4	8.7	40.5	0.14	7.8	4.96	1.13	0.31
0%P	2.22	0.19	2.05	0.52	0.26	0.42	49.7	334	34.8	9.4	52.7	0.14	5.39	5.31	1.08	0.15
0%P	2.41	0.21	1.97	0.48	0.25	0.41	60.7	349	41.6	8.37	52	0.07	4.13	5.81	1.22	0.17
0%P	2.02	0.21	1.6	0.38	0.2	0.26	52.8	274	35.2	7.47	44.4	0.12	4.99	7.67	1.27	0.19
0%P	2.07	0.18	1.73	0.49	0.23	0.46	57.5	295	36.4	7	44.3	0.13	3.81	4.48	1.2	0.19
0%P	2.25	0.2	1.83	0.5	0.24	0.42	56.6	356	38	7.61	49.2	0.11	6.52	5.39	1.23	0.16
0%P	2.04	0.2	1.98	0.5	0.24	0.34	46.6	304	29.1	7.52	56.8	0.1	5.86	6.01	1.03	0.15
0%P	2.24	0.24	2.27	0.53	0.26	0.5	51.2	273	40	9.21	51	0.08	3.67	4.45	0.99	0.19
0%P	2.32	0.22	2.01	0.47	0.22	0.39	48.6	405	34.8	8.33	60.2	0.1	2.92	6.03	1.16	0.12
0%P	2.13	0.24	1.89	0.45	0.22	0.37	52.3	295	27.8	8.48	42.5	0.15	6.41	5.72	1.12	0.18
0%P	2.13	0.22	1.89	0.42	0.22	0.37	60	304	35.1	7.48	42.2	0.07	6.5	5.74	1.12	0.2
0%P	2.23	0.21	2.08	0.51	0.24	0.58	49.2	264	31.3	6.84	44.4	0.07	4.57	3.85	1.07	0.19
0%P	2.04	0.19	1.85	0.52	0.26	0.41	73.6	281	32.7	8.08	46.1	0.11	6.15	5.02	1.1	0.26
0%P	2.29	0.2	1.9	0.35	0.17	0.31	53.9	262	33.1	8.83	39.1	0.07	11.8	7.43	1.2	0.21
0%P	2.07	0.19	1.79	0.42	0.22	0.36	61.9	294	36.7	9.32	39.8	0.12	14.3	5.7	1.15	0.21
0%P	2.13	0.25	1.64	0.53	0.27	0.62	62.2	399	50.5	10.3	55.1	0.15	5.61	3.44	1.3	0.16
0%P	2.72	0.24	1.92	0.54	0.27	0.45	52.4	286	38	9.77	53.8	0.11	6.27	5.99	1.42	0.18

Appendix D(j). Standard laboratory foliar nutrient concentrations for the **0% K HNS regime at 30 days post-treatment.**

Treatments	N	P	K	Ca	Mg	S	Fe	Mn	Zn	Cu	B	Na	Al	N:S	N:K	Fe:Mn
0%K	2.27	0.35	1.12	0.63	0.33	0.45	126	339	35.7	8.5	49.6	0.1	4.26	5.01	2.02	0.37
0%K	2.02	0.31	1.03	0.54	0.27	0.32	55.7	324	29.5	6.55	42.7	0.07	11.3	6.25	1.96	0.17
0%K	2.07	0.28	0.96	0.69	0.34	0.33	62.8	312	27.2	6.96	54.3	0.14	3.4	6.23	2.14	0.2
0%K	2.41	0.32	1.04	0.51	0.28	0.42	54.9	353	44.5	8.83	40	0.1	6.21	5.75	2.33	0.16
0%K	1.83	0.25	1.05	0.47	0.23	0.31	45.8	215	17.3	4.74	42.4	0.1	4.43	5.85	1.75	0.21
0%K	2.36	0.28	1.01	0.53	0.29	0.4	115	218	25.3	7.18	38.9	0.11	6.01	5.87	2.32	0.53
0%K	2.13	0.28	0.89	0.58	0.31	0.38	46.6	378	23.6	6.68	43.6	0.12	8.13	5.62	2.39	0.12
0%K	2.05	0.31	1.04	0.52	0.28	0.4	55.9	312	32.5	6.54	51.7	0.05	10.4	5.16	1.98	0.18
0%K	1.74	0.27	1.03	0.53	0.26	0.35	44.6	288	22.8	6.82	40.3	0.13	6.73	4.96	1.7	0.15
0%K	2.03	0.28	1.03	0.49	0.28	0.29	68.6	225	39.4	8.78	42.1	0.12	5.61	6.93	1.97	0.31
0%K	2.42	0.31	1.21	0.57	0.32	0.47	48.9	338	24.3	8.27	42.9	0.11	4.32	5.16	2	0.14
0%K	2.32	0.28	1.14	0.55	0.31	0.29	42.1	340	18.5	6.78	51.2	0.05	4.46	8.04	2.03	0.12
0%K	2.17	0.31	1.07	0.62	0.32	0.4	59	265	27	7.84	43.3	0.13	7	5.41	2.02	0.22
0%K	1.78	0.28	1.08	0.65	0.35	0.39	53.7	284	26.4	6.29	49.9	0.16	5.45	4.63	1.64	0.19
0%K	1.95	0.29	0.98	0.64	0.34	0.36	53.9	252	23.1	6.06	56.1	0.14	5.8	5.4	1.99	0.21
0%K	2.07	0.31	1.1	0.53	0.32	0.4	48.3	348	28.6	8.39	43.3	0.11	3.77	5.17	1.88	0.14
0%K	2.3	0.39	1.17	0.68	0.36	0.58	50.9	342	31.2	9.35	58.8	0.11	2.83	4	1.97	0.15
0%K	2.16	0.31	1.02	0.55	0.33	0.46	53.6	325	29.3	7.99	40.3	0.11	3.59	4.72	2.12	0.16
0%K	2.23	0.31	1.24	0.7	0.34	0.52	43.9	352	27.1	8.33	53.1	0.12	4.36	4.31	1.8	0.12
0%K	2.25	0.31	1	0.46	0.26	0.31	56.4	328	24.8	7.83	39.3	0.11	6.8	7.25	2.26	0.17